Development and Characterization of Biomass Lignin and Plant Protein-Based Adhesives

by

Sarocha Pradyawong

B.S., Mahidol University, 2010
M.S., Asian Institute of Technology, 2013

AN ABSTRACT OF A DISSERTATION

submitted in partial fulfillment of the requirements for the degree

DOCTOR OF PHILOSOPHY

Department of Biological and Agricultural Engineering
College of Engineering

KANSAS STATE UNIVERSITY
Manhattan, Kansas

2018

Abstract

The depletion of petroleum feedstock along with significant concerns about health and environment lead to an interest in alternative green products. Soy protein (SP) adhesives have great potential as a renewable material for wood industries. The obstacle of applying SP-based adhesives is its relatively low water resistance. The overall objective was to enhance the water resistance of SP adhesives through protein and lignin interaction. An improvement of adhesion performance, flowability, and thermal properties of SP adhesives was achieved through the protein and lignin interaction and formation of protein and lignin copolymer.

pH adjustment is a simple process to change protein folding and lignin properties. Cleavage of β-O-4 linkage was observed at pH 8.5 and pH 12, resulting in an increase in lignin active groups and the changes in lignin particle size and thermal properties. Cross-linking of protein with lignin took place via carbonyl, amino, and hydroxyl groups. Multiple-point and non-specific interactions between lignin and protein resulted in stronger lignin-protein networks and changes in properties, which improved wet adhesion strength of protein adhesives. In addition, lignin was depolymerized by laccase enzyme with the presence of mediator, TEMPO, to induce a formation of the strong lignin-protein network. The formation of the strong lignin-protein network increased the wet adhesion strength by 106% and the partial wood failure was observed after the three-layer wood test. A better performance was also observed on the three-cycle soaking test.

The adhesion performance of SP adhesives was also greatly affected by lignin particle size and the protein to lignin ratio at pH 4.5. The wet adhesion strength of SP adhesives increased as lignin particle size decreased. The protein-lignin adhesive with protein to lignin ratio of 10:2 (w/w) at 12% solid content had the lowest contact angle and the highest wet adhesion strength of 4.66 MPa, which is 53.3% higher than that of 10% pure SP adhesive.

Lignin-protein interactions, water resistance property, and glue line pattern had strong influences on an adhesion performance. Lignin and soy protein were modified at pH 4.5, 8.5 and 12. The maximum increase (620%) in water resistance was found at pH 12 with an addition of lignin. After the protein was unfolded (pH 8.5) and denatured (pH 12), it was refolded by shifting pH to 4.5. The better wet adhesion performance was obtained at pH 4.5, 8.5-4.5 and 12 with rigid glue line. Shifting pH from 8.5 to 4.5 promoted lignin-protein interaction and increased adhesion performance.

The protein-lignin adhesives using absolutely renewable materials and practical processes showed an excellent potential to replace the petroleum-based adhesives and fulfill the global demand for green products and technologies.

Development and Characterization of Biomass Lignin and Plant Protein-Based Adhesives

by

Sarocha Pradyawong

B.S., Mahidol University, 2010
M.S., Asian Institute of Technology, 2013

A DISSERTATION

submitted in partial fulfillment of the requirements for the degree

DOCTOR OF PHILOSOPHY

Department of Biological and Agricultural Engineering
College of Engineering

KANSAS STATE UNIVERSITY
Manhattan, Kansas

2018

Approved by:

Major Professor
Donghai Wang

Copyright

Abstract

The depletion of petroleum feedstock along with significant concerns about health and environment lead to an interest in alternative green products. Soy protein (SP) adhesives have great potential as a renewable material for wood industries. The obstacle of applying SP-based adhesives is its relatively low water resistance. The overall objective was to enhance the water resistance of SP adhesives through protein and lignin interaction. An improvement of adhesion performance, flowability, and thermal properties of SP adhesives was achieved through the protein and lignin interaction and formation of protein and lignin copolymer.

pH adjustment is a simple process to change protein folding and lignin properties. Cleavage of β-O-4 linkage was observed at pH 8.5 and pH 12, resulting in an increase in lignin active groups and the changes in lignin particle size and thermal properties. Cross-linking of protein with lignin took place via carbonyl, amino, and hydroxyl groups. Multiple-point and non-specific interactions between lignin and protein resulted in stronger lignin-protein networks and changes in properties, which improved wet adhesion strength of protein adhesives. In addition, lignin was depolymerized by laccase enzyme with the presence of mediator, TEMPO, to induce a formation of the strong lignin-protein network. The formation of the strong lignin-protein network increased the wet adhesion strength by 106% and the partial wood failure was observed after the three-layer wood test. A better performance was also observed on the three-cycle soaking test.

The adhesion performance of SP adhesives was also greatly affected by lignin particle size and the protein to lignin ratio at pH 4.5. The wet adhesion strength of SP adhesives increased as lignin particle size decreased. The protein-lignin adhesive with protein to lignin ratio of 10:2 (w/w) at 12% solid content had the lowest contact angle and the highest wet adhesion strength of 4.66 MPa, which is 53.3% higher than that of 10% pure SP adhesive.

Lignin-protein interactions, water resistance property, and glue line pattern had strong influences on an adhesion performance. Lignin and soy protein were modified at pH 4.5, 8.5 and 12. The maximum increase (620%) in water resistance was found at pH 12 with an addition of lignin. After the protein was unfolded (pH 8.5) and denatured (pH 12), it was refolded by shifting pH to 4.5. The better wet adhesion performance was obtained at pH 4.5, 8.5-4.5 and 12 with rigid glue line. Shifting pH from 8.5 to 4.5 promoted lignin-protein interaction and increased adhesion performance.

The protein-lignin adhesives using absolutely renewable materials and practical processes showed an excellent potential to replace the petroleum-based adhesives and fulfill the global demand for green products and technologies.

Table of Contents

List of Figures

List of Tables

Acknowledgements

I would like to express my deep gratefulness to Dr. Donghai Wang, my advisor, for giving me an opportunity to pursue the doctoral degree and work as a graduate research assistant in his research group. He gave me his constant guidance, mentorship, advice, and financial support during the entire course of my Ph.D. I deeply respect Dr. Donghai Wang's enthusiastic working attitude and inspiration. His perspective and training will be significant benefit my future career. I could never thank him enough for the support and guidance he has given to me. I would like to thank Dr. Xiuzhi Susan Sun, member of my academic committee, for her advices and research facilities. My family and I do really appreciate Dr. Donghai Wang and Dr. Xiuzhi Susan Sun for their flexibility, kindness and support, especially throughout the difficult time.

I would like to thank the other members of my committee - Dr. Meng (Peter) Zhang, Dr. Yonghui Li and Dr. Lisa Wilken, for their time in serving as the supervisory committee, providing valuable suggestions and research facilities. I would like to thank Dr. Praveen Vadlani for his serving as a former committee member. Many thanks also go to Dr. Xiaojiang Jack Xin for willing to serve as outside chair of my supervisory committee.

I am also grateful to Dr. Guangyan Qi and Dr. Ningbo Li, Dr. Ke Zhang and Mr. Edwin Brokesh for the technical support and advice. I thank all the members of my research group: Ms Kaelin Saul Mr. Youjie Xu, Mr. Nana Baah Appiah-Nkansah, Mr. Bairen Pang, Mr. Xiwen Cao, Mr. Jun Li, Ms. Haijing Lui, Mr. Xiangwei Zhu, Mr. Yizhou Zheng, Ms. Zhu Xin, and MS. Quan Lifor their support and enjoyable experience.

Profound thanks to Dr. Joseph Harner, Dr. Naiqian Zhang, Ms. Barb Moore, Ms. Arlene Jacobson, Ms. Kerri Ebert, Mr. Randy Erickson, and other faculty and staff members in the Department of Biological and Agricultural Engineering for their help.

Most importantly, I am deeply appreciate to the unconditional love, support, and care from my Parents, Sarin and Wasan Pradyawong, grandmother and aunts. I am also thanks to Zimmerman, Watson, Chuwonganant, Yaege, Spires and Akins families, and Mr. Marut Saensukjaroenphon, Mr. Kedron Brock, Ms. Pui See Chung, Mr. Takashi Taguchi, and Mr. Taihao Yang for their support in my daily life.

Dedication

I would like to dedicate this thesis to my family and friends.

Chapter 1 - Introduction

1.1 Problem Statement

Formaldehyde-based adhesives are mainly used in wood-based industries due to their great adhesion performance. They occupy more than 70% of wood adhesive market due to its great adhesion performance (Grand View Research Inc. 2017a). Formaldehyde-based adhesives are widely applied in pressed wood products, such as particle board, plywood and fiber board in the United States (Wool and Sun 2005). However, formaldehyde can be emitted out from wood products, especially in high humidity area, and become volatile organic pollutant. Formaldehyde is the most concerning pollutant and classified as a human carcinogen with high chronic toxic effects. Exposure to formaldehyde for a short time, results in skin, throat, nose, and eye irritation (EPA 2013b; Sofuoglu et al. 2011). Moreover, formaldehyde causes negative effects on the environment. As a result, United States Environment Protection Agency (EPA) proposed a more strict regulation for formaldehyde emission standards for composite wood products (EPA 2013b). In addition, petroleum-based products including formaldehyde are not sustainable as petroleum is subjected to depletion in the near future. Therefore, there are strong demands for safe, environmental friendly, and sustainable wood adhesives. Soybean, a potential eco-friendly adhesive source, is largely available with reasonable price (Frihart et al. 2010; Maestri et al. 1998). Soy protein-based adhesive is one of the most popular bio-adhesives with good adhesion performance and safety. Recently, soy protein adhesives (SPA) have been commercially available with a small market share (Grand View Research Inc. 2017a) due to their excellent adhesion performance on wood and other materials under dry conditions. The significant disadvantage of SPA is relatively low water resistance which limits its application and market attraction

(Pradyawong et al. 2017). Therefore, most of the research has focused on improving wet strength of SPA through various methods (Frihart et al. 2010).

Lignin, a renewable aromatic polymer, has high potential to provide basic subunits that can enhance water resistance of protein-based adhesives. Interactions between small aromatic compounds which resembles lignin structure and protein have been reported (Le Bourvellec and Renard 2012) but the mechanisms of these interactions are yet to be elucidated (Ozdal et al. 2013). Recently, interactions between soy protein and lignin were studied (Salas et al. 2012). Some studies reported lignin has functuion to improve the wet strength of soy protein by lignin (Doherty et al. 2011; Luo et al. 2015a; Pradyawong et al. 2017; Xiao et al. 2013). The understanding of lignin-protein interactions will lead to significant breakthrough in the development of liginin-soy-protein adhesives with high water resistance property.

1.2 Review of Literature

1.2.1 Biomass Lignin

Recently, lignin draws strong interest as a renewable and environmentally friendly resource. Lignin is the most abundant aromatic polymer in the world (Pye 2008). Plants contain 15-30% of lignin which varies depending on plant species (El Mansouri and Salvadó 2006). About 70 million tons of lignin are produced by pulping industries annually (Mankar et al. 2012) and there is more lignin produced from biorefinery and lignocellulosic ethanol production. Lignin is mostly burned as a low-value energy source in factories (Stewart 2008). Only small amount of lignin (1–2% of annual production) are isolated from a wide range of specialty products (El Mansouri and Salvadó 2006). Lignin is an amorphous highly branched polyphenolic polymer with 23 subunits. It mostly concentrates on primary plant cell wall and middle lamella. It surrounds

cellulose and hemicellulose, and provides plants rigidity and protection. Lignin contains three major subunits, p-coumaryl or p-hydrophenol alcohol (H), coniferyl alcohol or guaiacyl (G), and sinapyl alcohol (S) as seen in Fig. 1.1. The structure consists of several active functional groups such as carbonyl, methoxyl, phenolic hydroxyl, and alcoholic hydroxyl groups. The molecules are linked by several types of ether and ester bonds. The majority are linked by β-O-4 bonds and the rest of them are α-o-4, and 4-O-5, and carbon to carbon linkages, and etc. (Christopher et al. 2014; El Mansouri and Salvadó 2006). Lignin structure is slightly different in subunit composition, functional groups, crosslink structures, and degree of depolymerization due to the varieties of plant species and separation techniques. Hence, the molecular weight of isolated lignin varies in the range of 1000-20000 g/mol (Doherty et al. 2011).

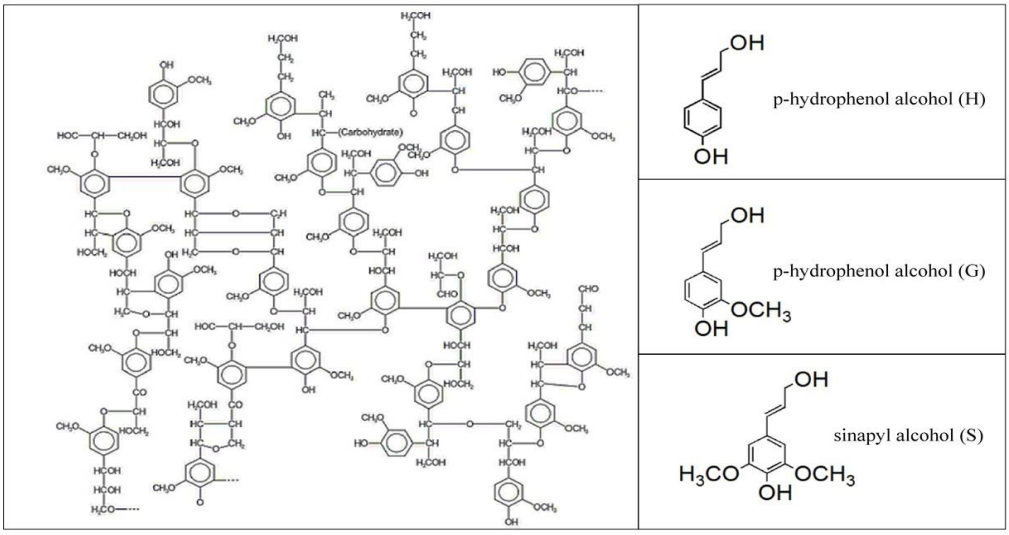

Figure 1.1. Lignin structure and major subunits (adapted from Christopher et al. 2014)

According to lignin structure that contains a lot of aromatic subunits, lignin has a high potential to replace the large market of petroleum-based chemicals and liquid fuel. Nowadays, lignin is used as a replacement for petroleum-based products such as phenolic resin, epoxy resin, antioxidants and aromatic resources (Pye 2008). A million tonnes of lignosulfonate lignin is also

applied as a dispersion and binding agents in many industries. However, compared to the total amount of lignin that is separated from the wood by chemical pulping industry, the amount of lignin that is recovered and sold commercially are very small (Pye 2008).

Lignin can be utilized for many applications such as emulsifiers, dispersants, surfactants, antioxidants, panel and door binders, phenol-formaldehyde resins, epoxy resins, friction materials, insulation materials, aromatic sources, and initial substrates for many value-added products (Pye 2008). Moreover, there is plenty of new market for lignin such as epoxies resin, printed circuit board resins, animal health applications and feed supplement, carbon fibers for vehicles (Gosselink et al. 2004; Lora and Glasser 2002; Pye 2008; Stewart 2008). However, there are a lot of technical changes need to be addressed. For instant, kraft lignin and soda-anthraquinone lignins are low molecular weight containing relative high amount of phenolic hydroxyl group which highly reactive with formaldehyde (El Mansouri and Salvadó 2006). The partial replacement of phenol formaldehyde-based adhesives have advantages of cost reduction and the decrease in formaldehyde emission. However, this replacement is not successful in the industrial scale due to due to the diverse function groups and the long pressing time (Pizzi 2006; Stewart 2008). Recently, lignin has been applied as a water resistance enhancer for plant protein-based adhesives. However, additional studies are needed to further increase the adhesion performance (Pradyawong et al. 2017). The detailed discussion will be mentioned in section 1.2.3. Therefore, studying and understanding lignin structure and depolymerization processes are necessary to add value to lignin and explore lignin applications.

Thermal degradation is a conventional methods used to break lignin into varieties of smaller or single subunits under high pressure and temperature. Lignin depolymerization processes such as pyrolysis, gasification, supercritical fluid, hydrogenolysis and hydrothermal degradation

are costly and operated under extreme conditions (Fisher and Fong 2014; Pandey and Kim 2011; Yang et al. 2015). Using a combination of chemicals, organic solvents and/or catalysts resulted in more specific reactions and provides a higher yield of designated products, but costs and process complexity restricts commercialization (Fang et al. 2008; Liu et al. 2013; Xin et al. 2014).

Lignin can also be degraded naturally by microorganisms, plants, and insects (Fisher and Fong 2014). Fungi secrete lignin peroxidase (LiP), manganese peroxidase (MnP), and laccase naturally to depolymerize lignin under mild condition. The operating conditions are safe and environmentally friendly (Díaz-Rodríguez et al. 2014). Among the three enzymes, laccase has a low redox potential (450-800 mV) but it has the advantage of utilizing atmospheric oxygen as an electron donor instead of hydrogen peroxide, which is used by LiP and MnP (>1000 mV) (Desai and Nityanand 2011). Fungal laccases have higher redox potentials and are easier to produce, therefore, laccase is an excellent candidate for diverse industrial applications and has received great attention in recent years (Christopher et al. 2014; Díaz-Rodríguez et al. 2014; Fabbrini et al. 2002; Fisher and Fong 2014). Laccase has four-copper active sites that gain oxidative potential by reducing oxygen to water. Then laccase with high redox potential will engages in an oxidation reaction. Laccase removes an electron and a proton from phenolic hydroxyl and aromatic amino groups (Leonowicz et al. 2001). Nevertheless, laccase itself can oxidize only phenolic compounds. To enhance the oxidation reaction of non-phenolic compounds, mediators are added to the system as an electron shuttle to transfer an electron to non-phenolic compounds (Barreca et al. 2003; Fabbrini et al. 2002). The mediator is a small compound that can be easily oxidized by laccase enzyme and subsequently reduced by the substrate (Christopher et al. 2014). It acts as an electron shuttle to transfer an electron from substrates to laccase (Fabbrini et al. 2002). The cleavage of C_α-C_β, aryl-alkyl and alkyl-alkyl bonds and oxidation of C_α in lignin was found (Ramalingam et al.

2017; Sánchez et al. 2011). Varieties of mediators such as ABTS, HPI, HBT, VLA and etc. were studied under different circumstances. TEMPO (2, 2, 6, 6-Tetramethylpiperidin-1-yl) is considered as the most effective mediator (Díaz-Rodríguez et al. 2014; Fabbrini et al. 2002). Laccase-TEMPO can oxidize both aromatic and non-aromatic primary or secondary alcohols of lignin and protein in water at room temperature using ambient air (Díaz-Rodríguez et al. 2014; Ramalingam et al. 2017). Phenolic and non-phenolic subunits of lignin were oxidized in the laccase-TEMPO system.

1.2.2 Soy Protein and Soy Protein Adhesives

Soybean is one of the major oilseed crops accounted for about 90 percent of U.S. oilseed production. According to the USDA oilseeds report in 2017, 119.52 and 42 million MT of soybean and soymeal are produced in the USA, respectively, and the world production capacity of soybean and soymeal are 340.86 and 236.70 MT, respectively in 2017/2018. Soybean and soymeal price ranged from $330.66 to $352.70 and from $294.84 to $322.05 per MT, respectively (USDA 2018). Soymeal is a permissible source to obtain protein (Hemmilä et al. 2013).

Soybean comprises of 18-26% lipid and 50-70% proteins. The majority (50-90%) of soy proteins are storage protein which contain ~30% of glutamic acid and aspartic acid with COO^- functional groups, ~22% of lysine, arginine, histidine, proline with NH, NH_2 and NH_3 groups and ~2.5% of cysteine and methionine with S element, while other amino acids make up the remainder (Wool and Sun 2011). The amino acids are linked by peptide bonds to form the primary structure, polypeptide chain. Hydrogen bonds within the chain results in a secondary structure, α-helix, and β-sheet. The more stable conformation, tertiary structure, is stabilized by disulfide linkage, hydrogen bond, ionic bond and non-specific interactions. The quaternary structure contains multi-polypeptide chain and maintains the structure by the same interactions and bonds. The differences

in protein functions and properties result from the diversity in the number, composition, and sequence of amino acids. The major components of soy protein are globulin: β-conglycinin (7S) and glycinin (11S), which are trimeric and hexameric complexes, respectively. 11S, with a molecular weight of 350 kDa, contains acidic subunit A and basic subunit B (Kim and Sun 2014). It shows better thermal and chemical stabilities than 7S because its subunits are linked by disulfide bonds, whereas non-covalent bonds and electrostatic force mainly present in 7S. 7S, with a molecular weight of 175 kDa, contains α, α' and β subunits (Qi et al. 2011). There are several factors that affect the properties of the subunits. In aquatic solutions, hydrophobic amino acids are arranged in the structural core and the hydrophilic amino acids are exposed to the surface. Protein structure, folding degree, and properties are sensitive to pH. Acidic and basic polypeptides of 11S are likely sensitive to pH change. As high pH shift breakdowns the disulfide bonds and low pH shift enhanced the cross-linking of 11S subunits; therefore, 11S became more soluble at high pH. In contrast, the solubility of 7S is not affected by pH shifting. High pH tended to increase the solubility of the protein. Protein FTIR spectra were found to be different depending on pH value of soy protein solution which imply changes in the structural arrangement and bond adjustment (Santoni and Pizzo 2013). Shear thinning behavior was observed and soy protein viscosity was very low at its pI and show plug-like behavior (Li et al. 2012b; Qi et al. 2013a).

Plants protein are ampholytic and contain a variety of functional groups such as carboxylic, amide, and hydroxyl which can interact with the wood surface. During the curing process, protein penetrates into wood surface pores and forms complex matrixes. The bond strength is significantly affected by entanglement and cross-linking between proteins. Covalent bonds between functional groups of protein and carboxylic and hydroxyl groups of cellulose fiber have been considered as the most durable and the strongest (Wool and Sun 2011). The optimal penetration and balance

between the adhesive and the wood tissue and the remaining adhesive in the bond line lead to the high adhesion performance (Nordqvist et al. 2013). Soy protein is most promising bio-adhesive product and it has been extensively investigated during last decades (Nordqvist et al. 2013; Santoni and Pizzo 2013; Wool and Sun 2005). Soy protein was used to reduce the formaldehyde emission of traditional phenol formaldehyde (PF) adhesive. PF-soy flour blended adhesive could reduce the cost of commercial PF resin by 30-40%, while maintaining the durable adhesion performance and providing the same adhesion strength as the control PF adhesive (Wescott et al. 2006; Zhong and Sun 2007). Besides, pure soy protein also provided great dry adhesion performance in the pH range of 3.6 to 7.6 whereas, the best-wet adhesion performance was found in the range of 3.6 to 5.6. The highest water resistance was found at the neutral surface charge at pI (Wang et al. 2009a). The significant weak point of bio-based adhesives including soy protein is poor water resistant (Hemmilä et al. 2013). Unfortunately, for exterior application, water uptake, irritation and air drying in plywood pay an important role for wood-based products. Glue lines were found to be a significant factor in the performance of plywood as high water resistance adhesives acted as a strong moisture barrier to prevent water penetration to the inner layer (Li et al. 2014). Therefore, water resistance improvement of soy protein-based adhesive is required to explore its outdoor applications. In general, the soy protein globular structure is formed by intermolecular interactions such as van der Waals forces, hydrophobic interactions, hydrogen, disulfide and electrostatic bonds. Protein exposes hydrophilic groups to surface, whereas hydrophobic amino acids are hidden in the structure core (Li et al. 2014; Wang et al. 2009a). Because of its weak-inter molecular interactions and hydrophilicity, soy protein has low water resistance and bonding strength (Zhang et al. 2014).

The majority of the research related to water resistance improvement of SPA focus on changing or modifying the protein folding structure by modified agents and strengthen the protein network by cross-linkers. SPA in the pH range of 1.6-9.6 with different protein folding structures were studied and the highest wet strength was obtained at pH 3.6-5.6 (~pI) (Wang et al. 2009a). The pH-shifting process was applied to expose hydrophobic core and increase surface hydrophobicity. Holding protein in extremely acidic and alkaline pH and adjusting pH back to neutral caused declining in water solubility because some buried hydrophobic side chains were exposed to the surface. The process had a significant effect on 11S as the alkaline shifting process induced cleavage of a disulfide bond, whereas acidic treatment promoted cross-linking (Jiang et al. 2010). Solubility decreased with longer holding time up to 4 h in extreme conditions (Jiang et al. 2009). However, salt increased the apparent solubility of soy protein due to a "salt in effect". Sodium chloride shielded protein, reduced protein-protein interaction, and formed protein aggregates which gave a negative impact on adhesion strength of the glue. A high concentration protein adhesive with acidic pH is an excellence glue for plywood applications (Mo and Sun 2013).

On the other hand, chemicals, cross-linkers, and modified agents have been used to modify protein structure and caused significant water resistance improvement of SPA (Kim and Sun 2014; Li et al. 2004; Li et al. 2012a; Liu et al. 2015). Millard cross-linking of soy protein was observed in food and film studies and caused a decrease in water sensitivity and other properties change (Gerrard et al. 2005; Su et al. 2010). Glutaraldehyde was claimed to be one of the most efficient reagents cross-linking the nucleophilic groups, such as the ε-amino group of lysine and N-terminal of peptide chains, thus strengthening the protein network (Gerrard et al. 2005). It provides chemically and thermally stable crosslinks, created larger molecular weight, decreased solubility, increased hydrophobic group from the attached glutaraldehyde, strengthened mechanical

properties and increased 115% of wet strength (Migneault et al. 2004; Park et al. 2000; Wang et al. 2007). Crosslinking of soy protein and better adhesion performance also could induce by sodium montmorillonite clay (Qi et al. 2016). Similarly, the other cross-linkers such as calcium silicate hydrate hybrids, undecylenic acid, polyisocyanate, and PAE shared the similar mechanism to increased molecular weight and improved water resistance of SPA (Frihart et al. 2010; Kim and Sun 2014; Li et al. 2004; Liu et al. 2015; Rowell et al. 2010; Zhang et al. 2014). In contrary, an increase in water resistance of plant protein also could be achieved by breaking disulfide bond and weaker intermolecular interactions and induced a negative charge on the protein surface. Dr. Sun's group studied plant protein such as soy and canola proteins modification by sodium bisulfite ($NaHSO_3$) and reported significant improvement in the adhesion performance together with other advantages such as longer shelf life, good flowability (Li et al. 2012a; Qi et al. 2013a). Cleavage of a protein molecule by enzymatic reaction also resulted in a significant increase in water resistance (Kim and Sun 2015). In addition, improvements in water resistance in SPA were also achieved by denaturing reagents such as cationic detergents, sodium dodecyl sulfate (SDS), sodium dodecylbenzene sulfonate, urea, and guanidine hydrochloride (Huang and Sun 2000a; b; Wang et al. 2005). However, the modifications generally change the globular structures of soy proteins, whereas weaken intermolecular interactions contribute to poor water resistance (Zhang et al. 2014). Therefore, more research is needed to further improve the water resistance of SPA.

1.2.3 Lignin-Protein Interactions and Adhesion Performance

As lignin is a phenolic compound and has a good thermostability, it has drawn a strong interest to be utilized as a substitution and replacement of phenol formaldehyde-based adhesives (Moubarik et al. 2013). Low molecular weight contains a high percentage of hydroxyl group and G subunit with open ortho-position, and is more reactive. Therefore, it is easier to form quinone

methide intermediate, and then form cross-link with another lignin molecule or soy protein. It is also more reactive for the synthesis of lignin-PF adhesives. Kraft and soda lignin have a good thermostability, low molecular weight and high hydroxyl group that are recommended for the production of lignin-based epoxy resin (El Mansouri and Salvadó 2006; El Mansouri et al. 2011; Mankar et al. 2012; Zhang et al. 2013). Lignin was pre-treated with several methods involving chemicals and catalysts to increase the lignin reactivity. Up to 50 wt % of phenol can be substituted by lignin and which resulted in an increase in bond strength (Khan and Ashraf 2005; Khan et al. 2004; Yang et al. 2014). More specific processes such as phenolation, glycosylation, and enzymatic reactions were investigated to enhance the bonding strength of lignin and lignin-phenol-formaldehyde-based adhesives for wood composite, wool floor covering, particle board, and fiberboard (Aracri et al. 2014; Bertaud et al. 2012; Cetin and Özmen 2002; Geng and Li 2006; Nasir et al. 2014; Pizzi and Salvadó 2007). Lignin substitute in PF adhesives passed the internal standard specification for interior grade panels and manufacture of exterior-grade wood particleboard (El Mansouri et al. 2011; Moubarik et al. 2013). However, substitution phenol from lignin in PF adhesive increases the panel pressing time and the production cost, because lignin is naturally less reactive compared to PF and requires additional preparation processes. It was not yet successful in medium density fiberboard and other pressed woods (Pizzi 2006). In addition, the replacement was mostly in the range of 40-70% (Mankar et al. 2012). Therefore, utilization of lignin by substituting phenol formaldehyde based resin does not completely remedy the formaldehyde emission problem.

A new innovation of completely safe and sustainable bio-based adhesives have drawn a strong interest recently. Lignin is blended to increase the water resistance in protein adhesives. There are few research studies about lignin-protein interactions and especially adhesion properties.

Lignin interacts with protein to form a lignin-protein network by the hydrophobic interactions and assisted by ionic and hydrogen bonds which are similar to the interactions between protein and polyphenol (Le Bourvellec and Renard 2012). The mechanism of these interactions still has not been fully elucidated (Ozdal et al. 2013). However, a cross-couple interaction, as a result of a nucleophilic attack of amino acids polar side chains (Nu), was found between coniferyl alcohol, a major lignin subunit, and amino acids (Cong et al. 2013). Hydroxyproline is more reactive toward lignin than other amino acids (Whitmore 1978; Whitmore 1982). The mechanisms and models between nucleophilic side group in amino acids and quinone methide were studied (Diehl et al. 2014). The adsorption of both glycinin (11S) and β-conglycinin (7S), soybean protein subunits, on the lignin surface occurred by nonspecific interactions, hydrophobic and electrostatic force, and hydrogen bonding (Salas et al. 2012). Unfolded soy protein could form a better interaction with lignin (Salas et al. 2014). The hydroxyl rich lignin was found to form extensive networks with soy protein isolate (Huang et al. 2003a). A lignin-protein aggregated network enhanced of mechanical property of materials (Chen et al. 2006a; Huang et al. 2003b; Wei et al. 2006). Cross-linking between lignin and protein enhanced the thermostability, Young modulus, water resistance and tensile strength of protein (Doherty et al. 2011; Huang et al. 2003b; Kunanopparat et al. 2012).

Lignin-based resin increased the viscosity of SPA (Luo et al. 2015a; Pradyawong et al. 2017). By reacting to itself and interpenetrating into the soy protein network along with cross-linking between the lignin-based resin and soy protein, there was a decrease in the hydrophilic groups and an increase in the water resistance of the adhesives. The wet strength of soy meal with 10% lignin-based resin increased by 200%, compared with soy meal adhesive (Luo et al. 2015a). Lignin with higher free hydroxyl and carbonyl groups showed higher thermostability and provided superior shear strength and water resistance (Xiao et al. 2013). A reasonable degree of water

resistance of laccase modified reduced lignin and soy protein was reported. Hydrogen or ester bond between the hydroxyl and carbonyl groups of soy protein and the laccase modified lignin. Acidic and basic conditions provide better adhesion performance than neutral pH, and alkaline soy-lignin adhesive showed the best performance for medium-density fiberboard and passed both internal bonding and modulus of rupture standards (Ibrahim et al. 2013; Nasir et al. 2014). Lignin-soy protein-based adhesives presented a great potential as a green adhesive. However, more investigation and improvement are needed to explore its applications.

1.3 Research Objectives

The long-term goal of this research was to develop affordable and durable bio-based adhesive for wood applications and to reduce the usage of phenol formaldehyde based-adhesives and reliance on fossil feedstocks. The specific objectives of this research are:

1. To study the effects of pH and pH-shifting process on lignin and lignin-soy protein interactions and properties.
2. To study the effects of lignin particle size on adhesion performance of soy protein adhesives.
3. To study the effects of pH and pH-shifting process on adhesion performance and properties of lignin-soy protein adhesives.
4. To study the effects of laccase-modified lignin on soy protein adhesion performance and properties.

Chapter 2 - Effect of pH and pH-shifting on Lignin and Protein Properties and Interactions

2.1 Abstract

Lignin modification and utilization remain a major challenge for sustainable lignocellulosic biorefineries due to its complicated structure. Innovation of high-value added lignin derivatives has become a topic of huge interest recently. In our previous study, we successfully improved water resistance and adhesion performance of soy protein adhesive using lignin. This study focuses more on lignin-protein modifications, properties, and interactions. Firstly, lignin modification was achieved by pH and pH-shifting modification processes. Cleavage of β-O-4 linkage was observed at pH 8.5 and pH 12, resulting in smaller particle sizes and changes in thermal properties. Partial repolymerization was found after pH-shifting treatments. Secondly, lignin-protein solutions were prepared by pH and pH-shifting modification processes. Lignin increased the strength of the protein film under high temperature, and significantly enhanced water resistance of soy protein at pH 12. Finally, the best conditions were selected to study lignin-protein interactions. Cross-linking of protein with lignin took place via carbonyl, amino, and hydroxyl groups. Multiple-point interactions between lignin and protein resulted in changes of properties and stronger lignin-protein network. Additional lignin-protein complexes with high-molecular weight were detected with elevated lignin concentration at pH 8.5. The binding interaction between lignin and protein, although of non-specific nature, was also observed by isothermal titration calorimetry (ITC). This primary study will motivate further development of green lignin-protein products.

2.2 Introduction

Lignin accounts for 30% of the carbon source on earth (Cong et al. 2013; Pye 2008). It is largely available as a renewable amorphous aromatic based bio-polymer. As lignin is a high potential sustainable material to be utilized as the source of monomers, building blocks and variety of chemicals, it has drawn significant interest as alternative bio-based products and materials in last few decades (Duval and Lawoko 2014; Huang et al. 2003a). Lignin, modified lignin, and its derivatives were found to be good fillers and property enhancers for both petroleum- and bio-based materials(Holladay et al. 2007; Lora and Glasser 2002; Pye 2008). Recently, the field of lignin has become is very trendy and is the subject of diverse fields of green researches such as polymers, plastics, adhesives and so on (Chen et al. 2006b; Frigerio et al. 2014; Huang et al. 2003a; Huang et al. 2003b; Ibrahim et al. 2013; Luo et al. 2015b; Pradyawong et al. 2017; Wei et al. 2006; Zhang et al. 2015). Even though, many studies have confirmed its great potential as an alternative aromatic source, very few percentages of lignin have been utilized as high value-added products (El Mansouri and Salvadó 2006). Most of the lignin by-products from paper, plumping and biomass industries are flamed to generate heat in factories (Mankar et al. 2012; Stewart 2008). Given the great potential and availability of lignin, along with the environmental concerns and the crisis caused by our dependence on fossil fuels, there is an urgent demand for more thorough studies on lignin and innovation of new lignin applications (Wei et al. 2006).

Lignin is polyelectrolyte in an aqueous solution. It can be depolymerized and modified to smaller phenolic compounds. The phenolic group can easily form H-bond with the carboxylic group of protein (Ozdal et al. 2013). Cross-linking interactions between protein and polyphenol have been reported by many studies(Damodaran 2008; Haslam 1996; Prodpran et al. 2012). Polyphenols can form multiple interactions and cross-link with peptide chains at more than one

point (Mulaudzi et al. 2012). The cross-linked networks are strengthened by hydrophobic and hydrophilic binding and Van der Waals forces. These interactions change physicochemical properties of proteins. It can lower solubility and increase the thermal stability of protein (Ozdal et al. 2013). The similar interactions between lignin and its derivatives and protein has also been reported. Reversible interactions such as hydrogen bonding, hydrophobic and electrostatic force, and non-specific interactions also occur in lignin-protein adsorption process (Salas et al. 2012). In addition, cross-coupling interactions are also formed between 3 types of polar amino acids and coniferyl alcohol, the major subunit of lignin (Cong et al. 2013).

Understanding the role of lignin-protein interaction is a key step in improvement of many adhesive and film works. This research will lead to further improvement of adhesion properties, and convey lignin-protein adhesives to markets. As a consequence, this novelty will play an important part in exploring lignin applications which contribute to a significant achievement of bio-material products.

However, no research has focused in depth on lignin-protein interactions. Few research groups have reported a new lignin application as a wet strength enhancer for soy protein-based adhesives, however very little supporting information or proof of interaction have been provided. Hence, the detail study of such system is still lacking and the mechanism is not yet fully elucidated (Ozdal et al. 2013). Moreover, no one has studied morphological changes in protein brought about by lignin interaction. Therefore, the objectives of this work are: firstly, to observe the morphological changes of protein caused by lignin; and secondly, to study and prove interactions between lignin and protein with various techniques at different pHs and pH-shifting processes.

2.3 Materials and Methods

2.3.1 Samples Preparation

ALDRICH alkali lignin (No. 370959) (AL) was purchased from Sigma-Aldrich, Inc. (St. Louis, MO) and dispersed in distilled water (DW) to reach the concentration of 10% (w/w). Sodium hydroxide (NaOH) and hydrochloric acid (HCl) were supplied from Fisher Scientific (Fair Lawn, NJ) and used as received to adjust pH of the lignin solutions to 4.5, 8.5 and 12. The samples were labeled as L4.5, L8.5, and L12, respectively. The pH was adjusted and maintained for 24 hr. For pH-shifted lignin samples, the pH of 8.5 and 12 lignin solutions were adjusted to 4.5 and kept constant for 2 hr after maintaining at pH 8.5 and 12 for 24 hr. They were labeled as L8.5-4.5 and L12.5-4.5. The fresh lignin samples were directly used to prepare adhesives. Some parts of samples were dried at 150 °C for 10 minutes for further analysis.

Defatted soy flour (Cargill, Cedar Rapids, IA) with the dispersion index of 90 was obtained as a protein source. Protein extraction process was conducted at 6.5% solid content in DW. The pH of the slurry was adjusted with NaOH (10N) to 8.5 to solubilize protein. Then the protein precipitation took place at pH 4.2 by HCl (10N). Protein part was collected by centrifugation at 12,000 g. The protein chunk was collected and neutralized with NaOH (10N). The isolated soy protein (SP) was then freeze-dried and ground with a cyclone miller with 1 mm screen (Udy Corp., Fort Collins, Colo.) and stored at 4 °C.

For the first part (non-pH-shifting adhesives), 10 percent of SP was dissolved in DW and adjusted pH to 4.5, 8.5 and 12.0 by 3 N HCl and NaOH. They were named as SP4.5, SP8.5, and SP12. For lignin-protein mixed adhesives, L4.5, L8.5, L12 fresh samples were added to SP4.5, SP8.5, and SP12, respectively, and named as SPL4.5, SPL-8.5, and SPL12. All samples were stirred at 300 rpm at room temperature for 2 hours. For the second part (pH-shifting adhesives),

the pH of SP and SPL samples at pH 8.5 and 12.0 from the first part were shifted to 4.5 and kept it constant for another 2 hr. The samples are called SP8.5-4.5, SP12-4.5, SPL 8.5-4.5 and SPL12-4.5, respectively. For dried samples, samples were dried at 150 °C for 10 minutes, ground by hand grinder (CoorseTek 60311 Ceramic, Coli-Parmer, IL, USA) and passed through 100 mesh screen.

2.3.2 Characterizations of Lignin Properties

The dried lignin samples from section 2.1 were coated with palladium and gold by sputter coater (Desk II Sputter/Etch Unit, Moorestown NJ), and observed under the scanning electron microscope (SEM), Hitachi S-3500N (Hitachi Science System, Ibaraki, Japan) to observe the morphological changes. The pictures were collected at an accelerating voltage of 10.0 kV. The specific quantum mechanical magnetic properties were analyzed by 2D-HSQC NMR technique. Approximately 40 mg of control and dried lignin samples from section 2.1 were dissolved in 0.5 mL DMSO. The spectra were measured by 500 MHz Bruker AVIII spectrometer equipped with a cryogenically-cooled carbon observe probe. The spectral widths were 8012 and 20883 Hz for the ^{1}H and ^{13}C dimensions, respectively. The number of collected complex points was 1024 for the ^{1}H dimension with a recycle delay of 2 s. The number of transients was 2 with 256 time increments were always recorded in the ^{13}C dimension. The $^{1}J_{C-H}$ used was 145 Hz. The data matrices were zero filled to 1024 points in the ^{13}C dimension. Data were processed by standard Bruker Topspin-NMR software. Thermogravimetric Analyzer (Perkin-Elmer TGA 7, Norwalk, CT) were used to analyze the thermostability of dried lignin samples. Approximately 5 mg of samples were heated from 25 °C to 700 °C. The heating rate was set as at 10 °C/min. The inert atmosphere in the chamber was control by N_2.

2.3.3 Evaluation of Morphological Properties

The particle sizes of lignin, SP and LSP fresh samples (see section 2.1.1) were measured using the laser scattering particle size distribution analyzer, LA-910 (Hiroba Scientific, NJ). Then the fresh adhesives were diluted to 0.1% with DW. The slurries were negatively stained with 2% aqua uranyl acetate and examined at 80.0 kV under the transmission electron microscope (TEM), TecnaiTM G2 Spirit BioTWIN (FEI Co., Hillsboro, OR.). The Film morphology and weight retain measurement was conducted by using the fresh SP and LSP adhesives to prepare films on premium micro slide plain (Fisherfinest, USA) and oven drying at 150 °C for 10 minutes. Dried film photos were taken by Samsung Galaxy S7 (Samsung, Korea). Morphology of adhesive films was observed under an optical microscope (Olympus BX51, Olympus Corporation, Tokyo, Japan), with 45° reflection of fluorescent light. The dried films were soaked under DW for 2 hr. The underwater films morphology was captured again by Samsung Galaxy S7 (Samsung, Korea).

2.3.4 Analysis of lignin-protein interactions

SDS-PAGE was run on 12% Bis-Tris separation gel and 4% Bis-Tris stacking gel in a discontinuous buffer system as described in (G Qi et. al., 2011) to study protein and lignin-protein network molecular weight distribution. The samples (20 mg/ml) were mixed with loading buffer containing 2.1% SDS, 26.3% glycerol and 0.01% bromophenol blue and 5% mercaptoethanol at pH 6.8 at the ratio of 1:1. SDS-PAGE was carried out under reducing condition. After boiling for 5 min, a total of 10 μl of the mixtures were loaded into wells. Electrophoresis was conducted under 150 V and 40 mA for 90 min. The molecular weight standard (10–250 kDa), (Precision Plus Protein^{TM} Standards, Dual color, BIO-RAD, CA, USA), was loaded with the mixtures. Then the gel was stained with 0.25% Coomassie brilliant blue R- 250 and destained in a destaining solution containing 30% acetic acid and 30% methanol and 40% distilled deionized water. Analysis of

binding interaction between lignin and soy protein was studied using isothermal titration calorimetry (ITC) (MicroCal iTC_{200}, GE Healthcare. For this lignin and protein solutions were prepared in plain water adjusted to pH 8.5 at final concentrations of 84 and 3 µM. Lignin solution in the syringe was injected into soy protein solution in cell set at temperature of 25^{o}C using 19 injections of 2 µL (5 s), injection intervals of 180 s, a reference power of 8 µcal/s, and a stirring speed of 750 rpm. Control experiment was also performed where lignin was injected to buffer alone. Thermograms were evaluated using Origin (version 7; OriginLab), and the data sets were fitted to "one set of sites" model. The elemental composition of lignin, protein and lignin protein samples was measured with CHNS/O Elemental Analyzer (PerkinElmer 2400 Series II, PerkinElmer Inc., Waltham, MA). Two to 2.5 mg of the dried samples from section 2.1 was weighted by a PerkinElmer AD-6 Autobalance (PerkinElmer Inc., Waltham, MA) and packed with foil. Then, the sample was burned under a pure oxygen atmosphere in the combustion chamber. The gaseous products from combustion (CO_2, N_2, SO_2, and H_2O) were separated in and detected in a quartz column by a thermoconductometer detector. PerkinElmer SpectrumTM 400 FTIR/FT-NIR spectrophotometer (Shelton, CT, USA) was used to scan the spectrum of the dried samples. The Fourier transform infrared (FTIR) data were collected in the range of 500–4000 cm^{-1}. The transmission spectra of 32 scans were collected at a resolution of 4 cm^{-1}. .

2.4 Result and Discussion

2.4.1 Lignin Properties

2D-HSQC analysis is a powerful method to determine lignin structure (Yuan et al. 2011). $^{13}C^{1}H$ correlation spectra in the 2D-HSQC analysis of the lignin samples were identified according to the previous literatures (Pu et al. 2009; Yang et al. 2015; Yuan et al. 2011). The side-chain

region (δ_C/δ_H 50.0–90.0/2.50–6.00) and aromatic region (δ_C/δ_H 100.0–150.0/5.50–8.50) of lignin are shown in Fig. 2.1A-1F and 1a-1f, respectively.

According to Fig. 2.1A, the original kraft lignin (control) showed prominent C-H correlations of β-O-4 linkages at C_α-H_α (δ_C/δ_H 71.3/4.76ppm), C_β-H_β (δ_C/δ_H 83.9/4.30ppm), and C_γ-H_γ (δ_C/δ_H 60.2/3.35-3.69ppm). A strong signal of methyl group was observed at δ_C/δ_H 55.7/3.77 ppm. A present of resinol (Fig. 2.1II) was confirmed by C-H correlations of C_α-H_α, C_β-H_β, and C_γ-H_γ at δ_C/δ_H 85.3/4.62,53.7/3.04 and 71.0/3.76 and 4.16 ppm, respectively. The major component of the kraft lignin is G subunit as dense signal of at δ_C/δ_H 109.6/7.16, 115.4/6.74, and 119.6/6.97 ppm represents C_2-H_2, C_5-H_5 and C_6-H_6 of guaiacyl units (G), respectively (see Fig. 2.1a). The light spot at δ_C/δ_H 103.5/6.63 of $C_{2,6}$-$H_{2,6}$ implies low amount of S unit in the kraft lignin. A correlations from $C_{2,6}$-$H_{2,6}$ in p-hydroxyphenol structure (*) were observed at δ_C/δ_H 128.2/7.17 ppm.

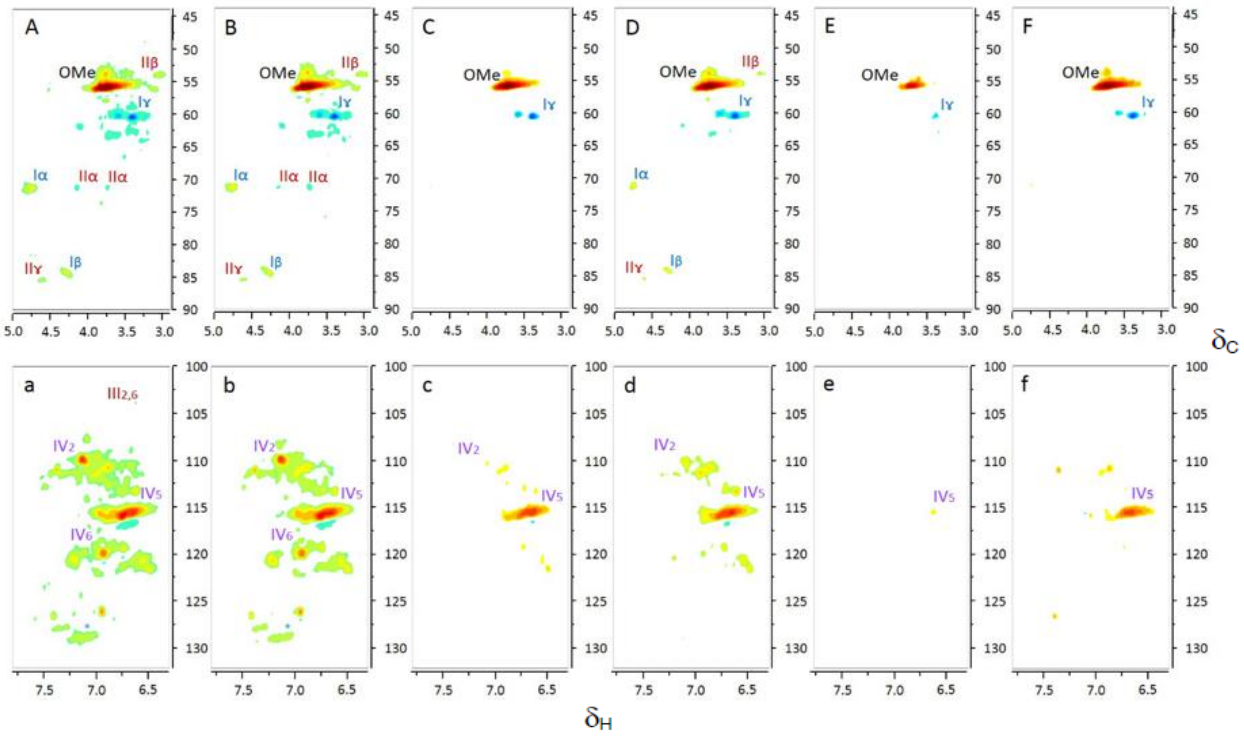

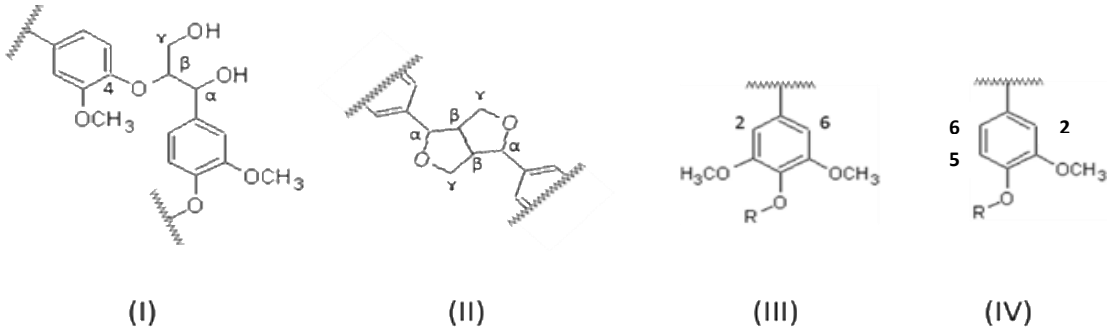

Figure 2 2D-HSQC-NMR spectra of lignin obtained at various pH. (A, a) kraft lignin control; (B, b) L4.5; (C, c) L8.5; (D, d) L-8.5-4.5; (E, e) L12; (F, f) L12-4.5. Main structures present in kraft lignin control: (I) β-O-4 ether linkage; (II) resinol; (III) syringyl units; and (IV) guaiacyl units.

Acidic pH (pH 4.5) had a small influence in lignin structure since similar spectra was observed between the control and L4.5. However, slight decrease of the correlation of ether bond after the mild acid treatment could indicate hydrolysis of aryl ether bond. Cle avage of aryl ether lignin bond increased with severity and lead to an increase of phenolic hydroxyl group (Moxley et al. 2012; Pouteau et al. 2005). On the other hand, alkaline environment caused significant changes in lignin structure. A decrease in correlation intensity of methoxyl group (δ_C/δ_H 55.7/3.77 ppm) was observed in all alkali treated lignin. The C-H correlations of C_α-H_α and C_β-H_β of β-o-4 linkages disappeared and a low response of C_γ-H_γ in L8.5, L12 and L12-4.5 indicated the cleavage of β-O-4 linkages and resulted in higher phenolic hydroxyl group (Kuo and Hse 1991). Some β-O-4 linkages could be reformed after pH-shifting process in alkali treatment (L8.5-4.5). However, reformation of β-O-4 linkages was not observed in the pH-shifting process from extremely high pH environment (L12-4.5). Similar scenario was also found in β-β linkage in resinol (Fig. 2.1II). The signal assigned to S unit was invisible in treated lignin samples. The C-H correlations of p-hydroxyphenol also disappeared in alkali and alkali-shifting treatments. Compared with untreated

lignin, alkali treated lignin samples have less signal intensity of C_5-H_5 and only faint response of C_2-H_2, and C_6-H_6 positions. These refers to replacement of H atom in C_2, C_6 and C_5 of G unit.

The changes in lignin structure after modification processes obtained from NMR were confirmed by the morphological images. The unmodified lignin was scanned at 400x magnification as seen in Fig.2.2a. The particles did not aggregate and were large compared to those under modified conditions and displayed both rough and smooth surface characters. Even though, no significant changes were found from the NMR spectrum (Fig.2.2B and b) compared to the control AL (Fig.2.2A and a), L4.5 was depolymerized and became smaller after acid treatment. These minute particles formed interactions and attached to each other as shown in Fig. 2.2b, indicating significant smaller particle size and change in electrostatic charge. On the other hand, alkaline treatments provided sharp-edge cut lignin as shown in Fig. 2.2c. a higher ratio of sharp-edged cut lignin was observed at extremely high pH (see Fig.2.2e) compared to L8.5 (see Fig.2.2e). Since acid hydrolysis broke down lignin into small particles, whereas base hydrolysis provided sharp-edged cut lignin, the pH- shifting process provided the mixture of both acid and based lignin characteristics. In addition, small linkages between 2 clamping particles were observed (see Fig. 2.2d and the red arrows) which implied additional lignin-lignin interactions and/or repolymerization occurred due to the pH-shifting processes. This evidences emphasize the repolymerization after pH-shifting process as mentioned in NMR analysis.

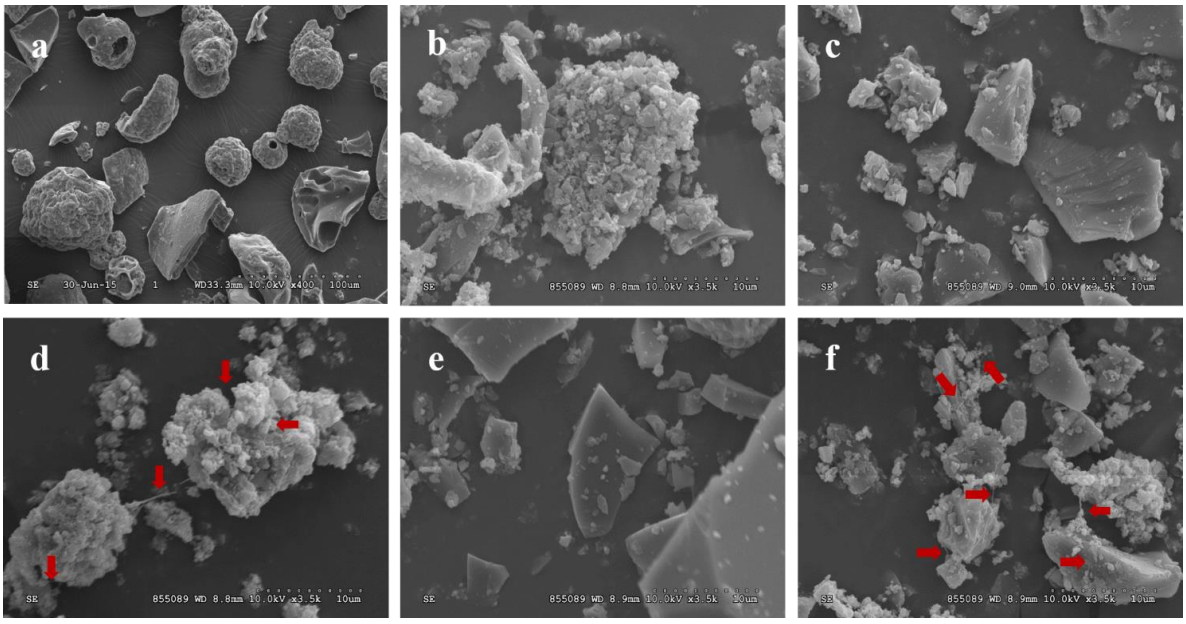

Figure 2.2 Scanning electron microscope images of lignin: (a) alkaline lignin at 400x magnifications, (b) L4.5, (c) L8.5, (d) L8.5-4.5, (e) L12, and (f) 12-4.5 at 1500x magnifications.

Lignin is stable at high temperature due to its condensed aromatic and highly branch structures. According to Fig.2.3, thermal degradation process of lignin occurs in a broad range since lignin contains various aromatic side chains and branches attached to different positions on the aromatic units. The weight loss at the beginning (25-200 °C) is mainly from evaporation of moisture (Cao et al. 2013). After that, pyrolysis occurs and contributes to major weight loss. The first degradation stage is dehydration of hydroxyl groups (150-275 °C) and breakage of ether bond (150-300 °C). Then aromatic rings start to loose aliphatic side chains. Higher temperature (370-400 °C) breaks C-C linkage. After that, backbone degradation, at the temperature between 500-700 °C results in gaseous products (Laurichesse and Avérous 2014). The degradation temperature range is affected by fragmentation of inter-unit linkage and highly related to the content of C-C bonds (Ibrahim et al. 2011; Kim et al. 2013). Therefore, lignin with higher degradation temperature contains a higher portion of high molecular weight compounds (Wen et al. 2013).

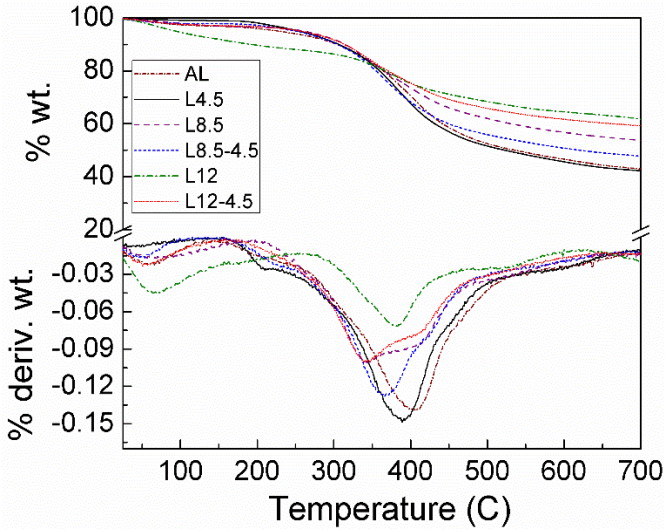

Figure 2.3 Derivative thermogravimetric curves of lignin at different pH and pH-shifting processes.

The thermal stability of unmodified lignin was slightly higher due to its high G content as mentioned in the NMR section (Wang et al. 2009b). Acid, base and pH-shifting process depolymerized lignin and provided lower molecular weight compounds as Tg of all modified lignins were in the range of 338.48-389.15 °C, whereas unmodified lignin Tg was 404.19 °C. Regarding Fig. 2.3, different derivative weight curve patterns implied different subunits were produced in different treatments. Acid modification caused lower Tg but did not significantly change the thermal profile of unmodified lignin. On the other hand, the shoulder around 410-430 °C showed up at L8.5 and both pH-shifting treatments, suggesting repolymerization of lignin. L12 presented distinctive thermoresistance profile as the first peak indicating water evaporation and dehydration of hydroxyl group was bigger than other lignins. L12 also showed a unique weight loss profile (see table 2.1). More than a quarter of total weight loss came from dehydration of hydroxyl groups and evaporation, whereas only 3-8 % of those was released in other modified

lignins. This indicates that extremely high pH treatment increased the amount of hydroxyl group and water binding capacity of lignin. Moreover, only approximately 55% weight was lost between 200-500 °C, whereas 74-81% were lost in other lignins. Suggesting that some part of lignin skeleton had already broken under extremely basic environment and some small compounds were released, for the smell of some odor compounds were observed during the sample preparation. As a result, a relatively smaller backbone degradation peak was observed and approximate 60% ash were recovered after the test. All lignins emitted approximately the same ratio of gaseous products after 500 °C. L12 showed the highest thermoresistance properties with ~60% residual after 700 °C. Modified lignins which exploded with high pH were likely more thermostable than L4.5 (acid treatment) or untreated lignin.

Table 2.1 Glass transition temperature (Tg) and weight loss (%) of lignin at different pH and pH-shifting processes

Lignin	T_g(°C)	Weight loss/Total weight loss (%)			Total loss (%)	Weight remain (%)
		25-200 (°C)	200-500 (°C)	500-700 (°C)		
AL	404.19	7.05	76.13	16.81	57.15	42.85
L4.5	389.15	3.3	80.51	16.19	57.81	42.19
L8.5	338.48	7.52	74.33	18.15	46.58	53.42
L8.5-4.5	365.05	5.32	79.1	15.58	52.36	47.64
L12	379.71	26.49	54.72	18.78	39.13	60.87
L12-4.5	338.96	8.01	75.53	16.47	41.02	58.98

2.4.2 Lignin-SP and SP Morphology

According to Fig. 2.4a, the average single agglomeration of pure SP was 60-70 nm. Larger agglomeration also formed with the size less than 500 nm. Lignin cross-linked protein network and resulted in a huge clamp (see Fig. 2.4b). Lignin connected protein network and resulted in a lignin-protein copolymer that was larger than 500 nm. The quantitative analysis of particle size

was shown in Table 2.2 Lignin particle became smaller and more uniform after treated with different pHs. In severe alkali environment (pH 12), the particle was undetectable as all samples were completely soluble. Exposing protein to alkaline conditions before aggregation resulted in the bigger cluster. The biggest cluster (131.559±32.526 μm) was observed after exposing protein to denaturing pH. That means the denatured protein can refold to looser structure which is different from the folding structure of the non-denaturing protein.

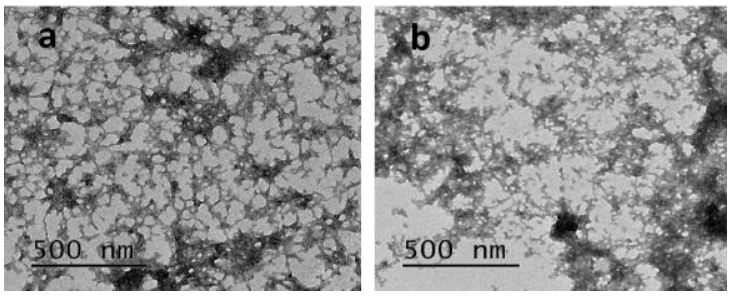

Figure 2.4 TEM images of (a) SP8.5 and (b) LSP8.5 at 11000x magnifications.

Comparing the particle size between protein and lignin-protein samples. The particle size of LSP8.5 was larger and broader than SP8.5 and L8.5. The bigger complex may be caused by covalent bonds and cross-links between lignin and protein. Since the average particle size of LSP8.5 was bigger than the single-pair binding of L8.5-L8.5, L8.5-SP8.5 or SP8.5-SP8.5, multiple-interactions and the lignin-protein network could have been formed. It implies multiple active sides of lignin and protein. This discovery supports the model that proposed in the previous study (Pradyawong et al. 2017). However, lignin-protein cluster at the isoelectric point of LSP4.5, LSP8.5-4.5, and LSP12-4.5 were smaller than that of SP4.5, SP8.5-4.5 and SP12-4.5, respectively. Since active sites of protein have already bonded to lignin, less number of the active sites are available to form interactions with protein when the pH was brought to the pI. Moreover, the presence of lignin in the system disturbed the formation of protein network. As a result, the cluster of LSP was smaller than that of SP samples in all conditions.

Table 2.2 Average particle size distribution of lignin, SP, and LSP at different pH and pH-shifting processes

pH	Particle Size (um)		
	Lignin	SP	LSP
4.5	5.91 ± 4.57	24.97 ± 17.78	10.10 ± 6.73
7	8.42 ± 16.06	-	-
8.5	4.80 ± 3.82	7.55 ± 1.91	32.65 ± 42.89
8.5-4.5	2.79 ± 1.16	29.52 ± 18.67	17.83 ± 11.41
12	-	-	-
12-4.5	7.14 ± 3.79	131.56 ± 92.53	40.19 ± 113.02

Dried film morphology was shown in Fig. 2.5 at higher pH, SP films became yellower. LSP film also turned darker brown due to the brown color of lignin. All pH 4.5 and pH-shifting films were flat and stick to the slide. At pH 8.5 film partially lifted from the slide and form a corrugated film with air inside. Small bubbles were spread along the film in both SP and LSP samples. In contrast, the big bubble was found in the middle of the SP12 film with big crack around (see Fig. 2.5d) which implied more cohesion at high pH. Light reflection was obviously seen in both SP12 and LSP12 dried film.

Film texture was observed by the optical microscope. More cracks were found in SP samples more than LSP samples. Small broken and complete bubble were found in SP8.5, whereas air was trapped and formed bigger unbroken bubbles in the LSP8.5 film (see Fig.2.5 B and G). This indicated stronger cohesion force in LSP than SP films. The film strength of LSP was obviously observed in pH 12 as some small fragments sprite out from the main film at the edge of the bubble in SP film, whereas it did not occur in LSP film (see Fig.2.5 D and I). Therefore, lignin strengthened and improved the cohesiveness of SP film.

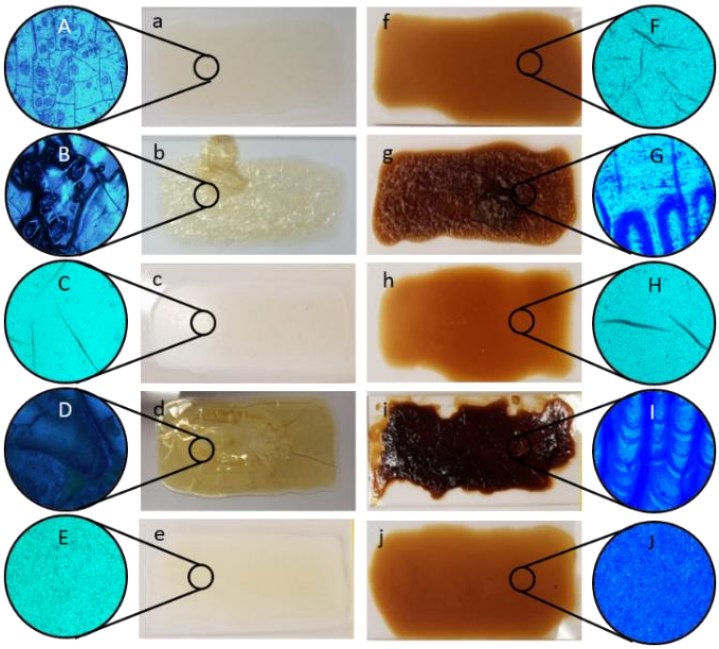

Figure 2.5 Dried film morphology of: (a) SP4.5, (b) SP8.5, (c) SP8.5-4.5, (d) SP12 (e) SP12-4.5 (f) LSP4.5, (g) LSP8.5, (h) LSP8.5-4.5, (i) LSP12, and (j) LSP12-4.5, and optical microscope images of dried film at 5x magnifications of: (A) SP4.5, (B) of SP8.5, (C) SP8.5-4.5, (D) SP12 (E) SP12-4.5 (F) LSP4.5, (G) LSP8.5, (H) LSP8.5-4.5, (I) LSP12, and (J) LSP12-4.5.

Film morphology under water strongly reflects water resistance of samples. Chemical and conformational changes strongly influence each other and cause significant changes in protein properties. The appearance of SP and LSP 4.5 was similar (see Fig. 2.6a and f). The difference was shown at alkaline conditions. At pH 8.5, a lot of small SP8.5 film pellets detached at the edge of the film, whereas the LSP8.5 film was intact and no free pellet was observed (see Fig. 2.6b and g). More remarkable improvement and interactions of lignin-blended samples were detected at extreme alkali pH since conformation change found at pH above 11 (Ishino and Okamoto 1975). As protein denatured and unfolded, polar and non-polar groups in protein were exposed and became more available to interact with lignin (Hettiarachchy et al. 1995). The SP12 film floated completely and dissolved (see Fig. 2.6d). In contrast, the floated LSP12 film was thick and partially dissolved in water. The film absorbed water and formed a strong jelly-liked pellet texture. The

improvement in morphology after soaking in water is a rigid evidence in concluding that lignin improves protein water resistance possibly by crosslinking and other lignin-protein interactions. According to Fig. 2.6c and h, mild pH-shifting process (8.5-4.5) did not change the film appearance of SP and LSP samples. However, extreme alkali-shifting process (12-4.5) affected protein solubility and led to exposures of hydrophobic groups and cleavages of native S-S bonds (Jiang et al. 2010). With the interference of lignin on protein aggregation as mention in section 3.1, the LSP12-4.5 film showed many fractures but SP12-4.5 film stayed intact (see Fig. 2.6e and i). Thereby, the water resistance of SP and SPL films were not only strongly influenced by protein structure but the strength of lignin-protein interactions were also impacted as a consequence of pH and pH shifting processes.

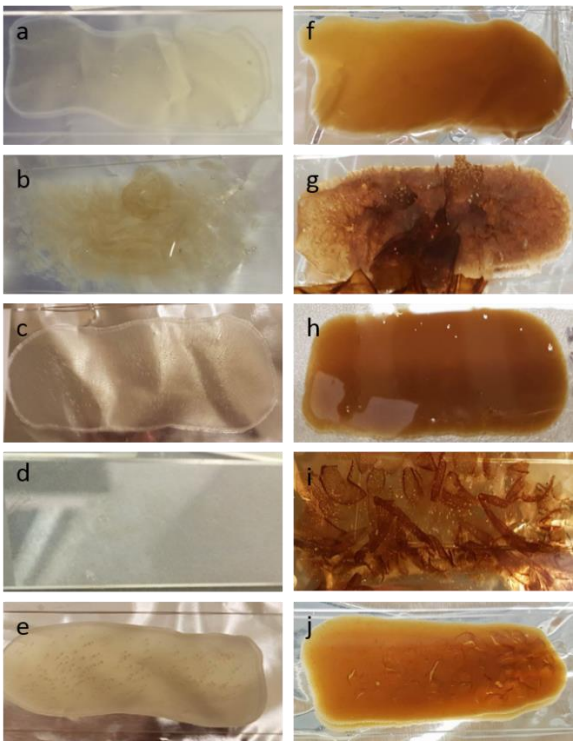

Figure 2.6 Submerge film morphology of: (a) SP4.5, (b) SP8.5, (c) SP8.5-4.5, (d) SP12 (e) SP12-4.5 (f) LSP4.5, (g) LSP8.5, (h) LSP8.5-4.5, (i) LSP12, and (j) LSP12-4.5.

2.4.3 Lignin-protein interactions

The binding interaction of soy protein with lignin was studied with the help of isothermal titration calorimetry (ITC). The exothermic peaks observed during the titration (Fig. 2.7) suggested some binding must be taking place. However, attempts to get reproducible 'N' values were unsuccessful which led us to propose that the binding must be of non-specific type. The interpretation of binding phenomenon was further complicated by the lack of specific molecular weight data for the lignin and soy protein. Hence, for current observation, the molecular weight was estimated as the sum total of molecular weights of all the subunits.

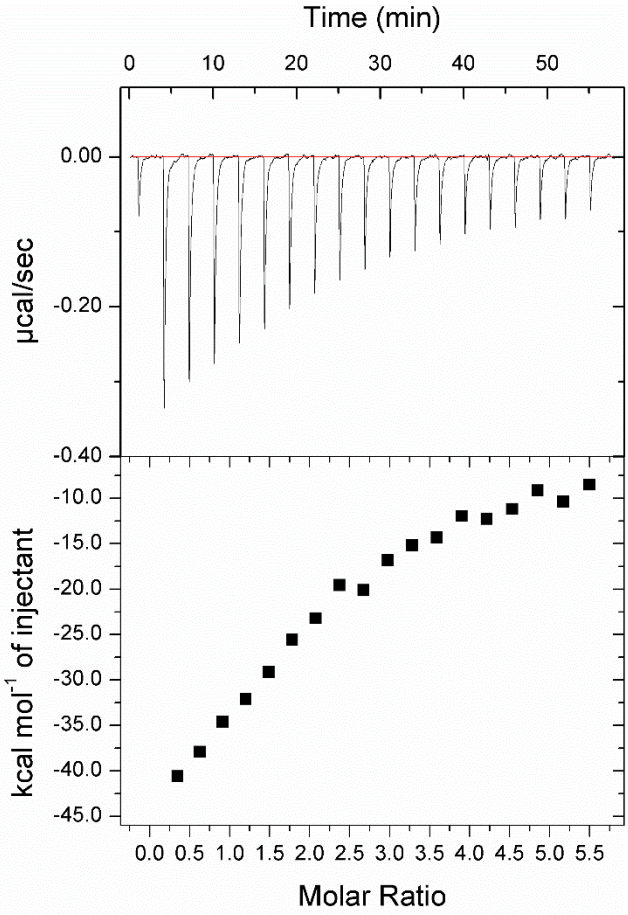

Figure 2.7 ITC of Soy protein with lignin The syringe contained 84 µM lignin and the cell contained 3 µM soy protein. The 1st peak is a mock injection. Raw data showing heat pulses obtained by multiple injections (upper panel); Integrated heat of binding as a function of molar ratio of ligand:macromolecule (lower panel). The graph shown is after subtraction of negative control where lignin was injected to the buffer.

The obvious differences between SP and LSP samples likewise mentioned in section 2.4.1 and 2.4.2 were found at pH 8.5. No band was detected in the lignin sample or the negative control (Fig. 2.8a, lane 1). Lane 2a represented pure SP sample. The distribution pattern of α0, α, and β subunits from 7S around 75 and 50 kD was pretty similar to Qi, et. al. study in 2011. Acid and basic polypeptides of 11S also appeared at lower molecular weights. Similar protein subunits distribution pattern also presented in LSP sample (Fig. 2.8a, lane 1) indicating that some polypeptides did not interact with lignin. According to Fig.8a, there was no bands on negative control lignin sample, (lane 1a). A significant band was clearly detected on LSP8.5 (lane 3a) around 250 kD and >250kD but not in SP8.5 (lane 2a), suggesting lignin-protein complex. As discussed previously in section 3.1, the networks that were formed by broad range particle size of lignin and protein leading to the extensive band (range from ~30 to >250 kD). High molecular weight fractions of cross-coupling products, coniferyl alcohol (a lignin major subunit)-amino acid, was also reported (Cong et al. 2013). The lignin-protein complex fractions also appeared at room temperature. The same protein subunits distribution pattern also showed in SP and all LSP samples. There was also no bands on lignin samples (Fig. 2.8b lane 1). The lignin-protein complex band also found in the same size range in Fig. 2.8a and the band intensity elevated from Fig. 2.8b lane 3 to 7 as the lignin concentration increased from 10 to 50%, indicating more lignin protein complex were formed with more lignin in the system.

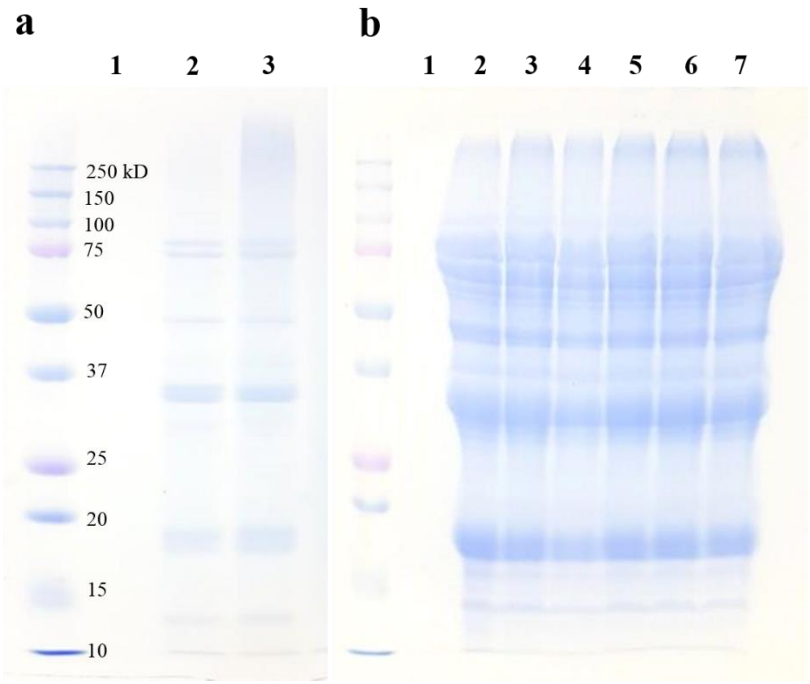

Figure 2.8 SDS-PAGE pattern of reducing lignin, SP and LSP at 150 °C samples: L8.5 (lane 1b); SP8.5 (lane 2b); LSP8.5 (lane 3B), and fresh samples: L8.5 (lane 1a); SP8.5 (lane 2a); SP+L8.5 (10%) (lane 3a); SP+L8.5 (20%) (lane 4a); SP+L8.5 (30%) (lane 5a); SP+L8.5 (40%) (lane 6a); SP+L8.5 (50%) (lane 7a).

The elemental composition analysis reflects the overall composition of samples. Table 2.3 shows the percentage of oxygen to carbon ratio (O/C) of lignin, protein, and lignin-protein samples. The O/C of lignin was 35.21% at pH 4.5. Then, the O/C of L12 and L12-4.5 increased to 84.51 and 75.28 %, respectively. An additional oxygen atom into the structure mainly resulted from cleavage of β-O-4 which created more active groups such as hydroxyl, and carboxyl groups. More active groups were generated after the treatments, especially in extreme alkali environments. These data confirmed the 2D-HSQC NMR results in section 2.2.1 that there are more reactions and changes occurred in extremer alkali treatments.

The O/C of protein were consistent in SP4.5, 8.5 and 8.5-4.5. The higher O/C was found at denaturing pH (pH 12). Hydrolysis of the peptide bond (-CO-NH-) on the polypeptide chain

resulted in –COOH and -NH_2 groups. An additional oxygen in –COOH group could mainly contribute to significantly higher O/C in SP12 and SP12-4.5. The changes in LSP samples also followed the trends of lignin and SP samples.

The O/C of lignin+SP was calculated regarding to the blending ratio of lignin and SP on an assumption that there were no chemical and bonding interactions between lignin and protein that could change the compositions in the molecule. The differences between the actual value from LSP samples and the calculated lignin+SP number that reports in the last column in Table 2.3 indicates changes in the oxygen content after reactions. The negative sign indicated an interaction between lignin and SP since LSP samples have less oxygen than the calculated lignin+SP values. Loss of oxygen could imply covalent crosslinks interactions between lignin and protein samples. Since lignin and protein have active groups such as amino, hydroxyl, carbonyl and carboxyl groups, the reactions that involved in oxygen could highly possible to be condensation and esterification.

Table 2.3 Percentage of oxygen to carbon ratio (O/C) of lignin, protein and lignin-protein samples

	O/C*				
pH	Lignin	SP	Lignin+SP**	LSP	**Difference (%)*** **
4.5	35.21±0.12	47.22±0.04	45.21±0.06	45.42±0.20	**0.45±0.33**
8.5	38.54±1.50	48.21±2.17	46.60±2.06	44.96±0.54	**-3.46±3.10**
8.5-4.5	41.11±0.08	48.98±0.36	47.66±0.28	45.84±0.47	**-3.84±0.41**
12	84.51±0.86	58.68±0.07	62.99±0.20	59.09±1.17	**-6.19±2.16**
12-4.5	75.28±0.21	62.94±2.34	65.00±1.99	57.73±.044	**-11.16±2.04**

* O/C = $\frac{O(\%)/16}{C(\%)/12} x\ 100$

** Lignin+SP = (([%O/C_{lignin} x 0.2] + [%O/C_{SP} x 0.2])/1.2)x100

*** **Difference** = (%O/C_{LSP} - %O/$C_{Lignin+SP}$) /%O/C_{LSP})x100

At the most extreme condition of pH 12-4.5, lignin, soy protein, and lignin-soy protein gave the clearest IR spectrums. IR spectrum of lignin shows aromatic skeleton vibrations at 1595, 1510 and 1422 cm^{-1}. The shoulder at 1701 cm^{-1} corresponds to the C=O stretching in conjugated carbonyl compounds with the aromatic rings. The absorption at 1457 is attributed to C-H bending and vibrations of aromatic groups. The absorption peak at 1213 and 1029 corresponds to C-O and bending vibrations of aromatic plane of G subunit, respectively (Ibrahim et al. 2006).

Amide I, II and III, protein major absorption bands were observed at 1640, 1520, and 1233, respectively. Amide I contains major stretching vibrations of the amide group (80%) and C-N bond. Amide II peak arises from N-H bending (60%) and C-N stretching (40%) vibrations. Amide III peak describes mainly C-N stretching vibrations and N-H in-plane bending vibrations.

According to Fig 2.4.3.3, compared to SP sample, LSP sample showed differences in all 3 amide peaks. Firstly, the amide I absorption peak of LSP was slightly weaker than that of SP. This indicates the stronger H-bond nearby C=O group. The stronger H-bond reduces electron density around C=O area and results in lower absorption intensity. In this extreme pH environment, extended peptide chains after unfolding are aligned closer to neighbouring chains which contributes to very strong intermolecular hydrogen bonds. Secondly, slight shift in peak position and changes in amide II peak shape and absorption, could be from the influence of lignin adsorption band or changes in the chemical environment. Frequency shift is caused by true frequency shift or relative intensities of component band variations (Stuart 2004). Thirdly, amide III peak of LSP became broader and the peak slightly shifted from 1233 to 1230 cm^{-1} with shoulder appearing at 1273 cm^{-1}. It is possibly caused by lignin absorption peak at the same position at the shoulder, 1273 cm^{-1}. However, it is difficult to interpret the amide III absorption band as it could be influenced by C=O in-plane bending, C-C stretching and CH_2 wagging vibrations. The

frequency and absorption bands of the amide I and II could be influenced by the strength of hydrogen bonds involving amide C=O and N-H groups. The stronger H-bond indicates stronger secondary structure in LSP samples. The absorption band at 1392 cm^{-1} is assigned to stretching and vibration of COO^- group (Luo et al. 2016a; Luo et al. 2016b). Considering that both samples with the same size absorption peak at 1447 cm^{-1}, the LSP sample showed relatively low 1392 cm^{-1} peak compared to that of SP sample indicating the highly possible interaction between lignin and COO^- group of protein. In addition, different absorption patterns between SP and LSP sample were observed between 1200 and 1000 cm^{-1}. As the spectrum in the 1300-1000 cm^{-1} region is related to the C-O stretching of alcohol, phenol, carboxylic group, the changes in LSP sample might be caused by the influence of lignin absorption, interactions of C-O, changes in the chemical environment, or the combination of those.

Fig. 2.9b is the difference spectrum where, the spectrum of SP is subtracted from that of LSP and compared with the spectrum of lignin. An additional peaks at 1728 and 1642 cm^{-1} represented stretching vibration of unconjugated and conjugated carbonyl groups (C=O), respectively (Ibrahim et al. 2006; Lisperguer et al. 2013; Poletto and Zattera 2013; Singh and Ekhe 2014). Considering Fig.2.9c, amide I peak shifted to higher frequency together with increase in peak intensity. These changes in both subtracted LSPs spectra indicated strong molecular interactions were formed between lignin and mostly the C=O group of protein. A conjugated carbonyl group represented inter- and intramolecular hydrogen bonds that generally occur between O-H and N-H atom, for example, $-COO^-$ and -OH groups of protein and lignin (Simon et al. 2003). An ester bond was possibly formed by alcoholysis and ammonolysis of -COOH in acid condition. Ester, ether and the bonds between C/N, C/S, S/S were observed (Cong et al. 2013; Fraenkel-Conrat and Olcott 1945; Ozdal et al. 2013). The bonds formed between amino acid side chains

such as the bond between lysine and aromatic ring, and disulfide bonds between lignin and protein (Le Bourvellec and Renard 2012). Moreover, the change in aromatic skeleton vibration was also observed. Firstly, the 1595 cm^{-1} peak indicated a mixed signal of aromatic skeleton vibration and C=O stretching. The reference lignin peak response was from aromatic skeleton vibration, whereas the subtracted LSP peak response was from both aromatic skeleton vibration and C=O stretching. The peak intensity of subtracted LSP was less than the referenced lignin indicating lower response came from aromatic skeleton vibration. Secondly, the spectrum at 1510 cm^{-1} corresponding directly to the aromatic skeleton vibration obviously disappeared after subtraction. Thirdly, the amide II absorption band shifted from 1520 to higher wavenumber 1540 cm^{-1} and the relative intensity of amide II increased compared to the amide I in the subtracted spectrum (Fig. 2.9c). The changes in those 3 areas indicated a new C-N bond formation between protein and lignin (Liu 2017). An interaction of amino group attached directly to C_2 and C_5 of phenolic compound through quinine intermediate (Ozdal et al. 2013) limits molecular movement and vibration of the aromatic ring.

On the other hand, compared to the reference lignin spectrum, some slightly shifted and stronger signals of C-O-C (1366), C-O of G subunit (1273), C-C and C-O (1213), C-H in plane deformation (1143), C-O deformation of secondary alcohol and aliphatic ethers (1092) and C-O of guaiacyl group and blending vibrations inside of aromatic plane of guaiacyl ring (1029) was detected from subtracted LSP spectrum. Stronger intensity in the range of 1000-1400 cm^{-1} indicated the formation of lignin-protein linkages. The new absorption peak at 1481, 900, and 836 $cm^{-1}$of the subtracted spectrum was obviously observed. The new peaks highly possibly indicated special covalent crosslinking between lignin and protein. However, further investigation is needed for more specific detail information. The changes in peak intensity in this range is likely affected

by non-specific interactions. These strong cross-links are supported by many kinds of electrostatic interactions. Hydrogen bonds (H-bonds) were claimed to be the dominant electrostatic interactions between protein and phenolic compounds in aqueous solutions (Hagerman and Butler 1981). Hydrophobic interactions and electrostatic forces were also observed between hydrophobic regions of soy protein and close by rings of lignin. In addition, when lignin and protein molecules are close to each other, attraction and repulsion between positive and negative regions takes place and lead to ion-dipole and ion-induced-dipole, and dipole-dipole interactions (Salas et al. 2012). However, the mechanism has not yet been clearly elucidated.

Nevertheless, it is ambiguous to predict or quantify lignin-protein interactions and networks since the formation of bonds and forces highly depends on the nature of lignin and protein, and environmental factors. Lignin has different structures, functional groups and molecular weights depending on plant species and extraction methods. In additions, various kinds of plant protein also have diverse amino acid sequences, subunit profiles and folding structures. Hence, the nature and structure of lignin and protein significantly determine the nature of interactions (Hagerman et al. 1998). Organic solvents and pH are simple environmental factors that not only sufficiently impact protein but also lignin. Changing pH or solvent strongly affects their solubility, folding degree, denaturing stage and exposure of functional groups, hydrophobic/hydrophilic properties and depolymerized degree. Therefore, reaction type and rate of lignin-protein highly affected by environmental conditions (Hagerman et al. 1998; Simon et al. 2003; Zhang et al. 2002).

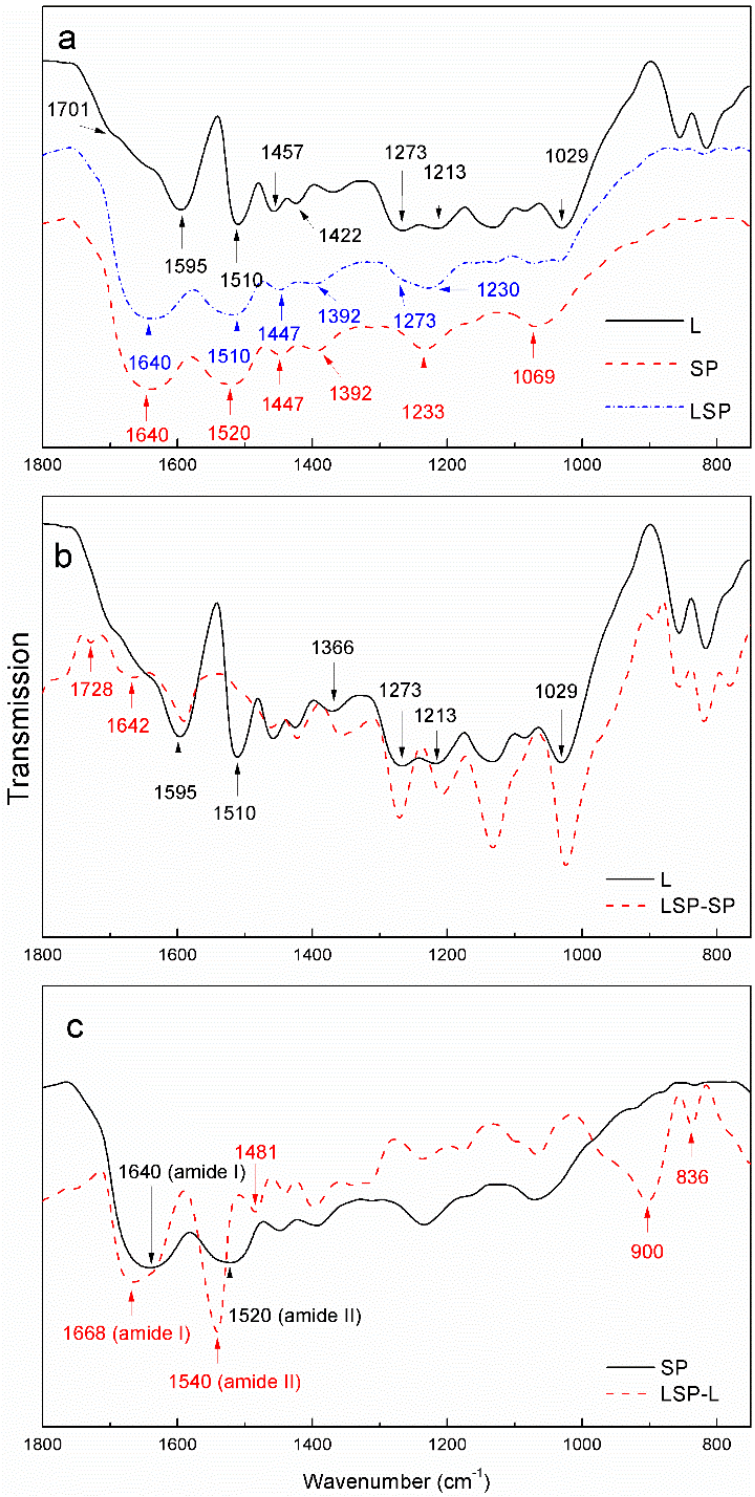

Figure 2.9 FTIR spectra of lignin, SP and LSP (a), lignin and subtracted LSP (b), and SP and subtracted LSP (c).

2.5 Conclusion

Lignin showed a great potential to be utilized to improve properties of resin in sustainable protein-based green products. Lignin depolymerized in alkaline environments and partially repolymerized via the shifting to a lower pH. Varieties in forms and properties of lignin derivatives could be obtained from simple pH and pH-shifting modifications in mild environments. Lignin was capable of cross-linking and forming non-specific interactions with protein, resulting in higher molecular weight compounds that were stable through chemical and heat treatments. The interactions primary occurred by oxygen and nitrogen-related functional groups such as –COO- and –OH, and $-NH_3^+$ associated with non-specific interactions. Lignin greatly improved protein properties and water resistance of protein upon alkaline treatments indicated by the interactions between smaller lignin derivatives and unfolded/denatured protein structure.

The use of lignin in bio-based applications is still a very challenge because the diversity of lignin structure and functional groups highly depend on delignification processes and plant species. The structure is complicated, consisting of varieties subunits and internal linkages which make it difficult to study the complete structure and obtain uniform derivatives. Moreover, lignin-protein interactions, network strength, film morphology and other properties are strongly influenced by modification methods and environmental conditions. Further study is required for deeper clarification of lignin-protein interactions, in order to effectively utilize lignin as bio-based products for high-value-added applications.

Chapter 3 - Adhesion Properties of Soy Protein Adhesives Enhanced by Biomass Lignin

This chapter has been published as a peer-reviewed research paper in the Journal of Renewable Energy. 2017. 114: 351-356.

3.1 Abstract

Soy protein adhesives have a great potential as a sustainable eco-friendly adhesives. However, low adhesion under wet condition hinders its applications. The objective of this research was to enhance water resistance of soy protein adhesive through protein and lignin interaction and protein. The focus of this research was to study the effect of protein to lignin ratio and lignin particle size (large (35.66 μm), medium (19.13 μm), and small (10.26 μm)) on the adhesion performance of soy protein adhesives as well as characterize its rheological and thermal properties. Results showed that the lignin particle size and the protein to lignin ratio greatly affected the adhesion performance of soy protein adhesive. The addition of lignin slightly increased the viscosity, spreadability, and thermostability of soy protein adhesives. The wet strength of soy protein adhesives increased as lignin particle size decreased. Soy protein mixed with small size lignin) at protein to lignin ratio of 10:2 (w/w) at 12% concentration presented the lowest contact angle and the highest wet adhesion strength of 4.66 MPa, which is 53.3% higher than that of 10% pure soy protein adhesive. The improvements of adhesion performance and physicochemical properties of soy protein adhesives by lignin were ascribed to the interactions between protein and lignin. Lignin with smaller particle size increased the wet shear strength of soy protein adhesives due to larger surface area of lignin was available to interact with protein.

3.2 Introduction

Approximately 8 million pounds of formaldehyde-based adhesives are supplied to the wood-based products industry annually (Wool and Sun 2005). Since formaldehyde-based adhesives provide durable adhesion performance, it is widely applied in pressed wood products, such as particle board, plywood and fiber board. However, Formaldehyde causes negative effects on the environment and human health because it induces high carcinogenic and chronic toxic risks (Sofuoglu et al. 2011). United States Environment Protection Agency (EPA) proposed a regulation for formaldehyde emission standards for composite wood products (EPA 2013a). In addition, petroleum demand is increasing while petroleum shortage issue has been a topic of concern. Therefore, there are strong demands for safe, environmentally friendly, and sustainable wood adhesives.

Soybean seed, a potential eco-friendly adhesive source, contains approximately 40% protein and is largely available at a reasonable price (Frihart et al. 2013; Maestri et al. 1998). Recently, most of studies have been focusing on soy protein-based adhesives (Frihart 2010). Soy protein-based adhesive has been considered as the alternative for urea formaldehyde-based adhesives due to its excellent adhesion performance on wood and other materials (Frihart et al. 2010). Nevertheless, the water resistance of soy protein-based adhesive is not compliable with formaldehyde-based resin for exterior applications (Qi et al. 2013a).

Lignin, the most abundant aromatic polymer is largely available as industrial residues from pulping and biofuel production (Pye 2008). Lignin is traditionally known as a low value by-product and is usually burned to generate energy (Pye 2008; Stewart 2008). Lignin provides basic aromatic subunits that can be utilized as building blocks for many monomers and polymers, which are currently obtained by synthetic chemistry from petroleum-based products (Duval and Lawoko

2014; Gosselink et al. 2004). Since only few percentages of lignin from pulping liquors are utilized for specialty applications, such as epoxy resins, and wood panel products (Lora and Glasser 2002; Stewart 2008), there is a high demand for lignin-based value-added research (Duval and Lawoko 2014).

The phenolic group in the lignin is an excellent hydrogen donor that can interact with functional groups of proteins such as carboxyl, hydroxyl, and amino and form covalent and hydrogen bonds with these carboxyl groups. Lignin reacts with protein to form a protein-lignin complex or network by the hydrophobic interactions, and ionic and hydrogen bonds which is similar to the interaction between protein and polyphenol (Le Bourvellec and Renard 2012) (Fig. 3.1). The mechanism of this interaction is still not yet fully elucidated (Ozdal et al. 2013). However, a cross-couple interaction, as a result of nucleophilic attack of amino acids polar side chains (Nu), was found between coniferyl alcohol, a major lignin subunit, and amino acids (Cong et al. 2013). Lignin and soy protein interaction studies were reported. The adsorption of both glycinin (11S) and β-conglycinin (7S), soybean protein subunits, on the lignin surface occurred by non-specific interactions, hydrophobic and electrostatic force, and hydrogen bonding (Salas et al. 2012). The sorghum lignin and lignin-based resin improved the wet strength of soy protein adhesive attributed to the increased wettability of adhesive to wood surface and cross-linking between lignin-based resin and reactive group on soy protein (Luo et al. 2015b; Salas et al. 2012; Xiao et al. 2013). By cross-linking with protein, lignin enhanced the tensile strength, thermal stability, young modulus and a decrease water absorption of soy protein (Doherty et al. 2011).

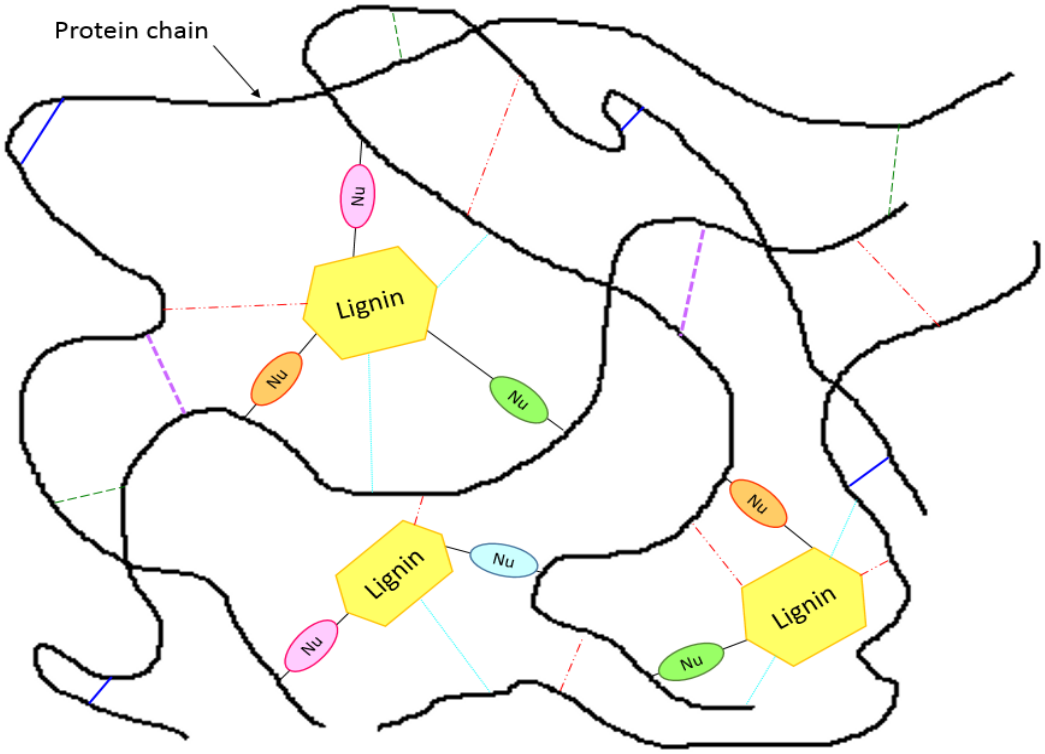

Figure 3.1 A model of lignin-protein network.

Lignin is more hydrophobic, whereas protein is more hydrophilic. Therefore, bio-based adhesives, derived from lignin and soy proteins, could improve the water resistance as well as reduce the cost as lignin is inexpensive and inexhaustible. Among all lignins, kraft lignin contains the highest level of aliphatic hydroxyl group, and more easier to be modified. Hence, kraft lignin was consider as an excellent substrate for producing lignin derivatives, especially for wood adhesive (Doherty et al. 2011; El Mansouri and Salvadó 2006). Therefore, the objective of this research was to study the effects of kraft lignin on adhesion performance of soy protein and rheological and thermal properties.

3.3 Materials and methods

3.3.1 Materials

Kraft Lignin (no. 370959) was purchased from Sigma-Aldrich, Inc. (St. Louis, MO). Defatted soy flour with the dispersion index of 90 was obtained from Cargill (Cedar Rapids, IA). Hydrochloric acid and sodium hydroxide were acquired from Fisher Scientific (Fair Lawn, NJ). Cherry wood veneers were supplied from Veneer One (Oceanside, NY)

3.3.2 Preparation of Kraft lignin

The kraft lignin was ground by the planetary ball miller ND 0.4L (Torrey Hills Technologies, LLC, CA) at 500 rpm. The samples were collected and measured the particle size by the laser scattering particle size distribution analyzer, LA-910 (Hiroba Scientific, NJ). Three particle sizes of 35.66±21.42, 19.13±22.90, and 10.26±9.98 μm called as large size (L), medium size (M), and small size (S) were used for this study. The particle size distribution of these 3 samples is showed in Fig. 3.2. All samples were kept at room temperature for future experiment.

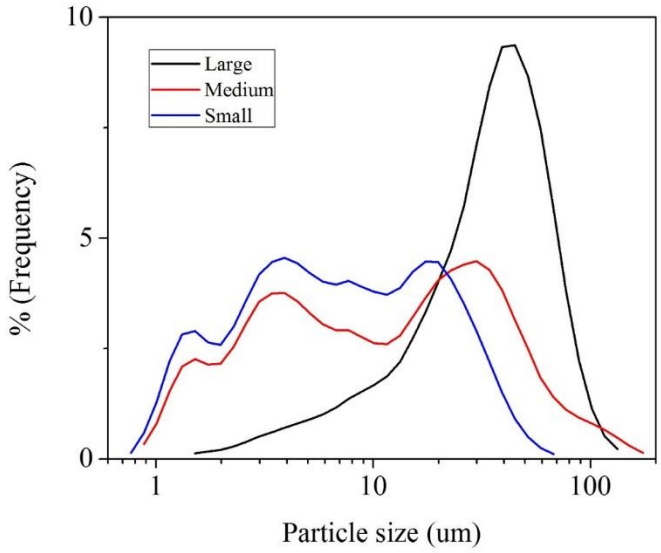

Figure 3 Particle size distribution of large size lignin, medium size lignin, and small size lignin.

3.3.3 Soy Protein Isolation

Soy flour was mixed with distilled water at the ratio of 1:15 (w/w), and the pH was adjusted with NaOH (10 N) to 8.5. Soy protein was precipitated and extracted at pH 4.2 then neutralized to pH 7.0 with HCl (10 N) (Mo et al. 2004). The soy protein was freeze-dried and ground with a cyclone miller with 1 mm screen (Udy Corp., Fort Collins, Colo.) and was stored at 4 °C for further test.

3.3.4 Preparation of Adhesives

Soy protein and lignin were mixed in distilled water to meet the designed protein to lignin ratios. In the first experiment, soy protein solution at 10% (w/w) was blended with 20% of large, medium and small size lignin (based on w/w of soy protein), respectively. Adhesive with 12% soy protein only was used as control. In the second experiment, soy protein and were mixed at ratio of 12:0, 10:2, 8:4, 6:6 (w/w) at the total solid content of 12%. For the third and the forth experiments, 10% and 12% of soy protein solutions were mixed with 10%, 20%, 30%, 40%, and 50% small size lignin (based on w/w of soy protein), respectively. The pH of all slurries were adjusted to 4.5 by 3 N HCl and then stirred at 300 rpm at room temperature (23 °C) for 2 hours.

3.3.5 Preparation of Plywood Specimen and Shear Strength Testing

Approximately 0.6 ml of adhesives were brushed on the surface of cherry wood veneer panels with dimension of 2 × 12 cm (width × length). The two panels were rested at room temperature for 15 minutes before assembled and hot-pressed (Model 3890; Auto ‘M’, Carver Inc., Wabash, IN) at 170 °C, for 10 min under the pressure of 2 MPa. The assembled panels were conditioned at 23 °C and 50% relative humidity for 7 days. Plywood specimens were cut to 20 mm length. The samples for wet strength test were soaked in water at room temperature (23 °C) for 48 hr. The dry strength samples were conditioned in a control environment for 48 hr according

to the ASTM standard method (ASTM D1183-03). The Instron testing machine (Model 4465; Canton, MA) was used to measure the tensile strength with crosshead speed of 1.6 mm/min. 10 replications for wet tensile strength and 5 replications for dry tensile strength were evaluated, respectively.

3.3.6 Rheological Properties

A Bohlin CVOR 150 rheometer (Malvern Instruments, Southborough, MA, USA) was used to measure apparent viscosity of the adhesive samples. The gap between a plate and a 20 mm-diameter parallel plate head was set to 500 μm. The apparent viscosity was measured at 23°C at the shear rate range of 0.01-1 s^{-1}. Silicone oil was applied to prevent water evaporation.

3.3.7 Contact Angle Measurement

The contact angle was observed by an optical contact angle meter (CAM100, KSV Instruments, Helsinki, Finland) on glass (plain microscope slides, Fisher Scientific, Fair Lawn, NJ). The polar surface energy, which highly related to contact angle, of glass and cherry wood were reported as 38.9 and 35.1-38.1 mJ/m^2, respectively (de Meijer et al. 2000; Hejda et al. 2010). Thus, the spreadability of adhesives on glass could be similar to cherry wood surface. Contact angle of 10 replications for each sample were measured every 1 s for 32 s.

3.3.8 Fourier Transform Infrared Analysis

The samples were dried overnight at 170 °C which is the curing temperature for samples in this study. Then the dry samples were ground to 100 mesh. The Fourier transform infrared (FTIR) data was collected in the region of 400–4000 cm^{-1} with a PerkinElmer Spectrum™ 400 FTIR/FT-NIR spectrophotometer (Shelton, CT, USA). The transmission spectra of 32 scans of each sample were collected at a resolution of 4 cm^{-1} in the reflectance mode.

3.3.9 Thermogravametric Analysis

The thermostability of dried samples were measured by thermogravimetric Analyzer (TGA) (Perkin-Elmer TGA 7, Norwalk, CT. Approximately 5 mg of samples were scanned from 25 °C to 700 °C with a heating rate of 10 °C/min. Nitrogen gas was flushed to provide an inert atmosphere.

3.3.10 Differential Scanning Calorimeter

The thermal properties of lignin-soy protein adhesives were analyzed by a differential scanning calorimeter (DSC) (Q200, TA instrument, Schaumburg, IL, USA). The oven dried adhesives (20 mg) was filled in Tzero aluminum hermetic pan. The samples were set at 25 °C for 1 min, then heated to 120 °C at a heating rate of 10 °C/min. Universal Analysis 2000 software was used to calculate peak temperatures and denaturation enthalpies.

3.3.11 Microstructural Properties

The fracture plane on the wood surface were observed by Stereo Microscope (SMZ1000, Nikon, Japan)

3.3.12 Statistical Analysis

The shear strength and contact angle were analyzed by statistical software (SAS Institute, Inc., Cary, N.C.). The P-value for significantly differences were adjusted for multiple comparison by using Turkey in the level of significant of 0.05.

3.4 Results and Discussion

3.4.1 Viscosity

According to Fig. 3.3, the apparent viscosity of soy protein and soy protein- lignin samples presented a shear thinning behavior as the viscosity decreased as shear rate increased. All the samples showed low viscosity compared to other soy protein based adhesives (Luo et al. 2015b; Wang et al. 2009a) which indicates good flow ability. All lignin blended samples resulted in higher viscosity than the soy protein which was very well in agreement with previous study (Luo et al. 2015b). Soy protein with small particle size lignin showed the highest viscosity than others, ascribed to the increased surface area of small particle size lignin and the more interaction between lignin and soy protein (Fig. 3.3a). The ratio of soy protein and lignin also affected the viscosity of the soy protein adhesive (Fig. 3.3b). In particular, the ratios of soy protein and lignin at 10:2 and 8:4 presented greater viscosity than that of 12:0 and 6:6. This is because at the ratios of 10:2 and 8:4, the soy protein and lignin exhibited the optimum interaction which resulted the slightly increased viscosity, and at ratio of 6:6, excessive lignin interrupted the interaction of soy protein and lignin, leading to decreased viscosity. 10% soy protein blended samples with 20% small size lignin showed the highest shear thinning properties at low shear rate (Fig. 3.3c). The higher viscosity was likely related to the high solid content and lignin particle size for 12% soy protein samples (Fig 3.3d).

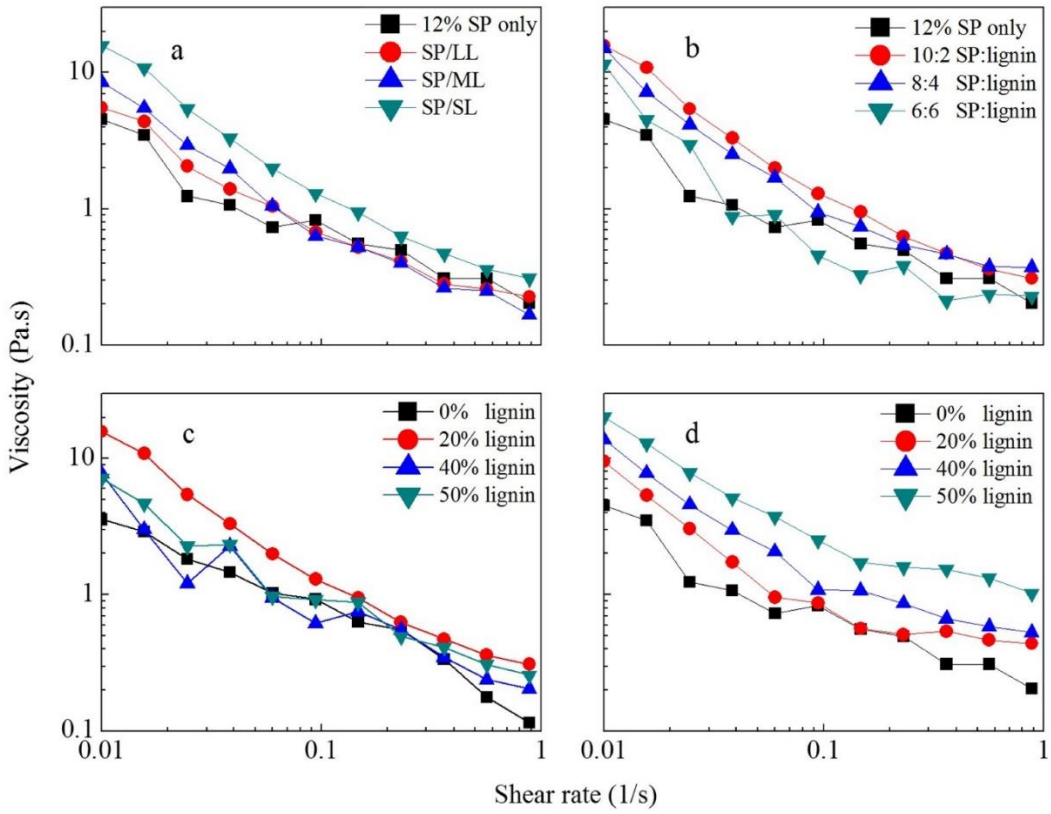

Figure 3.3 Impact of shear rate on apparent viscosities of soy protein samples with different lignin particle size (a), different ratios of soy protein and small size lignin (b), different ratios of soy protein and small size lignin at 10% soy protein (c), and different ratios of soy protein and small particle lignin at 12% soy protein (d). SP: soy protein; LL: large particle size lignin; ML: medium particle size lignin; SL: small particle size lignin.

3.4.2 Contact Angle

Contact angle indicating the ability of adhesives to wet or spread on solid surface was presented in Fig. 3.4 The lower contact angle implies the low surface tension and better adhesive spreadability. The contact angle of adhesives significantly reduced as lignin particle size decreased (Fig. 3.4a) because there was more surface area available to lignin with smaller particle size for the soy protein-lignin interaction. The ratios of soy protein and small size lignin affected the

contact angle significantly. Soy protein adhesives with small particle size lignin at 10:2 ratio and 12% total solid content exhibited the lowest contact angle of 43.64° compared to 54.44° and 48.43° at ratios of 12:0, and 6:6, respectively (Fig. 3.4b), indicating lignin improved the wettability of soy protein adhesives at the proper ratios of soy protein and lignin as reflected by the decrease of contact angle. However, excessive amount of lignin in higher solid content could significant increase in contact angle (Fig. 3.4d).

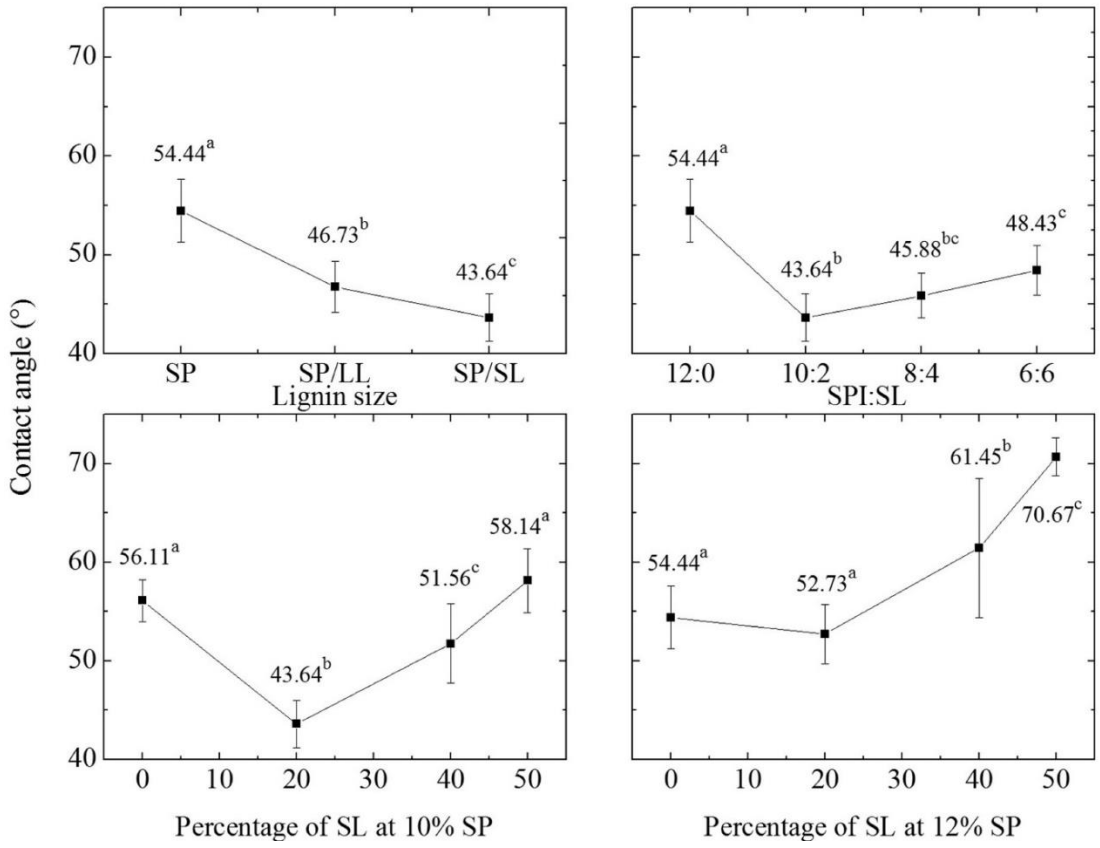

Figure 3.4 Contact angle of soy protein with different lignin particle size (a), Contact angle of soy protein with different lignin particle size (a), different ratios of soy protein and small size lignin (b), different ratios of soy protein and small size lignin at 10% soy protein (c), and different ratios of soy protein and small particle lignin at 12% soy protein (d). Means followed by different letters are significantly different at $P < 0.05$. SP: soy protein; LL: large particle size lignin; SL: small particle size lignin.

3.4.3 Fourier Transform Infrared

The grinding process or the particle size of lignin did not affect the chemical structure of lignin as large particle size and small particle size lignin showed the similar spectra pattern (Fig. 3.5a). The wide adsorption band of aromatic and aliphatic OH group was presented at 3400 cm-1. The peaks at 2973, 2939, 2837 and 1457 cm-1 were related to the C-H vibration of CH_2 and CH_3 (Toledano et al. 2010). The aromatic ring skeleton vibrations and stretching could be identified at 1594, 1509 and 1423 cm-1 (Schorr et al. 2014). The lignin contained the main absorption bands of guaiacyl (G) at 1268, 1129, 858, and 813 cm-1 and the non-esterified phenolic OH group at 1366 cm-1 which also found in elsewhere (Tejado et al. 2007).

The board peak at 3281 cm-1 referred to N-H stretching and sharp absorption peak at 2957, 2929 and 2873 (Fig. 3.5b) are assigned to antisymmetric and symmetric C-H stretching of protein (Chen et al. 2006b). The absorption bands of protein signature, amide group, were presented at 1642, 1515 and 1231 cm-1 which attributed to C=O stretching (amide I), N-H bending (amide II), and C-N stretching and N-H vibration (amide III), receptively (Luo et al. 2015b). The COO- and –C-NH2 groups showed at 1391 and 1067 cm-1, respectively (Lei et al. 2014).

In Fig 3.5b, the amide I and II peaks shape slightly changed and presented a peak shoulder, and the shoulder was getting more obvious with increasing the S content (Fig 3.5c and d). These might be caused by the interactions between the -NH group in soy protein and lignin or the overlapping between lignin and soy protein peaks. The $-COO^-$ cm^{-1} peak intensity at 1391 gradually decreased with the more lignin added. Hence, the $-COO^-$ of soy protein possibly acted as an active group and interacted with L.

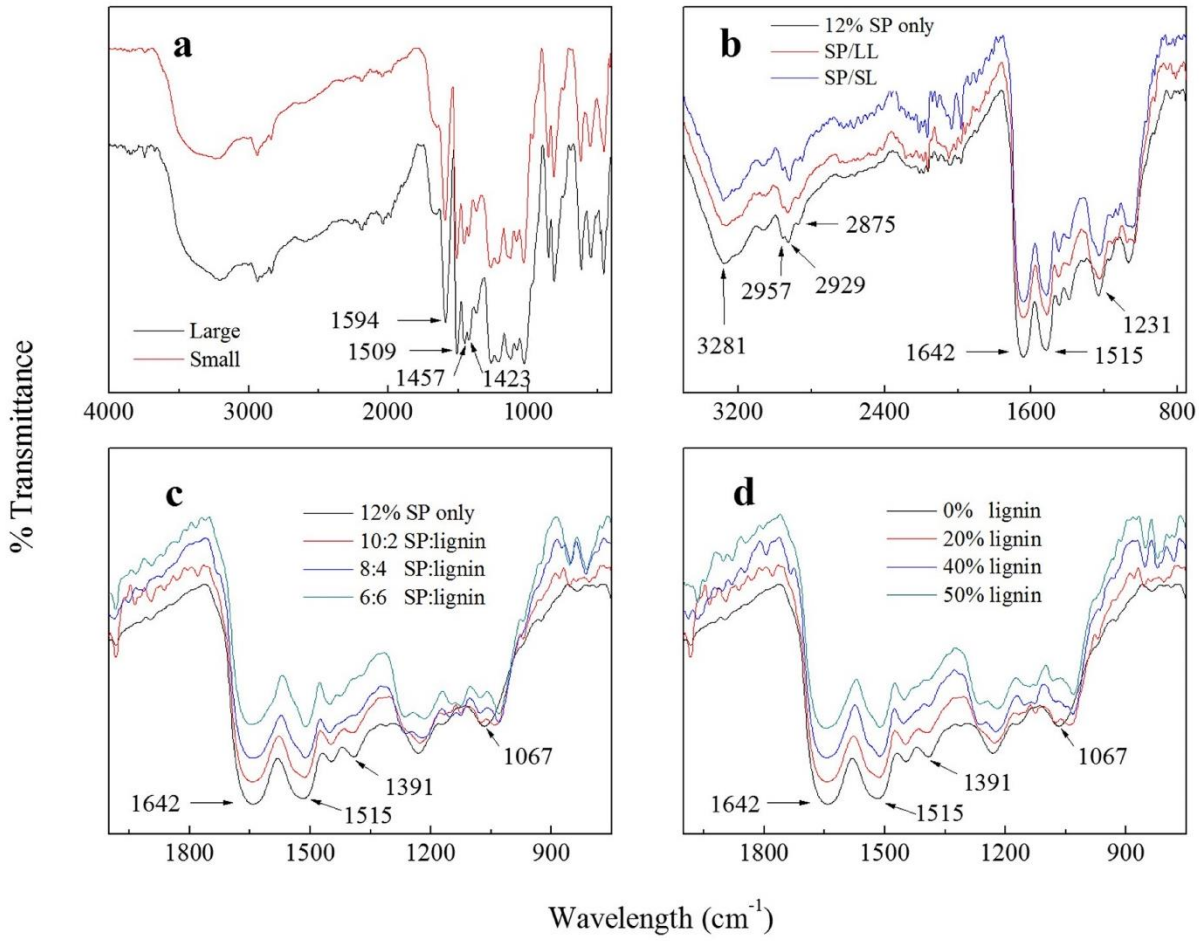

Figure 3.5 FTIR spectra of large size and small size lignin (a), soy protein with different lignin particle size (b), different ratios of soy protein and small size lignin at 12% soy protein (c), and different ratios of soy protein and small particle lignin at 10%FTIR spectra of large size and small size lignin (a), soy protein with different lignin particle size (b), different ratios of soy protein and small size lignin at 12% soy protein (c), and different ratios of soy protein and small particle lignin at 10% soy protein (d). SP: soy protein; LL: large particle size lignin; SL: small particle size lignin.

3.4.4 Thermogravametric Analysis

The slightly weight loss below 200 °C was ascribed to moisture evaporation in the samples (Fig 3.4.4). At 210-280 °C, the initial degradation was related to the breakage of unstable bonds of small molecules fractions (Luo et al. 2015b). Then the mid-degradation of the cross-links and skeleton structure of soy protein and lignin occurred at high temperature (280-360 °C). Finally, the C-O, C-C and C-N bonds and peptide bond of soy protein were destroyed and H_2N, NH_3, CO, and CO2 were released with the further increasing of temperature (Luo et al. 2015b). According to Fig. 3.6, degradation of soy protein started at the temperature above 200 °C and reached to the peak when temperature was in the range of 342-347 °C. The weight loss rate of lignin was slower as particle size increased, indicating lignin with smaller particle size are more capable to thermally stabilize the soy protein adhesives (Fig. 3.6a) as the soy protein adhesives presented approximately 3% less weight loss at 700 °C compared to pure protein adhesive. The peak areas of derivative thermogravimetric analysis were decreased as the soy protein to lignin ratios decreased due to the decrease of protein content in the soy protein adhesives (Fig. 3.6b).

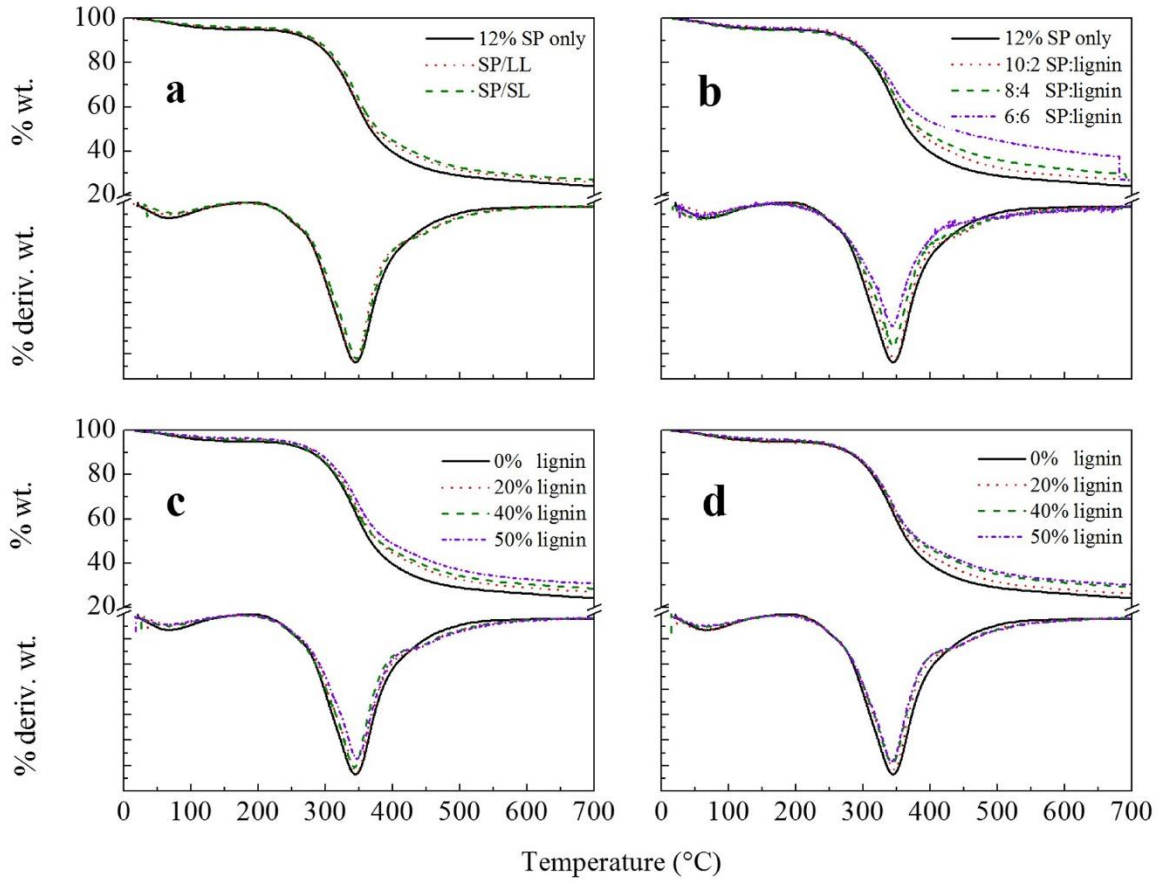

Figure 3.6 Thermogravimetric (TG) and derivative thermogravimetric curves soy protein with different lignin particle size (a), different ratios of soy protein and small size lignin (b), different ratios of soy protein and small size lignin at 10% soy protein (c), and different ratios of soy protein and small particle lignin at 12% soy protein (d). SP: soy protein; LL: large particle size lignin; SL: small particle size lignin

3.4.5 Differential scanning calorimeter

The DSC endothermic thermogram of the samples displayed 2 major peaks at temperatures of approximately 77.70 and 93.05 °C which are assigned to the denaturation behaviors of 7S and 11S protein subunits (Table 3.1) (Wang et al. 2009a). The 11S peak became flatter at addition of small particle size lignin with low ratios of soy protein and lignin, whereas, no endothermic

differences were observed when the large particle size lignin was added to protein adhesives. All samples gave approximately the same 7S T_d, whereas there were slight changes of T_d to 11S especially with small particle size lignin. The addition of lignin requires more energy to denature the structure as Table 3.1 showed that the ΔH_d of 12% soy protein with 50% lignin was 6.87 J/g compared to 4.16 J/g for soy protein only. It is possible that the formation of soy protein-lignin network strengthened the soy protein structure, thus enhanced the denaturation temperature of soy protein-lignin blends.

Table 3.1 Denaturation temperature (Td) and total enthalpy of protein denaturation (ΔHd) of soy protein adhesive with lignin.

Soy protein/lignin ratio at different lignin particle size	7S T_d °C	11S T_d °C	Total Heat Flow/g protein (ΔH_d)
SP	77.70	93.05	4.164
10:2 (SP:LL)[a]	77.86	93.94	4.834
10:2 (SP:SL)[b]	77.52	94.63	5.089
8:4 (SP:SL)	77.65	94.26	4.924
6:6 (SP:SL)	77.96	94.21	4.915
10:2 (SP:SL)	77.52	94.63	5.089
10:5 (SP:SL)	77.22	93.73	5.808
12:2 (SP:SL)	77.64	93.65	6.383
12:5 (SP:SL)	77.52	93.39	6.873

[a] SP: Soy protein; LL: large particle size lignin.

[b] SL: Small particle size lignin.

3.4.6 Shear Strength

Preliminary tests were conducted to find the best pH to improve the wet strength of the adhesive. As a consequence, lignin-protein adhesives at pH 4.5 gave the highest stability under wet condition. Moreover, the highest wet strength was reported at pH 4.6 upon the exposure of the buried hydrophobic group to the protein surface at pH 4.5 (pI), the water resistance is greatly improved (Wang et al. 2009a). Therefore, the experiment was conducted at pH 4.5. Our result showed that the 12% pure soy protein dry strength was 6.4 MPa. The particle size did not affect dry strength at all (fig. 3.7a) whereas, reduction of protein to lignin ratio caused weaker dry strength. The lowest ratio (6:6) showed significantly lower dry strength to 5.0 MPa (fig. 3.7b). An additional lignin to 10% and 12% did not significantly change or reduce dry strength (Fig 3.7c and d). On the other hand, the wet shear strength of soy protein adhesives increased with the decrease of lignin particle size, and the increase of wet shear strength was significant to soy protein adhesives with medium and small particle size lignin compared to pure soy protein adhesive due to larger surface area of medium and small lignin particle size was available to interact with protein (Fig. 3.7a). The wet strength of soy protein to lignin with small particle size ratio of 10:2 adhesive was 4.7 MPa which is about 53.3% greater than that of 10% soy protein adhesive only. The wet strength did not improve with the further decrease of protein to lignin ratio, but reduced the strength to approximately the same as the pure soy protein adhesive (fig. 3.7b). In addition, the wet strength of protein adhesive with 40% and 50% lignin reduce to 4.2 MPa with is about 9% decrease compared to that of soy protein adhesive with 20% lignin (Fig. 3.7c). On the other hand, adding small size lignin to 12% soy protein slightly increased the wet strength. Wood cohesion failure presented in all conditions of dry samples, whereas partial wood failures were found in

most of soy protein adhesives with lignin during wet strength testing, especially significant partial wood failures were also observed in the soy protein to small lignin ratio of 10:2.

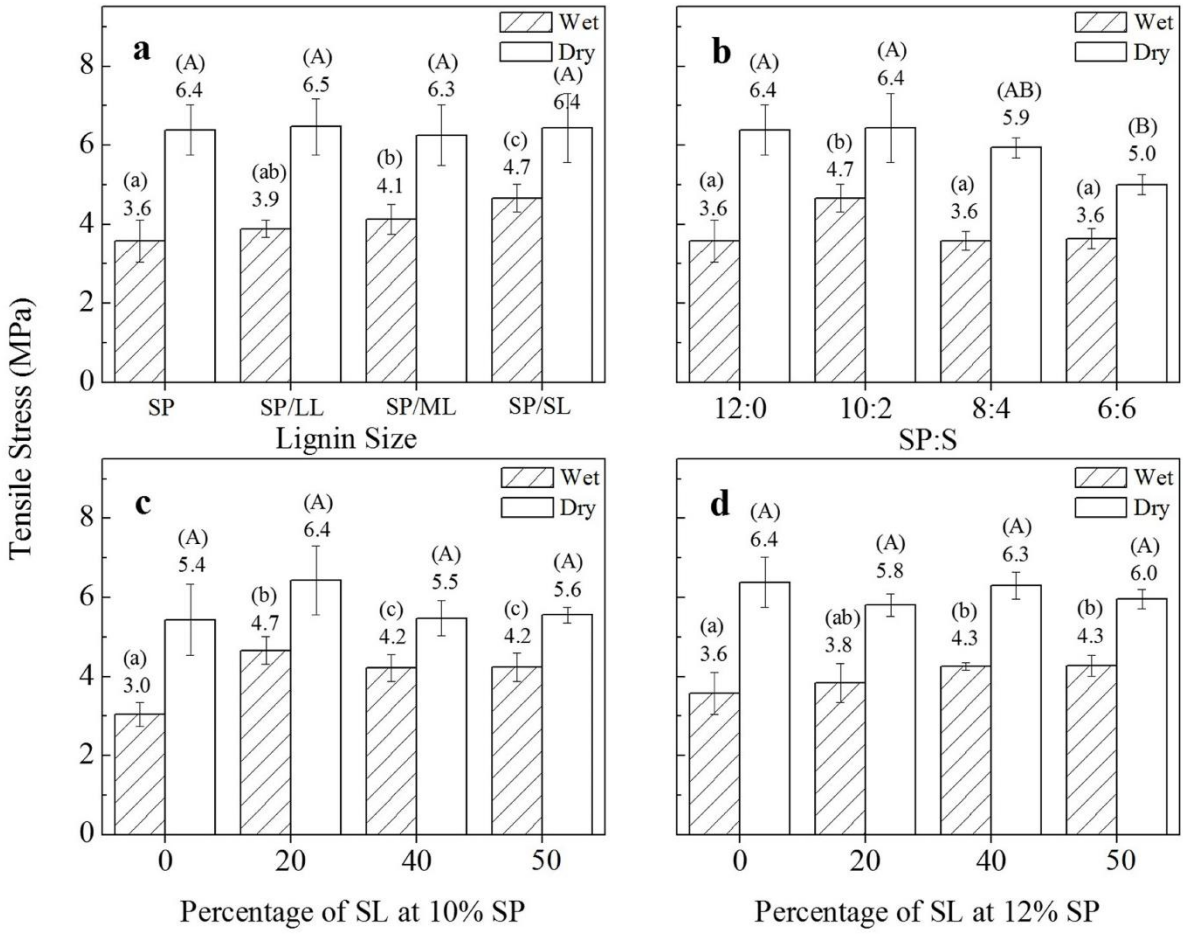

Figure 3.7 Wet and dry shear strength of soy protein with different lignin particle size (a), different ratios of soy protein and small size lignin (b), different ratios of soy protein and small size lignin at 10% soy protein (c), and different ratios of soy protein and small particle lignin at 12% soy protein (d). Means followed by different letters are significantly different at $P < 0.05$. SP: soy protein; LL: large particle size lignin; ML: medium particle size lignin; SL: small particle size lignin.

Adhesion mechanism has been discussed by several theories. Mechanical bonding theory explains how the adhesive wet the wood surface, penetrate into the wood pore and form complex matrix during the curing process. Flow behavior and covalent bonds between protein and cellulose are important factors affecting the adhesion performance (Wool and Sun 2011). In this study, the

10% soy protein mixed with lignin at the ratio of 10:2 showed the highest wet strength because of 4 major reasons. First, as discussed, the lowest contact angle referred to the best spreadability leading to good penetration into wood surface. Second, the entrapment effect of soy protein and lignin also enhanced water resistance properties (Qi and Sun 2011; Xiao et al. 2013). Third, the interactions of active groups between lignin and protein or in lignin itself and the formation of the cross-linked network in soy protein and lignin polymer leaded to a stronger adhesion property (Luo et al. 2015b). Forth, suggested an appropriate lignin concentration at 20% of soy protein caused optimum penetration and left adequate amount of protein active group to form covalent bond with wood surface. Therefore, the adhesive layer still remained intact after the wet adhesion test (Fig. 3.8a). On the other hand, higher amount of lignin (i.e. 50%) disturbed the network, enlarged the contact angle and reduced degree of penetration. The gradually decreased of COO^- peak at 1391 cm^{-1} (Fig. 3.5c, d) referred to more soy protein and lignin interaction and left less active group to adhere with wood surface. Exceeded soy protein and lignin interaction contributed to deteriorated bonding to the wood surface and the breakage of adhesive layer (Fig. 3.8b, c, d) resulting in relatively low adhesion strength.

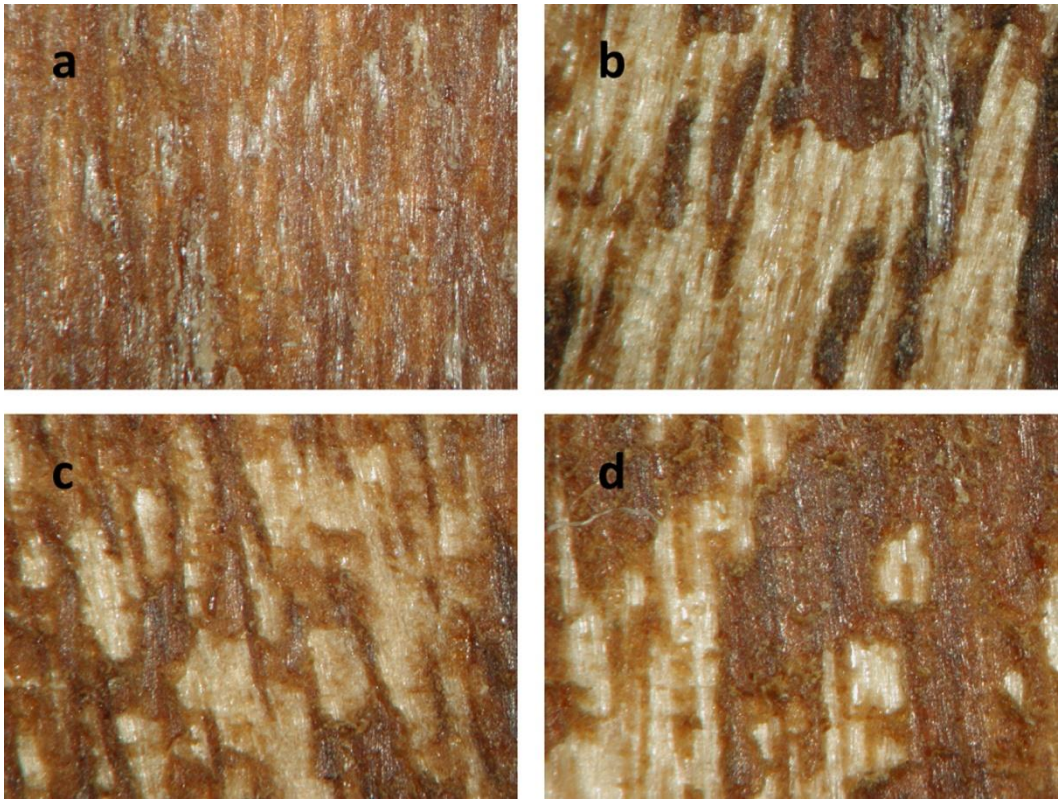

Figure 3.8 Stereomicroscope images of wood surface of cured adhesives after shear strength test with small size lignin at 4x magnifications. (a) at soy protein to lignin ratio of 10:2, (b) at soy protein to lignin ratio of 6:6, (c) at soy protein to lignin ration of 10:5, and (d) at soy protein to lignin ratio of 12:5.

3.5 Conclusion

The addition of lignin improved wet shear strength of soy protein adhesives, and the wet shear strength increased with decreasing the lignin particle size. The optimum soy protein and lignin ratio of 10:2 (w/w) led to 53.3% increase in wet strength compared to 10% soy protein adhesive only. In addition, the addition of lignin increased the spredability and thermal stability of soy protein adhesives. It is believed that lignin has a great potential to improve the water resistance of protein-based adhesives.

Chapter 4 - Effect of pH and pH-shifting on Adhesion Performance and Properties of Lignin-Protein Adhesive

4.1 Abstract

Public concerns about health and environment draw a strong interest in alternative green products research. The focus of this research was to study the effect of lignin and understand the consequence of pH and pH-shifting treatments on adhesion performance of soy protein (SP) adhesives as well as characterized the solubility, glue line patterns, and thermal properties. In this study, lignin and soy protein were depolymerized and modified, respectively at pH 4.5, 8.5 and 12. After the protein was unfolded (pH 8.5) and denatured (pH 12), the protein was refolded by shifting pH to 4.5. Lignin showed a great potential for being used to increase the wet strength of soy protein (SP) adhesive. By interacting and strengthen protein network, lignin improved water resistance and thermal stability of SP adhesives. In an extremely high pH, water resistance of SP increased from 5 to 40% with an additional lignin. SP and lignin-soy protein (LSP) properties and adhesion performance could be adjusted and improved by pH and pH-shifting processes. Different characteristics and properties varied in different treatments. The good wet adhesion performance was obtained at pH 4.5, 8.5-4.5 and 12 with rigid glue line. Shifting pH from 8.5 to 4.5 promoted lignin-protein interaction and provided the best improvement on adhesion performance. Even though an increase in water resistance and lignin-protein network were clearly observed at pH 8.5 but the poor adhesion performance was obtained due to excessive penetration of an adhesive into the wood specimen. Lignin-SP interactions, water resistance property, and glue line pattern were proved to be significant factors contributing to an adhesion performance.

4.2 Introduction

Nowadays, depletion of petroleum fossil feedstock along with significant concern about health and environment lead to an interest in seeking alternative sources for green products. Lignin, non-food biomass, draws a strong interest as a sustainable and environmentally friendly resource. According to lignin structure, lignin has a high potential to replace the large market of petroleum-based chemicals and liquid fuels. Lignin is utilized as a replacement for petroleum-based products such as phenolic resin, epoxy resin, antioxidants and other aromatic-based products (Pye 2008). Even though lignin is the most abundant aromatic polymer in the world and more than 70 million tons of lignin are produced by pulping, paper and ethanol industries annually, only 1–2% are isolated for a wide range of those specialty products (El Mansouri and Salvadó 2006; Mankar et al. 2012; Pye 2008). The majority of lignin is burned as a low-value energy source in factories (Stewart 2008). Hence, there is urgent demand for searching new application on lignin. Nowadays, formaldehyde-based adhesives occupy more than 70% of for wood adhesive market due to its great adhesion performance (Grand View Research Inc. 2017a). However, formaldehyde has been known to be a human carcinogen (Morgan 1997). In addition, formaldehyde price has exponentially increased recently. Therefore, safe, bio-based products like soy protein-based products is an outstanding eco-friendly candidate to replace formaldehyde-based adhesives and petroleum-based chemicals with the comparative price (United Soybean Board 2012). Nevertheless, soy protein-based adhesives have a small market share (Grand View Research Inc. 2017b).

The most important factor that limits its market attraction is poor water resistance. The adhesion strength is low in a wet environment (Mo et al. 2004; Wang et al. 2009a). Recently, few publications and our preliminary studies have found that lignin has a capability to improve the

water resistance of soybean protein adhesives (Luo et al. 2015b; Pradyawong et al. 2017; Xiao et al. 2013). The improvement of this property significantly contributes to more durable wood panel products, especially in high humidity area, since high water resistance glue acts as a barrier to prevent water and moisture penetrate into inner layer wood (Li et al. 2014).

Consequently, soy protein has been modified to obtain better water resistance. Protein modification mainly breaks disulfide linkage and hydrogen bond, unfolds protein structure and exposes hydrophobic groups to the globular surface. pH significantly affects protein conformation, folding degree, and denaturation behavior. Alkali treatment leads to denaturation, the explosion of hydrophobic and -SH groups, and enhance interaction of polar and non-polar groups to materials which drive to a conformation change and more accessible structure (Hettiarachchy et al. 1995; Ishino and Okamoto 1975). On the other hand, acid treatment below the isoelectric point of protein results in partially unfold, charge repulsion, loose side chain interactions, and become flexible but still remains relatively intact conformation. Acid-shifting promoted cross-linking of glycinin, whereas alkali-shifting induced cracking of native S-S bond. pH-modifications and pH-shifting processes led to better properties in food applications (Jiang et al. 2009; Jiang et al. 2010).

Nevertheless, no one has studied the effects of pH-shifting treatments on adhesion performance. Only a few publications focused on the pH-modifications. Therefore, this research desires to study an adhesion performance and properties of protein and lignin-protein adhesives in different protein configuration stages: aggregation (pH=4.5), soluble stage (pH=8.5), and denaturation (pH=12). The effects of the pH-shifting process from soluble or denature stages to isoelectric point, pH 8.5-4.5 and 12-4.5, respectively, also be characterized.

4.3 Materials and Methods

4.3.1 Materials

Defatted soy flour (Cargill, Cedar Rapids, IA) with the dispersion index of 90 was obtained as a protein source. Sodium hydroxide (NaOH) and Hydrochloric acid (HCl) were supplied from Fisher Scientific (Fair Lawn, NJ) and used as received. 370959 ALDRICH alkali lignin (L) was provided from Sigma-Aldrich, Inc. (St. Louis, MO). Cherry wood veneers with dimensions of 12.7 x 50 x 5 mm (length x width x thickness) were purchased from Veneer One (Oceanside, NY)

4.3.2 Preparation of lignin

Ten percent of alkali lignin was dispersed in distilled water (DW) and adjusted pH to 4.5, 8.5 and 12 by 1 N NaOH and HCl. The samples were labeled as L4.5, L8.5, and L12.0, respectively. The pH was kept adjusting and maintained for 24 hr. After that, a part of pH 8.5 and 12 lignin solutions were shifted to 4.5 and kept it constant for 2 hr. They were labeled as L8.5-4.5 and L12.5-4.5. The fresh lignin samples were directly used to prepare adhesives. Some parts of samples were dried at 150 °C for 10 minutes.

4.3.3 Scanning Electron Microscopy (SEM)

The dried lignin samples from section 2.2. were coated with palladium and gold by sputter coater (Desk II Sputter/Etch Unit, Moorestown NJ), and observed under the scanning electron microscope (SEM), Hitachi S-3500N (Hitachi Science System, Ibaraki, Japan). The pictures were collected under an accelerating voltage of 10.0 kV

4.3.4 Soy Protein Isolation

Soy protein (SP) extraction process was conducted at 6.5% solid content in DW. The pH of the slurry was adjusted with NaOH (10N) to 8.5 to solubilize protein. Then the protein precipitation took place at pH 4.2 by HCl (10). Protein part was collected by centrifugation at

12,000 g. The protein chunk was collected and neutralized with NaOH (10N). Protein was then freeze-dried and ground with a cyclone miller with 1 mm screen (Udy Corp., Fort Collins, Colo.) and stored at 4 °(Mo et al. 2004).

4.3.5 Preparation of Adhesives

In the first part (non-pH-shifting adhesives), Ten percent of SP was dissolved in DW and adjusted pH to 4.5, 8.5 and 12.0 by 3 N HCl and NaOH. They were named as SP4.5, SP8.5, and SP12. For lignin-protein mixed adhesive, lignin, L4.5, L8.5, L12.0, that prepared from section 2.2. were added to SP4.5, SP8.5, and SP12, respectively, and named as SPL4.5, SPL-8.5, and SPL12 respectively. All samples were stirred at 300 rpm at room temperature for 2 hours. In the second part (pH-shifting adhesives), the pH of SP and SPL samples at pH 8.5 and 12.0 from the first part were shifted to 4.5 and kept it constant for another 2 hr. The samples are called SP8.5-4.5, SP12-4.5, SPL 8.5-4.5 and SPL12-4.5, respectively. For dried samples, samples were dried at 150 °C for 10 minutes, ground by hand grinder (CoorseTek 60311 Ceramic, Coli-Parmer, IL, USA) and passed through 100 mesh screen.

4.3.6 Transmission Electron Microscopy (TEM)

Fresh adhesives from section 2.5. was diluted to 0.1% with DW. After the slurries were negatively stained with 2% aqua uranyl acetate and examined at 80.0 kV under the transmission electron microscope (TEM), TecnaiTM G2 Spirit BioTWIN (FEI Co., Hillsboro, OR.)

4.3.7 Particle size

The L, SP and SPL fresh samples from section 2.5. particle size was measured by the laser scattering particle size distribution analyzer, LA-910 (Hiroba Scientific, NJ).

4.3.8 Solubility

Ten percent of alkali lignin was prepared with the same process as mentions in section 2.2. After that, the slurries were centrifuged at 13,000 g for 5 minutes. The absorbance of the supernatant was measured with BiomateTM 3 spectrophotometer (Thermo electron corporation, WI, USA), at 280 nm (Dence 1992). The absorbance was measured in duplicate.

4.3.9 Water resistance measurement

Fresh adhesives from section 2.5 were prepared films on premium micro slide plain (Fisherfinest, USA) and oven dried at 150 °C for 10 minutes. Dried film photos were taken by Samsung Galaxy S7 (Korea). Morphology of adhesive films was observed under an optical microscope (Olympus BX51, Olympus Corporation, Tokyo, Japan), with 45° reflection of fluorescent light. The dried films were soaked under DW for 2 hours and dried again at 150 °C for 10 minutes. The weight differences were recorded.

4.3.10 Differential Scanning Calorimeter (DSC)

Twenty mg of fresh adhesives were packed in a Tzero aluminum hermetic pan. The thermal properties of SP and SPL adhesives were measured by a differential scanning calorimeter (DSC) (Q200, TA instrument, Schaumburg, IL, USA). The samples were scanned from 25 °C to 130 °C at a heating rate of 10 °C/min. Peak temperatures and denaturation enthalpies were calculated by Universal Analysis 2000 software.

4.3.11 Thermogravimetric Analysis (TGA)

Thermogravimetric Analyzer (Perkin-Elmer TGA 7, Norwalk, CT) were used to analyzed the thermostability of dried samples from section 2.5. Approximately 5 mg of samples were heated from 25 °C to 700 °C. The heating rate was set as at 10 °C/min. The inert atmosphere in the chamber was control by N_2.

4.3.12 Elemental analysis

All lignin samples were dried and grounded to fine uniform particle size and weighted into tin capsules by PerkinElmer AD-6 Auto-balance (PerkinElmer Inc., Waltham, MA). Approximately 2.0-2.5 mg (accurate to 0.001 mg) were packed with foil. The elemental composition the samples were measured with CHNS/O Elemental Analyzer (ParkinElmer 2400 Series II, PerkinElmer Inc., Waltham, MA). The samples were burned in a pure oxygen environment in the combustion chamber at 975 °C. The combustion gases (CO_2, N_2, SO_2 and H_2O) were separated and detected by quartz column containing copper wires and thermoconductometer detector.

4.3.13 Fourier Transform Infrared Analysis (FTIR)

The dried samples from section 2.5. were scan by PerkinElmer SpectrumTM 400 FTIR/FT-NIR spectrophotometer (Shelton, CT, USA). The Fourier transform infrared (FTIR) data were collected in the range of 500–4000 cm^{-1}. The transmission spectra of 32 scans were collected at a resolution of 4 cm^{-1}.

4.3.14 Preparation of Plywood Specimen and Shear Strength Testing

The glue area 2 × 12 x cm (width × length) on cherry wood veneer panels were cleaned and spread with 0.6 ml of fresh adhesives. After the two panels were rest for 15 minutes, they were assembled and hot-pressed (Model 3890; Auto ‘M’, Carver Inc., Wabash, IN) for 10 min under the pressure of 2 MPa at 150 °C. The glued panels were conditioned in the chamber at 23 °C and 50% relative humidity for 7 days before cutting to 20 mm length. The samples for the dry strength test were still conditioned in the same controlled environment, whereas the samples for the wet strength test were soaked in water for 48 hr. according to the ASTM standard method (ASTM D1183-03). Both wet and dry tensile strength tests were conducted by the Instron testing machine

(Model 4465; Canton, MA) with a crosshead speed of 1.6 mm/min. Five replications for dry tensile strength and 10 replications for wet tensile strength were evaluated, respectively.

4.3.15 Optical microscopy

Cross sections of the plywood specimens were prepared and stained with 0.01% aqueous Safranin-O (Ward's Science, ON, Canada) (Nordqvist et al. 2013). Then glue line was observed under an optical microscope (Olympus BX51, Olympus Corporation, Tokyo, Japan), equipped with a fluorescent filter (MF2).

4.3.16 Statistical analysis

The data were adjusted by using Tukey adjustment and analyzed through analysis of variance by statistical software (SAS Institute, Inc., Cary, N.C.). Pairwise comparisons were performed at a significance level of 0.05.

4.4 Results and Discussion

4.4.1 SEM

The majority (small) particle size region of unmodified lignin was captured at low magnification (see Fig. 4.1a), whereas higher magnification pictures of modified lignins are showed to clearly emphasize their detailed morphologies. Changes in lignin morphology were observed after-pH and pH-shifting processes. Before the modifications, a mixture of big rough and smooth particles was observed and stayed individually. Acid hydrolysis depolymerized lignin to small particles. These small particles had a tendency to clamp together as shown in Fig. 4.1b. On the other hand, sharp-edge cut and small particle mixtures were observed in higher pH treatments (see Fig. 4.1c and e). Since acid hydrolysis broke lignin into a small particle, whereas base hydrolysis likely provided sharp-edged cut lignin, the pH- shifting processed provided the mixture of both acid and basic modification characters. Acid and alkali treatments resulted in lower

molecular weight lignin fractions with a more phenolic hydroxyl group (Kuo and Hse 1991; Moxley et al. 2012). Moreover, acid treatment decreased polarity of lignin and provided more phenolic group (Pouteau et al. 2005) which potentially beneficial to wet adhesion performance. The smaller lignin size also advantaged to adhesion properties as our previous studies have proved that the smaller particle size of lignin showed better adhesion performance and other properties (Pradyawong et al. 2017).

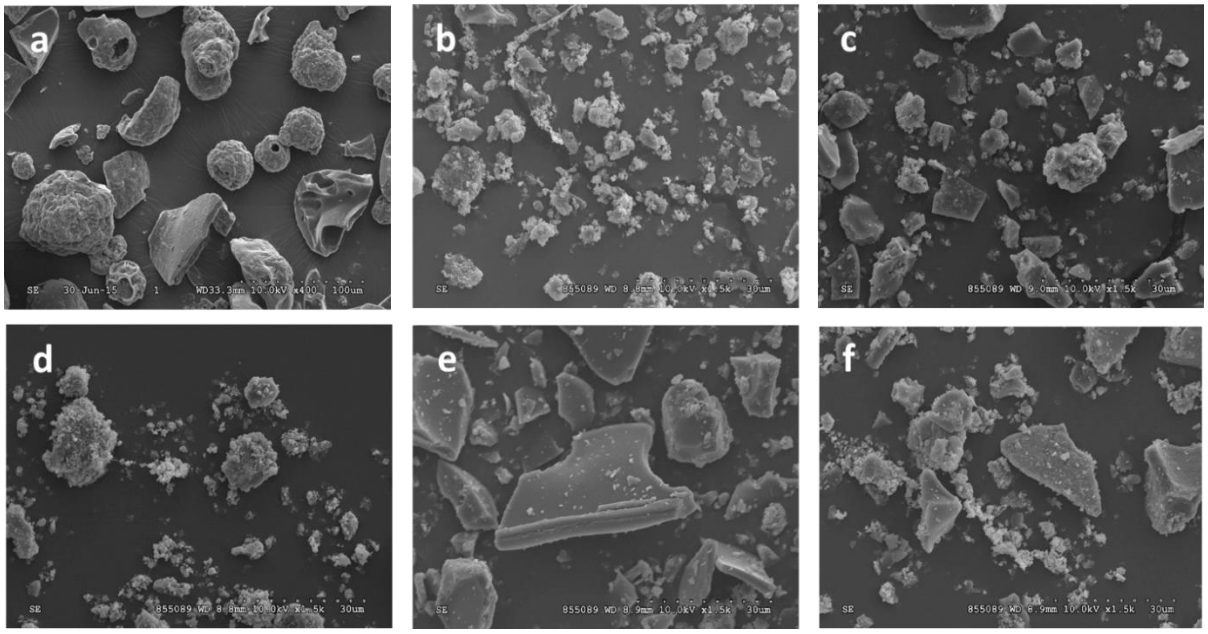

Figure 4.1 Scanning electron microscope images of lignin: (a) AL at 400x magnifications, (b) L4.5, (c) L8.5, (d) L8.5-4.5, (e) L12, and (f) 12-4.5 at 1500x magnifications.

4.4.2 Elemental analyzer

The elemental composition analysis reflexes the overall component of samples. Table 4.1 shows the elemental carbon (C), hydrogen (H), nitrogen (N), sulfur (S), and oxygen (O) contents in the samples. For all lignin samples, the average percentage of N and S was low. They could integrate into the structure during the krafting process. The percentages of carbon and hydrogen decreased, whereas the percentage of oxygen increased with extremer treatments. The ratio of

oxygen to carbon atom *O/C(%) rose with pH treatments. In extreme alkali treatments, L12 and L12-4.5, *O/C(%) are 2-3 folds of the unmodified kraft lignin Moreover, *O/C(%) slightly declined with the pH-shifting process from alkali environments to pH 4.5. There were more changes occurred in extremer alkali treatments and some reactions are reversible after shifting pH to 4.5. The greater number of *O/C(%) indicated an addition of phenolic hydroxyl group and more availability of active groups in lignin structure which are beneficial for further interactions (Kuo and Hse 1991; Moxley et al. 2012).

Table 4.1 Elemental composition of lignin, protein and lignin-protein samples and ratio of oxygen to carbon (O/C*)

Samples	C(%)	H(%)	N(%)	S(%)	O(%)	(%) O/C*
L control	61.50 ± 0.14	8.17 ± 0.28	1.51 ± 0.26	1.50 ± 0.12	27.34 ± 0.52	33.33 ± 0.55
L4.5	61.90 ± 0.19	6.05 ± 0.37	0.86 ± 0.07	2.14 ± 0.11	29.06 ± 0.01	35.21 ± 0.12
L8.5	60.71 ± 0.73	5.91 ± 0.18	0.57 ± 0.01	1.64 ± 0.06	31.19 ± 0.84	38.54 ± 1.50
L8.5-4.5	59.00 ± 0.17	6.32 ± 0.60	0.62 ± 0.01	1.73 ± 0.41	32.34 ± 0.03	41.11 ± 0.08
L12	43.72 ± 0.50	4.70 ± 0.23	0.36 ± 0.01	1.98 ± 0.81	49.26 ± 0.06	84.51 ± 0.86
L12-4.5	46.20 ± 0.02	4.73 ± 0.04	0.97 ± 0.13	1.75 ± 0.08	46.37 ± 0.15	75.28 ± 0.21
SP4.5	46.84 ± 0.04	7.67 ± 0.08	14.02 ± 0.06	1.99 ± 0.06	29.49 ± 0.05	47.22 ± 0.04
SP8.5	46.64 ± 0.33	7.65 ± 0.24	14.18 ± 0.10	1.56 ± 0.47	29.98 ± 1.14	48.21 ± 2.17
SP8.5-4.5	46.01 ± 0.00	8.22 ± 0.49	13.99 ± 0.00	1.74 ± 0.27	30.05 ± 0.22	48.98 ± 0.36
SP12	43.66 ± 0.00	7.38 ± 0.01	12.88 ± 0.04	1.93 ± 0.01	34.16 ± 0.04	58.68 ± 0.07
SP12-4.5	42.55 ± 0.62	7.07 ± 0.11	12.84 ± 0.03	1.84 ± 0.04	35.70 ± 0.81	62.94 ± 2.34
LSP4.5	49.25 ± 0.00	7.16 ± 0.19	11.83 ± 0.04	1.95 ± 0.02	29.83 ± 0.13	45.42 ± 0.20
LSP8.5	49.03 ± 0.18	8.07 ± 0.37	11.73 ± 0.02	1.80 ± 0.28	29.39 ± 0.25	44.96 ± 0.54
LSP8.5-4.5	48.70 ± 0.15	7.99 ± 0.33	11.79 ± 0.04	1.77 ± 0.30	29.76 ± 0.21	45.84 ± 0.47
LSP12	44.97 ± 0.40	7.23 ± 0.00	10.59 ± 0.01	1.79 ± 0.01	35.43 ± 0.39	59.09 ± 1.17
LSP12-4.5	45.24 ± 0.08	7.69 ± 0.19	10.81 ± 0.16	1.45 ± 0.08	34.82 ± 0.20	57.73 ± 0.44

*O/C(%) = $\frac{O(\%)/16}{C(\%)/12}$ x 100

The percentages of carbon and oxygen of protein were likely consistent in mild treatments. In strong basic condition, protein unfolds and denatured polypeptide chain was hydrolyzed as seen in fig.4.2d. Hydrolysis of polypeptide bond (-CO-NH-) resulted in –COOH and -NH_2 groups in reducing and non-reducing end of the polypeptide chains. The additional oxygen leads to a higher *O/C(%) in SP12 and SP12-4.5. The similar scenario also occurred with LSPs.

Changes in the elemental compositions are one of the significant factors that led to changes in physical, chemical, adhesion and other properties which will be discussed in the following sections.

4.4.3 TEM

Single sphere aggregation of protein was observed in SP and LSP 4.5. Protein became looser globular structure with an increasing pH to 8.5. With an additional of L8.5, the globules connected and clamped to be big agglomerations as seen in Fig. 4.2b and g indicating lignin-protein networks. However, no differences between SP and LSP 8.5 were found after shifting pH to 4.5. Protein denatured at extremely high pH. A chain like structure was observed in SP12. The chains like structure became smaller and did not quite group to other chains after blending with lignin. In addition, protein agglomerated after adjusting the environment to acidic pH (see Fig. 4.2e), whereas protein aggregation was observed in LSP12-4.5. These circumstances indicated that L12 interfere the interactions between polypeptide chains after exposed to extremely high pH and disturbed protein aggregation during the pH-shifting process to 4.5. Lignin caused changes in aggregating clamping and agglomerating behavior of protein which could cause differences in properties and adhesion performance.

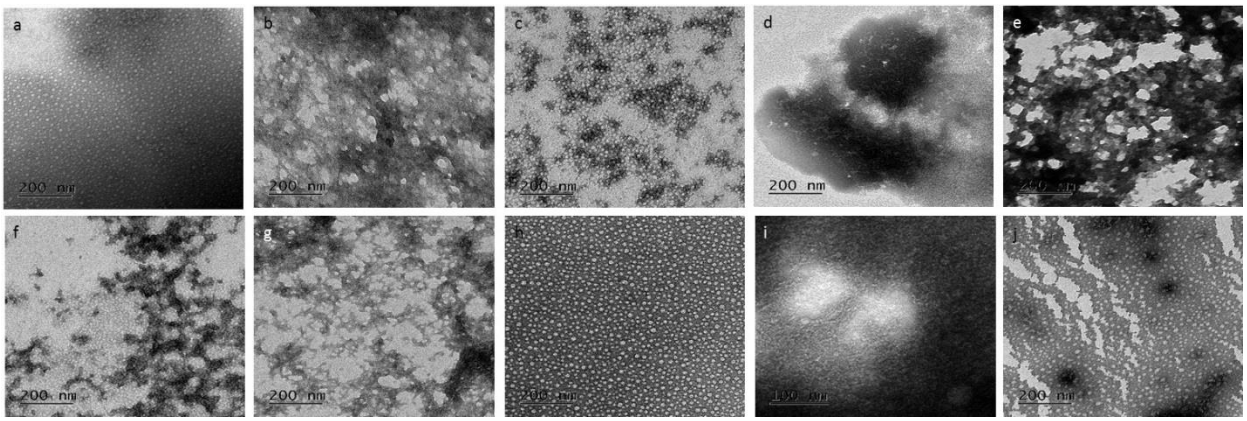

Figure 4.4 TEM images of (a) SP4.5, (b) SP8.5, (c) SP8.5-4.5, (d) SP12, (e) SP12-4.5, (f) LSP4.5, (g) LSP8.5, (h) LSP8.5-4.5, (i) LSP12, and (j) LSP12-4.5 (Except that i was taken at 39000x magnification, the rest of them were taken at 23000x magnification).

4.4.4 Particle size distribution

Particle size analyzer can show an overall particle size distribution of adhesives. According to Figure 4.3a, lignin particle size distributions were measured after it was exposed and stirred in certain pHs for 24 h. Neutral pH environment could not break the big particles around 100 μm that presented in the unmodified lignin (control) at pH 7. Acid, base and pH-shifting treatments could depolymerized lignin and provided smaller particle sizes as the huge particles around 100 μm that presented in unmodified lignin at neutral pH, L7, were all broken. Lower molecular weight lignin fractions also obtained after exposing to basic and acidic environments (Kuo and Hse 1991; Moxley et al. 2012). Single or less clamping particle sizes were smaller than 1 μm, whereas big clamping particles size was close to 30 μm. The broad range distribution likely caused by different clamping degree of particles. At extremely high pH (pH 12), the particle sized was undetectable as L12 was completely soluble. However, the overall particle size became bigger after shifting pH to 4.5, L12-4.5, suggesting that lignin could repolymerize to the different structure as the peak shifted to the right.

According to figure 4.3b, Protein in water showed smallest particle size and narrow of distribution range at soluble pH (SP8.5). The pH-shifting process from 8.5 to 4.5 did not cause much differences in aggregation as the average particle size and distribution pattern of SP8.5-4.5 were not different from SP4.5. In contrast, pH-shifting of denaturing protein after exposing to extremely high pH (SP12-4.5) induced the formation of the 4-5 times to average particle size of SP8.5-4.5 or SP4.5.

According to figure 4.3c, broad range particle size distribution of LSP8.5 sample was observed. The distribution ranged from less than 1 to 300 μm which refer to a non-reacting molecule, and a broad range of cross-couple cluster and lignin-protein network. This information supports the model that proposed in the previous study (Pradyawong et al. 2017). However, the smaller network was formed with an existing of lignin in other 3 conditions at the final pH of 4.5. Lignin interfered protein aggregation as all medians and peak of LSP samples shift to the left.

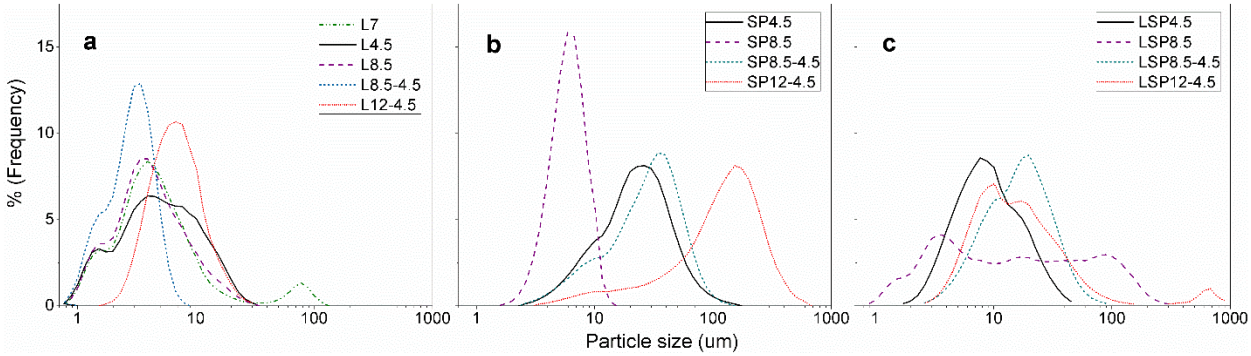

Figure 4.3 Particle size distribution of lignin (a), SP (b), and LSP (c) at different pH and pH-shifting processes.

4.4.5 Solubility

The solubility of lignin, SP and LSP can be compared within the group but cannot be compared with different groups as the solubility of lignin was calculated from the standard curve, whereas the solubility of SP and LSP are relative values.

In an acidic environment, phenolic groups (negative charge) on molecule surface were the protonated and neutralized by H^+. Attractive forces, hydrophobic forces, and van der Waals were favorable (Zhu 2015). Most of the lignin precipitated and coagulated. Therefore, solubility was low (~1.6 g/l) at pH 4.5. Lignin solubility increased significantly with increasing pH. In alkaline condition, repulsive electrostatic forces became dominant and caused dissociation of lignin (Zhu 2015). L12 showed significantly highest solubility (~78 g/l). Shifting pH from alkali conditions to 4.5 greatly reduced lignin solubility. L8.5-4.5 showed significant higher solubility than L12-4.5. Kraft lignin precipitate in acidic pH but soluble in alkali environment (Kunanopparat et al. 2012).

Table 4.2 Solubility of lignin, SP, and LSP at different pH and pH-shifting processes.

pH	Solubility		
	Lignin (g/l)	SP (relative OD)	LSP (relative OD)
4.5	1.59 ± 0.03[a]	0.172 ± 0.000[a]	0.049 ± 0.002[a]
7	11.22 ± 0.10[b]	-	-
8.5	27.41 ± 0.42[c]	0.882 ± 0.010[b]	0.396 ± 0.004[b]
8.5-4.5	12.23 ± 0.73[b]	0.162 ± 0.001[a]	0.047 ± 0.000[a]
12	77.91 ± 3.96[d]	0.899 ± 0.001[b]	0.688 ± 0.018[c]
12.5-4.5	1.37 ± 0.01[a]	0.177 ± 0.004[a]	0.060 ± 0.000[a]

Means followed by different letters are significantly different at $p < 0.05$.

Protein solubility was low at pI (pH4.5). In contrast, SP8.5 and SP12 showed high solubility. The pH-shifting process significantly decreased protein solubility and seen in Table 4.2 The similar result also published in Jiang study (Jiang et al. 2010) The solubility trend of LSP was pretty similar to lignin and SP. The significantly highest solubility was observed on LSP12 which could be strongly influenced by L12 that also show the greatest solubility as mentioned above. The solubility of LSP12-4.5, LSP4.5 and LSP8.5-4.5 were not a significant difference. An interesting result was observed in LSP8.5-4.5. Even it contained L8.5-4.5 with a moderate and SP with low

solubility, respectively, LSP8.5-4.5 showed the significantly lowest solubility within the LSP group. It could possibly imply appropriation interactions between lignin and protein causing by pH-shifting process from 8.5 to 4.5 that significantly decreased the solubility of LSP8.5-4.5.

4.4.6 Water resistance measurement

The change in morphology and weight of adhesives film upon water treatment reflect their water resistance. The weight remaining after 2 hr soaking in water was found to be different under various pH environments because surface hydrophobic properties is a function of pH (Hettiarachchy et al. 1995). Protein aggregated at pI (pH=4.5) and showed the highest weight remaining on the slide (see table 4.3). At higher pH protein became more soluble; hence, less weight was recovered at pH 8.5. Conformation change also found at pH above 11 (Ishino and Okamoto 1975). At extremely high pH, protein denatures and unfolds, (Gennadios et al. 1993). Therefore, SP12 presented the lowest protein weight remaining (5%).

Table 4.3 Weight remaining of adhesives after soaking in water for 2 hrs.

pH	Weight remaining (%)	
	SP	LSP
4.5	95.05 ± 0.29	94.8 ± 0.11
8.5	75.93 ± 4.61	89.4 ± 0.81
8.5-4.5	94.96 ± 0.24	93.72 ± 0.25
12	5.71 ± 0.60	41.09 ± 2.40
12-4.5	86.35 ± 0.09	84.87 ± 0.08

As pure SP has an excellent water resistance at pH 4.5; consequently, no improvement was found at pH 4.5 and both pH-shifting processes after blending lignin. However, as SP had poor water resistance in alkali environment, lignin could increase water resistance of SP at pH 8.5 and 12. Lignin slightly increased water resistance of SP 8.5 by 17.7%. Moreover, the

percentage of weight remaining on the slide greatly increased from approximately 5% (SP12) to 40% (LSP12). Morphology and texture of SP adhesive also obviously changed to be jelly-like appearance. A stronger network could be formed between denatured protein and lignin with a great number of reactive groups. More active groups in lignin and better accessibility to protein structure lead to stronger lignin-protein network and more improvement in water resistance property. Therefore, this improvement confirmed that lignin is an effective natural additive to improve the water resistance of soy protein adhesives, for the networks and bonds could not be destroyed by water and moisture. Specific interactions and cross-linking between protein and lignin were mentioned in several studies (Huang et al. 2003b; Ibrahim et al. 2013; Luo et al. 2015b; Salas et al. 2012; Xiao et al. 2013). In addition, kraft lignin also decreased water sensitivity of wheat protein (Duval et al. 2013; Kunanopparat et al. 2012).

4.4.7 DSC

Thermograms of soy protein generally displayed two endothermic peaks corresponding to denaturation temperature (T_d) of 7S (β-conglycinin) and 11S (glycinin) subunits. As β-conglycinin (7S) is less sensitive than glycinin (11S) to pH and pH-shifting environments (Jiang et al. 2009), the changes in denaturing temperature of 11S were more obvious than that of 7S.

According to Table 4.4, compact SP conformation was strong and difficult to denature as maximum heat flow were used to degrade SP4.5 and SP8.5-4.5. Lignin strengthened and enhanced thermostability of SP. The 7S and 11S peaks temperature of LSP4.5 increased approximately 2 and 3 °C from those of SP4.5, respectively. L4.5 could form interactions with soy protein and strengthen protein network which resulted in an increase of thermoresistance and denaturation energy requirement. In contrast, protein structure became looser with an increase of pH; thus, a lower amount of energy was needed to denature the uncompact protein structure as

seen in SP8.5. Merging of two endothermic peaks at pH 8.5 indicated dissociation of 7S and 11S units. After blending with L8.5, the merged peak T_d of LSP8.5 was almost 6°C higher than that of SP8.5 and double ΔH_d were observed. More interactions were formed between SP8.5 with looser structure and L8.5 with more active groups; therefore, the improvement of thermoresistance after adding lignin was more obvious in higher pH environment. Considering the pH shifting treatment from 8.5 to 4.5, LSP8.5-4.5 showed less change in T_d and no change in ΔH_d comparing to SP8.5-4.5. Even though, pH-shifting process disturbed the tertiary structure of globulin and changed subunits compositions (Jiang et al. 2010), no improvement in thermal property was detected.

Even though high 7S and 11S T_d were observed in SP12, less energy was required to denature the denaturing protein structures comparing to other protein samples. Special interactions could form between L12 and denatured SP12 as LSP12 showed approximately 3 folds ΔH_d of SP12. The extreme alkaline treatment induced cleavage of a disulfide bond and led to the more accessible structure. The interactions formed in LSP12 could be unique since only 1 endothermic at 87.13 °C were detected which could explain jelly-like texture that was observed during the adhesive preparation step. Even if the pH was shifted back to 4.5, SP12-4.5 still showed high T_d but very low ΔH_d. The interactions between lignin and SP that occurred at pH 12 disturbed a majority of protein-protein interactions and aggregation while the pH was shifting down to 4.5. Nevertheless, some lignin-protein interactions endured through the shifting process as LSP12-4.5 still required 3 times ΔH_d of SP12-4.5.

Table 4.4 Denaturation temperature (Td) and total enthalpy of protein denaturation (ΔHd) of SP and LSP at different pH and pH-shifting processes.

Sample	7S T_d °C	11S T_d °C	Merged T_d °C	Total heat flow/g protein (ΔH_d)
SP4.5	77.73	92.87	-	4.43
SP8.5	73.38	85.12	83.22	2.11
SP8.5-4.5	78.27	94.15	-	4.68
SP12	81.38	104.70	-	1.64
SP12-4.5	81.54	107.26	-	0.97
LSP4.5	80.04	95.85	-	5.47
LSP8.5	76.23	90.61	89.98	4.82
LSP8.5-4.5	80.52	96.07	-	4.61
LSP12			87.13	4.34
LSP12-4.5	77.87	92.61	-	2.84

The different tertiary structure of protein and various subunits of lignin were formed at different pH. By shifting pH from 8.5 to 4.5, soy protein showed the highest increase in thermoresistance because the protein was unfolded but not denatured. In contrast, the protein denatured at extremely high pH. Shifting process from pH 12 to 4.5 caused some changes but not gave much positive aspect to thermal property. More change in thermal property and interactions were observed in the more open structure of soy protein. Some interactions and changes could sustain or reform through the shifting process and resulted in different T_d and ΔH_d. More interactions and changes were achieved between unfolding or denature protein and depolymerized lignins, compared to our previous study that used unmodified lignin (Pradyawong et al. 2017). No significant change and less than 2 °C increasing were observed in 7S and 11S T_d. The change in ΔH_d was also less than this study.

4.4.8 TGA

According to Fig. 4.4a, the initial stage weight loss from 25-200 °C causes by a moisture evaporation. The middle stage weight loss from approximately 200-400 °C attributes to crack of covalent bonds between amino acids, cleavage of inter- and intra-molecular hydrogen bonds and electrostatic bonds. The final stage weight loss between 400-670 °C indicates decomposition of protein skeleton and disulfide bonds. Further degradation at a higher temperature results in complete decomposition of protein and releasing of gaseous products (Qi and Sun 2011; Swain et al. 2004). The major weight loss for SP4.5 and pH-shifting processes was in the range of 200-500 °C which majorly contributes to breakage of covalent linkages between amino acids. The solid residual were black and compact. On the other hand, at high pH treatments, SP8.5 and SP12, there were 2 major peaks assigned to middle and final stages. The middle stage T_g of SP12 shifted to lower temperature region but temperature range remained the same with others with few spike peaks. These could represent different configurations and bonds in extremely high pH environment. The weight loss around 500-700 °C obviously represented the decomposition of the protein backbone. The solid residual was black and white puffy ash. High pH causes unfolding and looserprotein structure; thereby, it could be easier for the dry protein chain to uniformly expose to heat and completely be decomposed. Approximately, only 4 and 9% residual left for SP8.5 and SP12, respectively, whereas about 40% weight still remained in SP4.5 after the samples were heated through700°C.

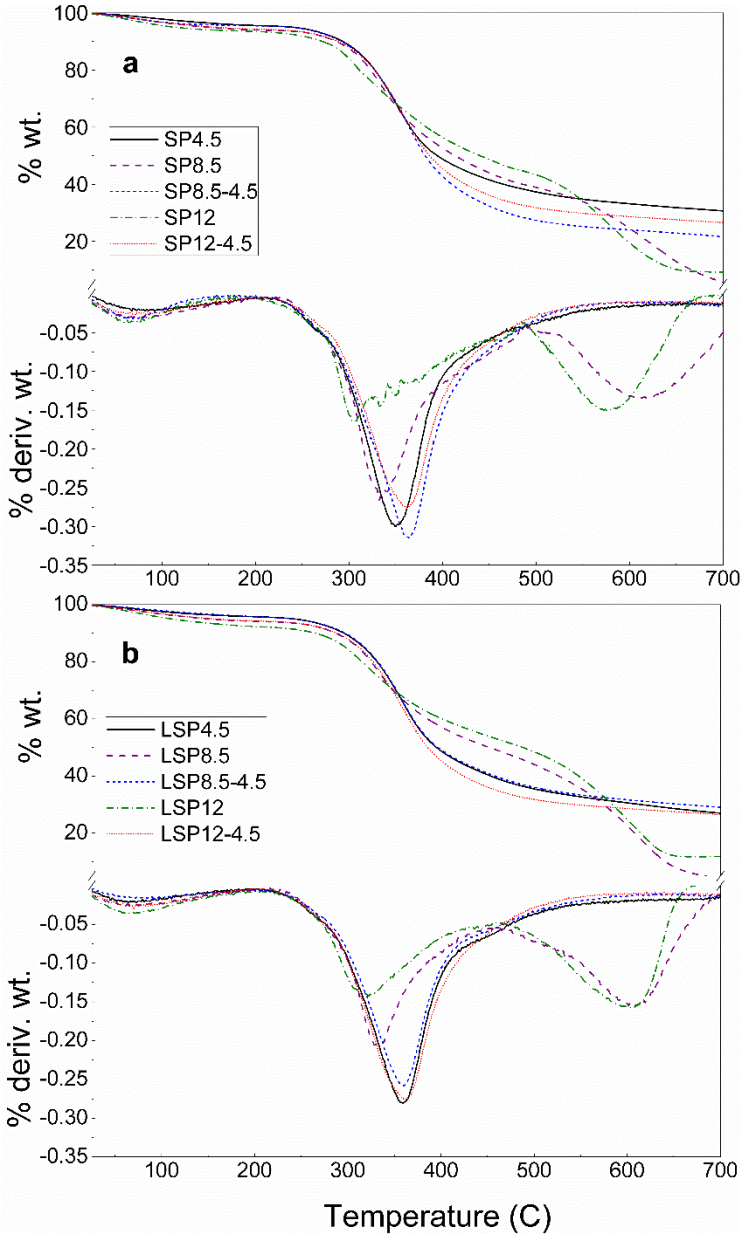

Figure 4.4 Derivative thermogravimetric curves of SP (a), LSP (b), at different pH and pH-shifting processes

Fig. 4.4b shows the same distribution pattern as Fig. 4.4a but most of T_g shifted to higher temperature with an addition of lignin to protein adhesives. The T_g of LSP4.5, 8.5-4.5, and 12-4.5 were close to 360 °C. This similar peak temperature was strongly influenced by the final pH of lignin-protein aggregation at 4.5. On the other hand, T_g of LSP8.5 was 1 and 6 °C higher than

that of SP 8.5 in the middle and last stages, respectively (Table 4.5). More obvious temperature shift was found in LSP12. T_g shifted from 306 to 323 °C and from 573 to 600°C, in the middle and last stages weight loss, respectively. More shifting in LSP 12 mainly influenced by the open structure of soy protein chain that allowed more interactions with lignin and resulted in the stronger lignin-protein network and special interactions.

Table 4.5 Glass transition temperature (Tg) and weight loss (%) of lignin at different pH and pH-shifting processes.

Lignin	T_g(°C)	Weight loss/Total weight loss (%)			Total loss (%)	Weight remain (%)
		25-200 (C°)	200-500 (C°)	500-700 (C°)		
AL	404.19	7.05	76.13	16.81	57.15	42.85
L4.5	389.15	3.3	80.51	16.19	57.81	42.19
L8.5	338.48	7.52	74.33	18.15	46.58	53.42
L8.5-4.5	365.05	5.32	79.1	15.58	52.36	47.64
L12	379.71	26.49	54.72	18.78	39.13	60.87
L12-4.5	338.96	8.01	75.53	16.47	41.02	58.98

4.4.9 FTIR

According to Fig. 4.5a, the broad peak around 3350 cm^{-1} assigns to aliphatic and aromatic –OH group. The absorption band at 2935 cm^{-1} attributes to C-H stretching of methoxyl and methyl groups. Different spectra were shown in L12 attributed to some changes in methoxyl and methyl groups which caused by extreme pH environment. All lignins showed aromatic ring vibrations of the phenyl-propane skeleton around 1592, 1509 and 1422 cm^{-1} (Ibrahim et al. 2011). Peaks shifting in the all 3 positions of L12 to 1582, 1496 and 1416 cm^{-1} could reflex changes associated with the

skeleton structure caused by the extreme pH treatment. Absorption peaks, 1265 and 1078 cm^{-1}, related to asymmetrical and symmetrical stretching of alkyl-aryl-ethers in the structures, respectively. The band ~1680 cm^{-1} was observed in the original alkali lignin, whereas broad-spectrum ~1700 cm^{-1}, was obviously found in L8.5-4.5 and L4.5 as a result of acid hydrolysis (Tejado et al. 2007). The band in this region is corresponding to carbonyl stretching from unconjugated ketones and carbonyl groups. The differences referred to the difference in a variation of double bonds in the backbone (Shadid 2016). This band did not present in L12-4.5 due to the lignin initially exposed to base hydrolysis. All lignin showed 1265, 1125, 853, 813 cm^{-1} bands of G signature which was favorable as G unit contains potential active sites (Ibrahim et al. 2011).

In Fig. 4.5b, the peak at 3270 cm^{-1} was assigned to the vibration and stretching of O-H and N-H in hydroxyl and amide groups, respectively. The protein signature absorption bands were found at 1635, 1533, and 1228 cm^{-1} which characterized C=O stretching (amide I), N-H blending (amide II), and N-H and C-N stretching (amide III), respectively. According to Fig. 4.5c, some changes in peak shapes were observed in amide II, amide III peaks, indicating interactions of the amino groups. In addition, compared to SP samples, slightly change was observed in 1447 cm^{-1} absorption peaks which are related to C-N stretching and vibration. These changes strongly indicated interactions of –NH group of protein and lignin. The similar suggestion also reported (Luo et al. 2015a; Pradyawong et al. 2017). Some changes also occurred in the region ~1056 cm^{-1}. The interactions were more obvious in SPL4.5 and SPL12-4.5 since the amide II peaks shifted from 1533 (SP sample, see Fig. 4.5b) to 1512 and 1510 cm^{-1}, respectively. This shifting was highly possibly caused by chemical reactions between SP and lignin. On the other hand, the band around 1393 cm^{-1} attributed to stretching and vibration of $-COO^-$ group (Luo et al. 2015a; Luo et al. 2016b). The overall 1393 cm^{-1} absorption peak of LSP blends were smaller than that of pure SP

samples. It possibly implied cross-link interaction between -COO^- groups of soy protein to lignin. Cross-link interactions on –NH and -COO^- groups of soy protein to lignin reduced the number of hydrophilic groups in the system which resulted in better water resistance properties (Luo et al. 2016b). The hydrophilic and charged amino acid composition of soy protein are approximately 17-19% and 46-47%, respectively (Aftabuddin and Kundu 2007; Santoni and Pizzo 2013). The interactions and cross-linking resulted in properties changes as discussed in prior sections.

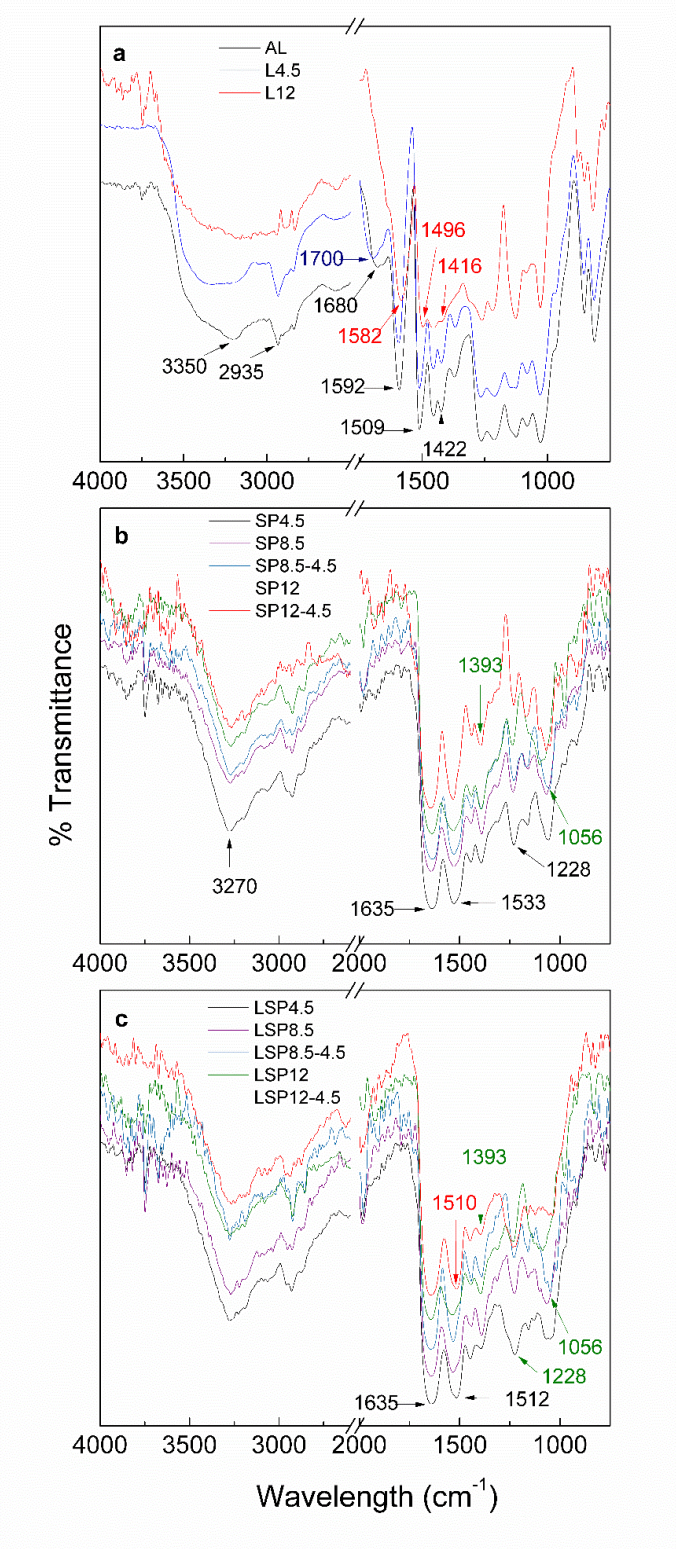

Figure 4.5 FTIR spectra of lignin (a), SP (b), LSP (c), at different pH and pH-shifting processes.

4.4.10 Shear strength testing and glue line

Fig. 4.7 represents the wet and dry shear strength of SP and LSP samples. The influenced of pH on adhesion strength were statistically studied at 95% confidential. According to Fig. 4.6A, SP12, and SP4.5 showed similarly high dry adhesion strength, despite the fact that, the nature of SP at pH 4.5 and 12 was completely different. SP12 provided a consistent glue line with little penetration into the wood specimen (see Fig. 4.6d). The denatured soy protein had a more flexible structure to penetrate into the wood grain and more accessible binding sites to form strong bonds to the wood specimen. The high wet strength of SP12 influenced by the explosion of sulfhydryl and hydrophobic groups at high pH. The groups could bind with wood surface and associated to form disulfide bonds and hydrophobic bonding forces again upon drying process(Gennadios et al. 1993) which strengthen both adhesion and cohesion forces. In addition, intra-and intercross links are very stable in alkali condition (Ishino and Okamoto 1975). Therefore, the SP12 significantly achieved the highest wet adhesion strength. Excellent adhesion performance presented in both wet and dry conditions. On the other hand, SP4.5 showed a strong rigid glue line and had high water resistance with stable conformation.

Table 4.6 Wet shear strength of SP and LSP at different pH and pH-shifting processes. (%) Percentage differences between LSP and SP following * are significantly different at $p < 0.05$.

pH	tests	SP (MPa)	LSP (MPa)	(%) differences
4.5	wet	2.76 ± 0.08	3.26 ± 0.17	**18.32***
8.5	wet	0.90 ± 0.35	1.03 ± 0.30	14.70
8.5-4.5	wet	2.59 ± 0.11	3.35 ± 0.28	**29.58***
12	wet	3.38 ± 0.26	2.92 ± 0.26	**-13.65***
12-4.5	wet	2.20 ± 0.07	2.81 ± 0.26	**27.75***

The pH-shifting of non-denaturing protein from 8.5 to 4.5 did not affect the adhesion property and no differences in adhesion strength were found comparing to SP4.5. In contrast, negative impacts on adhesion strength were observed on the pH-shifting process of denaturing protein (SP12-4.5). As the protein denatures at extremely alkali environment, the configuration and folding structure of aggregates in the following step are not as strong as the non-denaturing protein. Therefore, the adhesion strength was weaker.

As, glue lines were found to be a significant factor in the performance of plywood as high water resistance adhesives acted as a strong moisture barrier to prevent water penetration to the inner layer (Li et al. 2014). Exceed penetration of the adhesive into the wood specimen as seen in SP8.5 (see Fig. 4.6b) resulted in significantly low adhesion strength in both wet and dry conditions.

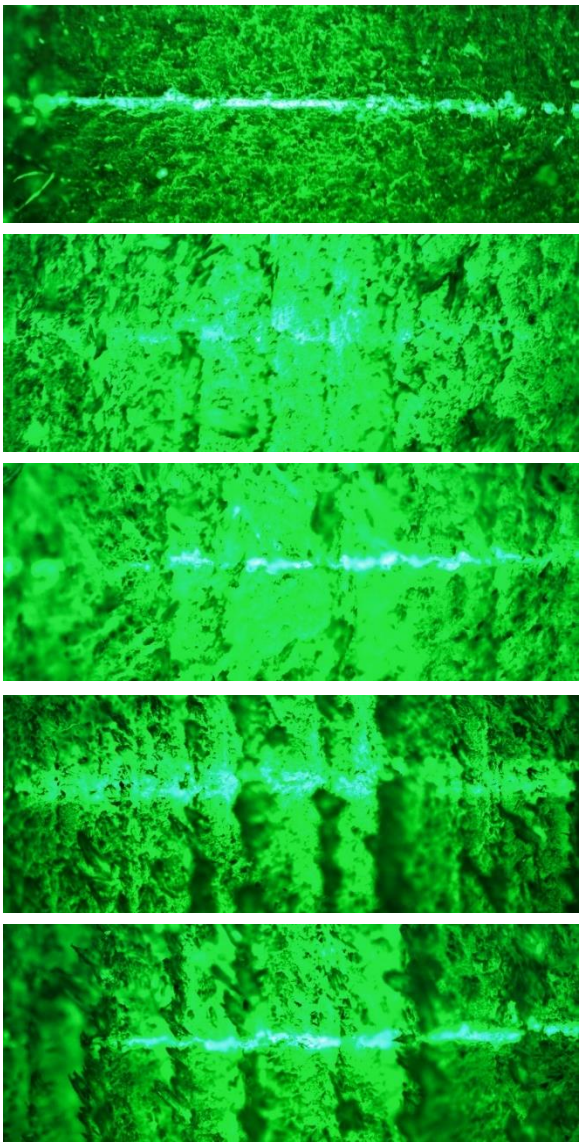

Figure 4.6 Optical microscope images of glue line of wood specimens 5x magnifications: (a) of SP4.5, (b) of SP8.5, (c) of SP8.5-4.5, (d) of SP12 and (e) of SP12-4.5.

Lignin did not show any effects on SP dry adhesion performance. Partial and 100% cohesion failure with sufficient dry adhesion strength was obtained in all samples except at pH 8.5. The differences and improvement of SP and LSP wet adhesion performance in the same environments were compared at the significant level at $p < 0.05$ as seen in table 4.6. Significantly improvement in wet adhesion strength after adding lignin was found in 3 conditions with the final

pH of 4.5. The increase in wet strength was close to 30% when blending lignin with loose structure protein at pH 8.5 and shifted to the aggregation pH in order to obtain a high water resistance property. The same scenario also happened with SP12-4.5. Less improvement was observed at pH 4.5 because fewer interactions took place under aggregation circumstances. A little higher wet adhesion strength also found at pH 8.5 but it is insignificant as the adhesion strength at pH 8.5 is relatively low and the SD of both SP and LSP samples were slightly high. In contrast, excessive interactions between protein and lignin at pH 12 significantly reduced the number of protein active groups adhering to the wood specimen and resulted in decreasing in adhesion strength.

As lignin and soy protein were the major components of the adhesives, their properties at certain pH have a strong influence on adhesion performance. In addition, cross-linked network and interactions of soy protein and lignin led to a stronger adhesion strength (Pradyawong et al. 2017). Solid glue line with an appropriate penetration degree also results in good adhesion properties. Therefore, lignin-SP interactions, solubility, the degree of penetration, adhesion and cohesion strength, and the balance of those factors contributed significantly to an improvement of the overall adhesion performance.

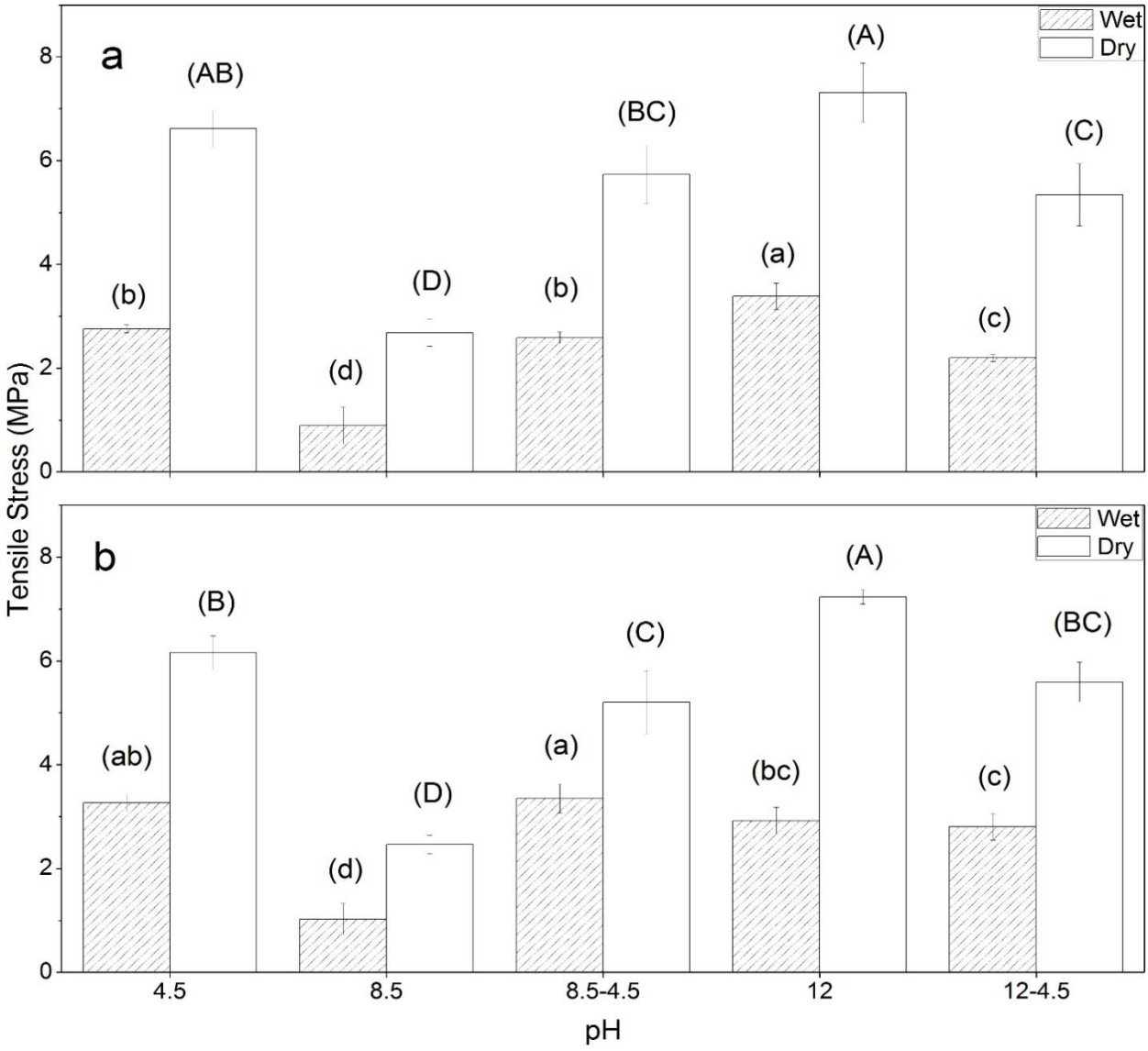

Figure 4.7 Wet and dry shear strength at different pH and pH-shifting processes: (a) SP and (b) LSP. Means followed by different letters are significantly different at $p < 0.05$.

4.5 Conclusion

Acidic and alkaline treatments depolymerized and broke down lignin to smaller particles with more active groups. Lignin strengthened protein network and resulted in an improvement of water resistance and thermal properties of protein adhesives. Water resistance, glue line characteristic, lignin-SP interactions, and the balance of those factors contributed significantly to

adhesion performance. This study found that pH and pH- shifting treatments are simple and effective methodologies to improve adhesion performance and properties of protein and lignin-protein based adhesives. Lignin showed a great potential for being used to improve water resistance and wet strength of soy protein adhesives.

Chapter 5 - Soy Protein-Based Adhesive Enhance by TEMPO Modified Lignin: Adhesion Performance and Properties

5.1 Abstract

The aim of this study was to enhance the water resistance of soy protein (SP) adhesive using laccase-TEMPO modified lignin. Kraft lignin was depolymerized by laccase enzyme with the presence of mediator, TEMPO, to expand the oxidation reaction to both phenolic and non-phenolic compounds. The simplified process was designed with the advantage of the laccase-TEMPO system enhancing the lignin-protein interaction. Compared to SP adhesive, lignin-protein adhesive from the simplified process showed a stronger elastic modulus and high thermal stability. The stronger interactions between $-COO^-$ and $-NH_2$ groups of protein and lignin led to a decrease in followability and spreadability The wet adhesion performance of SP adhesive was successfully increased through lignin-protein interaction. Lignin improved the wet adhesion strength of SP. The simplified process increased the wet shear strength of SP adhesive by 106% from 0.693 to 1.429 MPa and the partial wood failure was observed after the test. The better performance was also observed on the three-cycle soaking test.

Keywords: adhesive, lignin, protein, laccase, TEMPO

5.2 Introduction

Lignin has great potential as a sustainable resource to replace bulk high-value petroleum-based chemicals. Lignin is the most abundant aromatic compound in the world. It can be directly obtained from plants or by-products from paper and cellulosic-based industries. Approximately 50–60 million tons of lignin are produced by the pulp and paper industry annually (Christopher et al. 2014). The production of lignin by-products are expected to further increase with biorefinery industries growing. The innovation of lignin value-added products will improve downstream cellulosic fermentations stream and overall economics of the lignocellulosic biorefinery industry. Since lignin is a heteroaromatic polymer the depolymerization of lignin to low-molecular-weight compounds, the key step to effectively utilizing lignin as the building blocks for chemical syntheses of high-value products (Christopher et al. 2014; Fisher and Fong 2014). Enzymatic depolymerization is a process to degrade lignin under mild condition. The operating conditions are safe and environmentally friendly (Díaz-Rodríguez et al. 2014). Lignin peroxidase (LiP), manganese peroxidase (MnP) and laccase are naturally produced by fungi, which can depolymerize lignin. Even though laccase has a lower redox potential comparing to LiP and MnP, it has the ability to utilize atmospheric oxygen as an electron donor instead of hydrogen peroxide, which is used by LiP and MnP. Therefore, laccase is an excellent candidate for diverse industrial applications and has received great attention in recent years (Christopher et al. 2014; Díaz-Rodríguez et al. 2014; Fabbrini et al. 2002). Laccase is capable of oxidizing a variety of aromatic hydrogen donors, which removes an electron and a proton from phenolic hydroxyl group in the oxidation reaction. Moreover, laccase can also oxidize aromatic amino groups to form free phenoxy radicals and amino radicals from protein (Leonowicz et al. 2001). However, laccase itself cannot oxidizes non-phenolic compound.(Barreca et al. 2003; Fabbrini et al. 2002). In order to

enhance the oxidation reaction of non-phenolic compounds mediators are added to the system as an electron shuttle. TEMPO (2, 2, 6, 6-Tetramethylpiperidin-1-yl) was considered as most effective mediator (Díaz-Rodríguez et al. 2014; Fabbrini et al. 2002). Laccase-TEMPO can oxidize both aromatic and non-aromatic primary or secondary alcohols of lignin and protein at room temperature using ambient air (Díaz-Rodríguez et al. 2014; Ramalingam et al. 2017). The oxidation diagram was shown (Fig. 5.1).

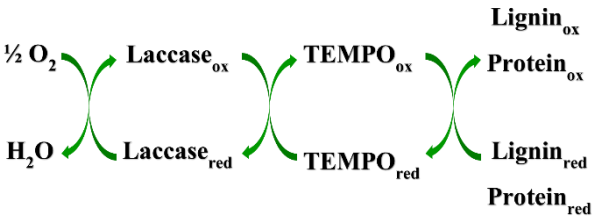

Figure 5.1 Laccase-TEMPO oxidation reactions.

A replacement of formaldehyde-based adhesives by bio-based adhesives like plant protein adhesives has been a topic of concern for decades. Many studies focused on several kinds of plant seed such as soybean, cottonseed, canola, and camelina which could be used as renewable resources for bio-based adhesives (He et al. 2014; Li et al. 2012a; Liu 2017; Qi et al. 2016). The most significant disadvantage point of plant protein adhesive is the low water resistance which limits its application and market attraction. A few research groups have tried to improve wet adhesion strength of soy protein adhesive by using lignin (Pradyawong et al. 2017; Xiao et al. 2013). Luo et al. improved the water resistance of bio-based adhesive by incorporating laccase modified lignin-phenol-formaldehyde resin into soybean meal (Luo et al. 2015b). However, the adhesive is not completely sustainable and formaldehyde-free. Laccase treated and chemically reduced lignin-soy protein showed good water resistance property (Ibrahim et al. 2013).

More studies and improvements are needed to produce a sustainable and high performance bio-adhesive. With the advantage of the laccase/TEMPO system, that oxidizes both phenolic and non-phenolic alcohols of lignin and protein, we simplified the laccase modified lignin-soy protein adhesive formula and compared the simplified adhesive with laccase modified lignin and unmodified lignin-protein adhesives. The two-layer and three-layer adhesion performance, contact angle, thermal properties and morphological characteristics of laccase modified lignin-soy protein adhesives were studied.

5.3 Materials and methods

5.3.1 Materials

Defatted soy flour with a dispersion index of 90 was provided by Cargill (Cedar Rapids, IA). Kraft Lignin (KL) (no. 370959) was purchased from Sigma-Aldrich, Inc. (St. Louis, MO). Laccase enzyme and 2, 2, 6, 6-Tetramethylpiperidin-1-yl (TEMPO) were purchased from Sigma Aldrich (St. Louis, MO). Sodium hydroxide and hydrochloric acid were acquired from Fisher Scientific (Fair Lawn, NJ). Cherry wood veneers were with a dimension of 50 × 120 × 0.5 mm supplied by Veneer One (Oceanside, NY). Yellow pine veneers with a dimension of 300 × 300 × 3.5 mm were purchased from Ashland Company (Covington, KY).

5.3.2 Preparation of laccase modified kraft lignin

The KL oxidation procedure was adapted from (Fabbrini et al. 2002; Ibrahim et al. 2013). Ten grams of KL was dispersed in 2 L of 20 mM acetate buffer with 200U of laccase enzyme and 56.25 mg of TEMPO. The lignin was stirred for 24 h at room temperature. The slurry was centrifuged at 5000 rpm for 15 min and the retentate was collected. The sample was dried at 50 °C

and was stored at 4 °C for future experiments. The laccase modified kraft lignin was labeled as LL.

5.3.3 Soy protein isolation

Defatted soy flour was mixed with distilled water at a ratio of 1:15 (w/w). The pH was adjusted to 8.5 with NaOH (10 N) and was stabilized for 2 h. Soy protein was precipitated at pH 4.2 with HCl (10N) then neutralized to pH 7.0 with NaOH (10 N) (Mo et al. 2004). The soy protein was freeze-dried and ground with a cyclone miller with 1 mm screen (Udy Corp., Fort Collins, Colo.) and was stored at 4 °C for further experiment.

5.3.4 Preparation of adhesives

In the control group, soy protein (10% w/w) was mixed with KL and LL (2% w/w) in distilled water. The pH of the slurries was adjusted to 4.5 with HCl (2 N) and then stirred at 300 rpm for 2 h. The samples were named as SP+KL and SP+LL. The process was simplified by blending 10% w/w of SP and 2% w/w KL with laccase and TEMPO all together at once at room temperature for 24 hr. The ratio of KL to laccase and TEMPO was the same in section 2.2. After that, the pH of the slurry was adjusted to 4.5 and continuously stirred at 300 rpm for another 2 h. The sample was named as SP+KL+Enz. Pure soy protein (10% w/w) adhesive (SP) was prepared and used as a reference.

5.3.5 Rheological properties

A Bohlin CVOR 150 rheometer (Malvern Instruments, Southborough, MA, USA) was used to measure viscosity and viscous (loss) modulus of the adhesives from section 2.4. The gap between a plate and a 20 mm-diameter parallel plate head was set to 500 μm. Silicone oil was applied to prevent water evaporation. The apparent viscosity was measured at 25 °C at a constant

shear rate range of 25 s^{-1}. The dynamic oscillation shear measurement was applied to measure viscous modulus (G'') at the angular frequency of 1 Hz.

5.3.6 Contact angle measurement

The spreadability of the adhesives from section 2.4 was studied on the glass slide (plain microscope slides, Fisher Scientific, Fair Lawn, NJ). Contact angles were measured by an optical contact angle meter (CAM100, KSV Instruments, Helsinki, Finland). The polar surface energy, of glass and cherry wood, were reported as 38.9 and 35.1–38.1 mJ/m^2, respectively (de Meijer et al. 2000; Hejda et al. 2010).

The contact angle is highly related to the polar surface energy, and the contact angle on the glass slide could be similar to a cherry wood surface. The contact angles of 10 replications for each sample were captured every 1 s for 32 s.

5.3.7 Differential scanning calorimetry

The denaturing behavior of lignin-soy protein adhesives from section 2.4 was analyzed by a differential scanning calorimeter (DSC) (Q200, TA instrument, Schaumburg, IL, USA). Approximately 20 mg of adhesives were placed in a Tzero aluminum hermetic pan. The samples were set at 25 °C for 1 min and then heated to 120 °C at a heating rate of 10 °C/min. The peak temperatures and denaturation enthalpies were calculated by Universal Analysis2000 software.

5.3.8 Thermogravimetric analysis

The samples were dried at 150 °C, the curing temperature in this study. Then, the dry samples were ground and passed through a 100 mesh screen. The thermostability was measured by a thermogravimetric analyzer (TGA) (Perkin-Elmer TGA 7, Norwalk, CT). Approximately 5 mg of samples were heated at the temperature changing from 25 °C to 700 °C, at a heating rate of 10 °C/min. Nitrogen gas was flushed to provide an inert atmosphere.

5.3.9 Fourier transform infrared analysis

The Fourier transform infrared (FTIR) data of the dried samples from section 2.9 were collected from 400 to 4000 cm^{-1} with a PerkinElmer SpectrumTM 400 FTIR/FT-NIR spectrophotometer (Shelton, CT, USA). The transmission spectra of 32 scans of each sample were collected at a resolution of 4 cm^{-1}.

5.3.10 Scanning electron microscopy (SEM)

The dried lignin samples from section 2.2 and 2.4 were coated with palladium and gold by sputter coater (Desk II Sputter/Etch Unit, Moorestown NJ), and were observed under a scanning electron microscope (SEM), Hitachi S-3500N (Hitachi Science System, Ibaraki, Japan) to study the morphological changes. The pictures were collected at an accelerating voltage of 10.0 kV under different magnifications.

5.3.11 Preparation of Plywood Specimen and Shear Strength Testing

The clean glue area of 2 × 12 x cm (width × length) on cherry wood veneer panels were spread with 0.6 ml of fresh adhesives. After the two panels were rest at the room temperature for 15 minutes, they were assembled and hot-pressed (Model 3890; Auto 'M', Carver Inc., Wabash, IN) for 10 min under the pressure of 2 MPa at 150 °C. The glued specimens were conditioned in the chamber at 23 °C and 50% relative humidity for 5 days before cutting to 20 mm length. The samples for the wet strength test were conditioned again for 2 days and soaked in water for 48 hr. The samples for the dry strength test were still conditioned in the same controlled environment for 4 days. The testing procedure was designed based on the ASTM standard method (ASTM D1183-03) (ASTM 2003). Both wet and dry tensile strength tests were conducted by the Instron testing machine (Model 4465; Canton, MA) with a crosshead speed of 1.6 mm/min. Five and ten replications were evaluated for dry tensile strength wet tensile strength, respectively.

The SP+KL+Enz sample was selected for future study of the three layers wood adhesion test for industrial uses. The yellow pine veneers with a dimension of 300 × 300 × 3.5 mm were conditioned in a 27 ℃, 30% RH chamber at 7 days before wood adhesion test. The testing procedure was the indicated in Qi et al.(Qi et al. 2013b). Briefly, a total of 40 g of adhesive were spread on both sides of the middle specimen. The top and the bottom specimens were assembled with the grain direction perpendicular to the middle specimen. The three-layer wood were pressed at room temperature for 15 min. The hot press condition was 150 ℃, 10 min at 1.03 MPa (G30H-15-B, Wabash MPI, Wabash, IN).

The hot-pressed samples were then conditioned in a chamber at 23 ℃ and 50% RH for 5 days before being cut into 8 small pieces (82.6 × 25.6 mm) and 5 large wood pieces (50 × 127 mm) based on the ASTM standard method D906-98 (19). Eight of the small wood pieces were soaked in water at room temperature for 24 h and then the shear strength was measured immediately. Another 8 of small wood pieces were conditioned in the same chamber and tested for dry shear strength. The three-cycle soaking test was performed by soaking the 10 wood panels (50 × 127 mm) at 23 ℃ for 4 h and then dried at 50℃ with air circulation for 19 h and repeated the process 2 more times. The wood panels were evaluated for delamination before and after drying process according to the American National Standard for Hardwood and Decorative Plywood and the delamination score was rated from 0 to 10 (HPVA 2004). Zero means no delamination and the wood specimen is intact, five is the maximum allowable delamination to pass the test, and 10 means complete veneer separation. Any wood panels that score higher than 5 is considered as a failure for the three cycles test.

5.3.12 Statistical analysis

The shear strength and contact angle were analyzed through analysis of variance by statistical software (SAS Institute, Inc., Cary, N.C.). Pairwise comparisons were performed for the means using the Tukey adjustment at a significance level of 0.05.

5.4 Results and discussion

5.4.1 SEM

Lignin and lignin-protein adhesives were captured at low magnification to show the overall particle size distribution of the samples (Fig.5.2A to F), whereas higher magnification images were showed to clearly emphasize their detail morphologies. There was a mixture of a large, medium and small particle in KL (Fig. 5.2A). The large particle was intact and the surface was smooth (Fig. 5.2a). Phenolic and non-phenolic subunits of lignin were oxidized in the laccase-TEMPO system. The cleavage of C_α-C_β, aryl-alkyl and alkyl-alkyl bonds and oxidation of C_α (Ramalingam et al. 2017; Sánchez et al. 2011) resulted in the majority of small lignin particles (Fig. 5.2B). At a closer look, the medium particles of LL were composed of many small particles (Fig. 5.2b)which confirmed oligomerization of phenolic compounds by laccase catalyzation that had been reported recently (Ramalingam et al. 2017). Still the overall particle size of LL was smaller than KL. LL had potential to provide better adhesion performance than KL in lignin-protein blends since the smaller lignin size showed the advantage on adhesion properties (Pradyawong et al. 2017). Not many differences were observed between SP and SP+KL samples in terms of particle size distribution and surface texture (Fig. 5.2C, c, D and d). The combination of laccase modified lignin-protein provided larger lignin-protein complexes (Fig. 5.2E and F) comparing to SP+KL (Fig. 5.2D) indicating more cross-links occurred between protein and lignin after being oxidized by laccase-TEMPO. Slightly larger lignin-protein particles were observed in SP+KL+Enz

compared to the SP+LL (Fig. 5.2E and F) as well as similar surface textures (Fig. 5.2e and f). Not many differences were found under microscopic observation. The differences of the lignin-protein blends were observed in the following sections.

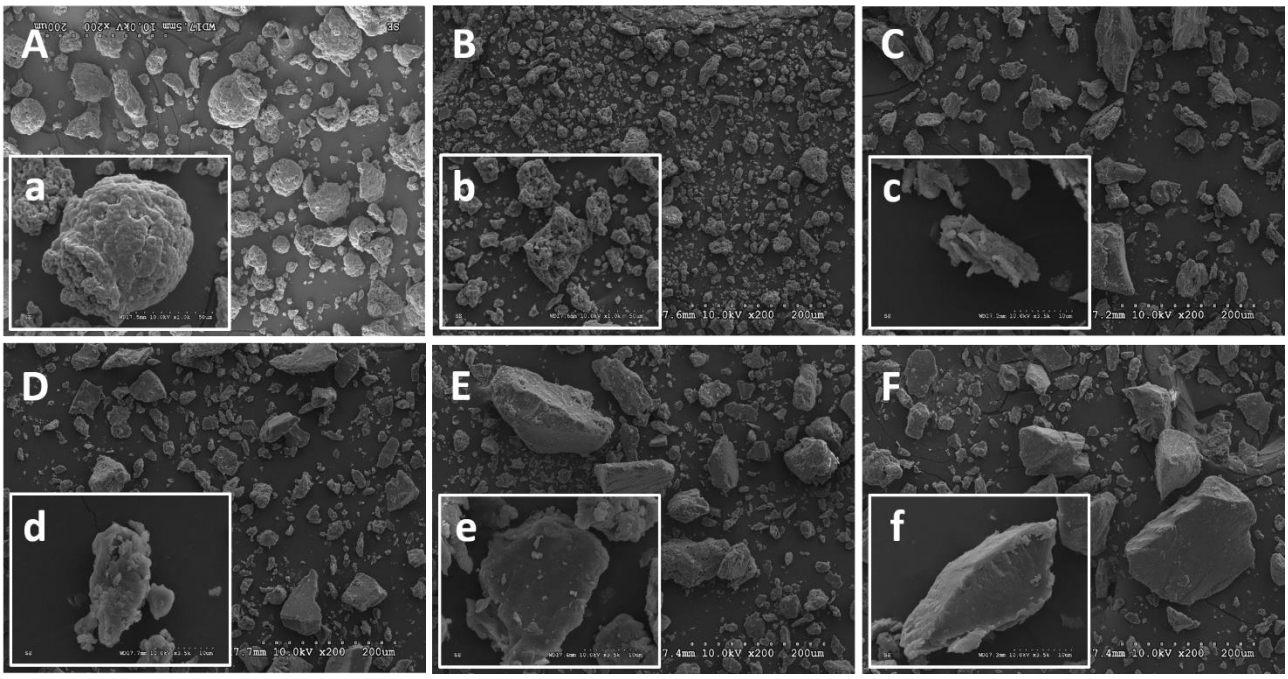

Figure 5.2 Scanning electron microscope images of: kraft lignin (KL) (A), laccase-TEMPO modified lignin (LL) (B), soy protein (SP) (C), kraft lignin-soy protein (SP+KL) (D), laccase TEMPO modified lignin-soy protein (SP+LL) (E), and laccase-TEMPO modified lignin-so soy protein (SP+LL) (E), and laccase-TEMPO modified lignin-soy protein from simplified process (SP+KL+Enz) (F) at 200x magnifications, KL (a), LL (b) at 1000x magnifications, and SP (c), SP+KL (d), SP+LL (e), and SP+KL+Enz (f) at 3500x magnifications.-

5.4.2 Rheological Properties

The physical properties of protein-based products are closely related to the rheological properties of the protein. The viscosity of the adhesives were measured at a constant shear rate. According to table 5.1, the viscosity of SP did not significantly change with the addition of KL or LL. In contrast, significantly higher viscosity was observed in SP+KL+Enz. The viscosity of the simplify SP+KL+Enz adhesive increased from 3.28-3.38 to 7.92. The change indicated a stronger molecular interaction between protein and lignin. On one hand, the LL was oxidized and

repolymerized while the protein was absent in the lignin modification system. On the other hand, both lignin and protein were present in the SP+KL+Enz system at the same time. Laccase-TEMPO oxidized both aromatic and non-aromatic primary and secondary alcohols of lignin and protein (Díaz-Rodríguez et al. 2014; Ramalingam et al. 2017); therefore, both reactive protein and lignin intermediates (quinone and radicals) could react to each other and formed cross-links easily in SP+KL+Enz system. An increase in the cross-link interaction resulted in a decreased in flowability.

Table 5.1 Viscosity and contact angle of soy protein (SP), kraft lignin-soy protein (SP+KL), laccase-TEMPO modified lignin-soy protein (SP+LL), and laccase-TEMPO modified lignin-soy protein from simplified process (SP+KL+Enz) adhesives. Means followed by different letters are significantly different at $p < 0.05$.

Samples	Viscosity (Pas)	Contact angle
SP	3.28 ± 0.12^{a}	57.63 ± 0.27^{A}
SP+KL	3.38 ± 0.02^{a}	40.81 ± 0.88^{B}
SP+LL	3.28 ± 0.01^{a}	38.41 ± 0.27^{B}
SP+KL+Enz	7.92 ± 0.05^{b}	54.45 ± 2.73^{A}

The strength of lignin and protein interactions were confirmed by the viscoelastic properties (Fig. 5.3). Elastic modulus or storage modulus (G') reflects the stiffness and compactness of the protein structure. G' is usually used to define protein's mechanical properties and intermolecular interactions (Zhu et al. 2017). G' was measured as a function of frequency. The stiffness of all adhesives increased as a response to an elevated level of frequency. SP+KL+Enz showed the highest elastic (storage) modulus which refers to high intermolecular protein interaction. The simplified process produced a stiffer lignin-protein network than the other conditions. The significant high viscosity and distinguish high elastic modulus occurring in the

simplified SP+KL+Enz strongly suggested more molecular interactions and cross-linkages of the lignin-protein network.

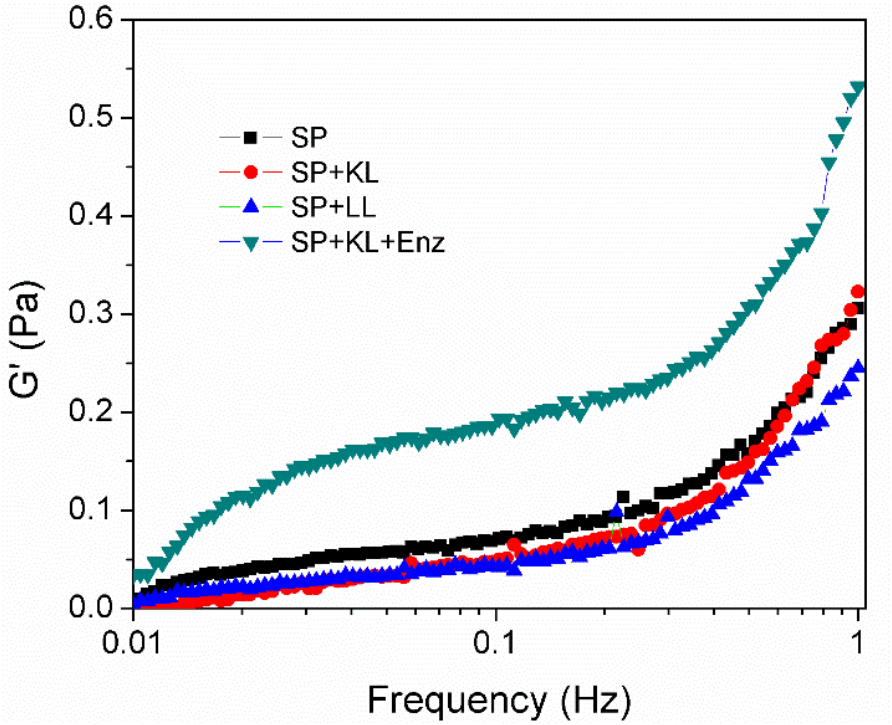

Figure 5.3 Elastic modulus of soy protein (SP), kraft lignin-soy protein (SP+KL), laccase-TEMPO modified lignin-soy protein (SP+LL), and laccase-TEMPO modified lignin-soy protein from simplified process (SP+KL+Enz) adhesives.

5.4.3 Contact angle

Contact angle reflexes the spreadability and wettability of adhesives on solid surfaces. The contact angle of the lignin-protein adhesives became significantly lower after blending with KL and LL. The low contact angle refers to low surface tension and better spreadability. Therefore, SP+KL and SP+LL samples were easier to wet the surface of the wood specimens. The result was similar to our previous study with the same blending procedure and lignin:protein ratio (Pradyawong et al. 2017). Lignin improved the wettability of soy protein adhesives. On the contrary, the contact angle of SP+KL+Enz adhesives were significantly higher than the other

lignin-protein adhesives, but not significantly different from the SP sample. The stronger intermolecular lignin-protein interaction as discussed in section 5.4.2 increased surface tension and contact angle of the SP+KL+Enz. The unfavorable spreadability could give a negative impact on an adhesion performance.

5.4.4 DSC

The adhesives were heated to study the denaturing behavior of the protein. The denaturing temperature (T_d) of 7S and 11S soy protein subunits, and heat flow/g protein are shown in Table 5.2 The 7S and 11S DSC endothermic peaks of SP appeared at 77.80 and 93.07 °C, respectively. The change in T_d of lignin-protein adhesives was observed on 11S denaturing peak temperature and ΔH_d. The similar result was reported (Pradyawong et al. 2017). Approximately 3.0-3.5 °C increase in 11S T_d was observed in SP+KL and SP+LL. Comparing to SP, significantly more energy was required to denature both SP+KL and SP+LL. The formation of soy protein-lignin networks strengthened the soy protein structure resulting in higher energy needed to denature the lignin-protein structure. LL had more surface area, active groups, and opening structure than KL, therefore, slightly more energy was absorbed to denature the LL-protein network. The simplified lignin-protein modification process provided the strongest network that resists the denaturation the most. The T_d and ΔH_d of SP+KL+Enz were noticeably higher than other adhesives. The T_d of 7S and 11S increased 1.69 and 4.41 °C, respectively, and the endothermic heat absorption was significantly (70%) higher than SP.

Table 5.2 Denaturing Temperature (Td) and total enthalpy of protein denature (ΔHd) of soy protein (SP), kraft lignin-soy protein (SP+KL), laccase-TEMPO modified lignin-soy protein (SP+LL), and laccase-TEMPO modified lignin-soy protein from simplified process (SP+KL+Enz) adhesives. Means followed by different letters are significantly different at $p < 0.05$.

Samples	Peak temperature (°C)		Total heat flow (J)/g protein
	7S	11S	
SP	77.80 ± 0.14	93.07 ± 0.02	4.21 ± 0.06[a]
SP+KL	78.68 ± 0.35	96.04 ± 0.04	6.01 ± 0.33[b]
SP+LL	77.76 ± 0.06	96.52 ± 0.58	6.56 ± 0.18[bc]
SP+KL+Enz	79.49 ± 0.18	97.48 ± 0.01	7.20 ± 0.27[c]

5.4.5 FTIR

The broad peak around 3000-3500 cm^{-1} is assigned to the aliphatic and aromatic –OH group (Fig. 5.4a). The absorption band at 2932 cm^{-1} is attributed to C-H stretching of methoxyl and methyl groups of lignin (Fig. 5.4a). Aromatic ring vibrations of the phenyl-propane skeleton were observed around 1594, 1510 and 1423 cm^{-1}(Ibrahim et al. 2011; Tejado et al. 2007). The peaks at 1454 and 1428 are corresponding to O-CH_3 deformation, CH_2 scissoring, and guaiacyl ring vibration. A stretching of C-O under different circumstances occurs in the range of 1033-1297 cm^{-1} (Adapa et al. 2009).

The change in peak shape around 3000-3500 cm^{-1} could define changes in aliphatic and aromatic –OH group position and composition. No change was observed on methoxyl and methyl groups as the spectrum at 2932 cm^{-1} of KL and LL were consistent. The peak ~1700 cm^{-1} corresponds to the C=O stretching in conjugated carbonyl compounds with the aromatic rings (Tejado et al. 2007). The peak at 1690 cm^{-1} likely disappeared in LL indicating depolymerization of lignin by oxidation reaction (Zhu et al. 2017). As the peaks intensity at 1454 and 1423 cm^{-1} slightly increased but no change was observed at 2930 cm^{-1}, it could reflex minor changes of CH_2

scissoring, and guaiacyl ring vibration. An obviously decrease in peaks intensity at 1082 cm^{-1} reflexed changes in C-O bonds in LL.

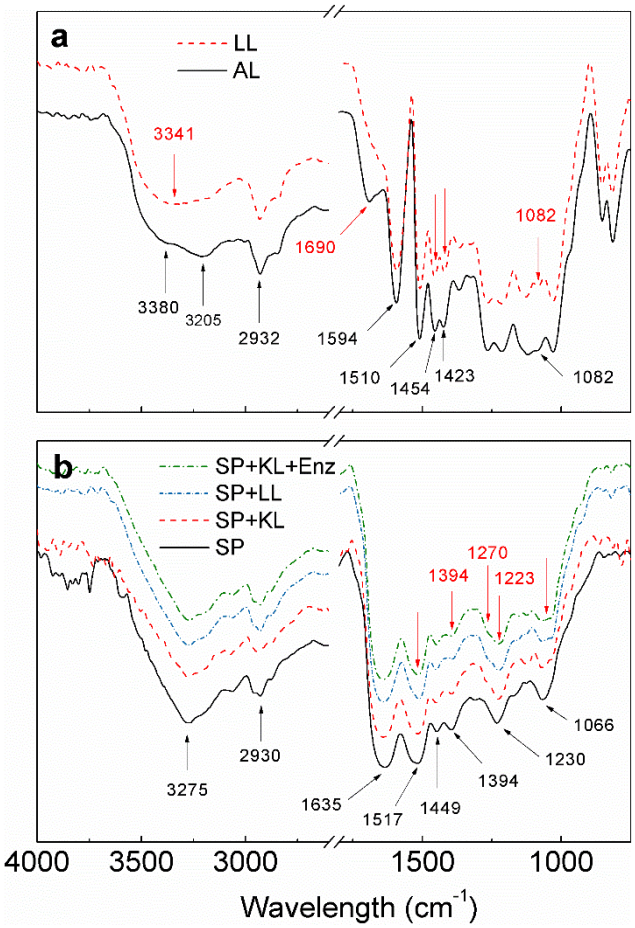

Figure 5.4 FTIR spectra of kraft lignin (KL) and laccase-TEMPO modified lignin (LL) (a), and soy protein (SP), kraft lignin-soy protein (SP+KL), laccase-TEMPO modified lignin- soy protein (SP+LL), and laccase-TEMPO modified lignin-soy protein from simplified process (SP+KL+Enz) adhesives (b).

The large peak at 3275 cm^{-1} refers to bending vibrations of free and bound O–H and N–H groups. The broad peak at 3281 cm^{-1} refers to N-H stretching and the sharp absorption peaks at 2957, 2930 and 2873 cm^{-1} are assigned to the antisymmetric and symmetric C-H stretching of the protein (Tejado et al. 2007). The three absorption bands of 1635, 1517 and 1230 cm^{-1} were responses from C=O stretching (amide I), N-H bending (amide II), and C-N stretching and N-H

vibration (amide III), receptively (Luo et al. 2015b). The COO^- and $–C-NH_2$ groups absorption band presented at 1394 and 1066 cm^{-1}, respectively (Lei et al. 2014). The change in of spectrum profile of SP with an additional lignin was consistent with our previous study (Pradyawong et al. 2017). Comparing to SP, the amide II peak of SP+LL and SP+KL+Enz became sharper. The amide III peak was broader and a small peak shoulder was discovered at 1270 cm^{-1}. The changes in amide II and III indicated the interactions between the -NH group of soy protein and lignin. The shoulder of SP+LL and SP+KL+Enz in amide III peak was slightly stronger than that of SP+KL as laccase-TEMPO enhanced the interaction between lignin and protein. The $-COO^-$ cm^{-1} peak intensity at 1391 cm^{-1}gradually decreased with an additional of KL and LL. Hence, the $-COO^-$ of soy protein interacted with lignin and more interaction was observed in SP+LL. Moreover, $-C-NH_2$ bond, C-O-C and C-O bending and stretching absorption were found at 1058 cm^{-1} and between 1249 and 833 cm^{-1}, respectively (Lei et al. 2014; Luo et al. 2015b). The absence of 1066 cm^{-1} peak and changes around that area supported the interaction of $-COO^-$ and $-NH_2$ of protein to lignin.

5.4.6 Adhesion tests

Two-layer adhesion strength of lignin-protein adhesives is shown (Fig. 5.5). The wet shear strength of soy protein adhesives increased with an addition of lignin. SP+LL and SP+KL+Enz showed a significantly higher wet adhesion strength than SP. An improvement of wet adhesion strength of 33% in SP+KL+LL was not as great as expected. According to the mechanical bonding theory both flow behavior and bonding between protein in the adhesive and cellulose on the wood panel are important factors affecting adhesion performance (Wool and Sun 2011). There was no doubt about an outstanding cohesion strength obtained from the simplified process. However, a higher surface tension and poor wettability were observed in SP+KL+Enz as discussed in section 5.4.3. Therefore, SP+KL+Enz had a disadvantages to get into the wood grain and pore and

uniformly form bonds throughout the wood specimens. The dry strength of the SP was excellent. Even if dry adhesion strength decreased significantly after adding lignin, it seemed not significant since wood failure was observed in all dry adhesion tests.

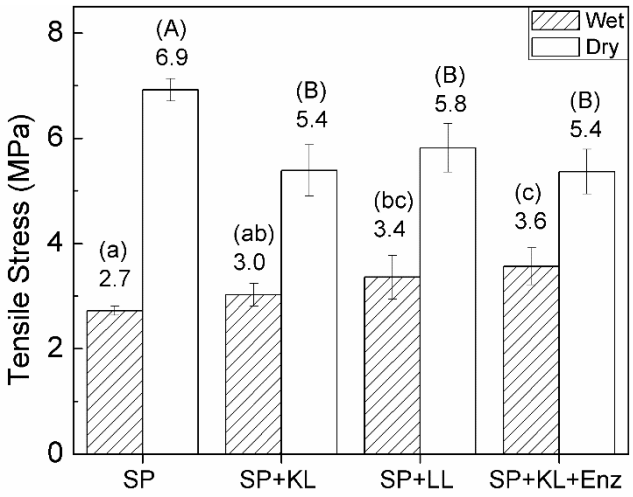

Figure 5.5 Wet and dry shear strength of soy protein (SP), kraft lignin-soy protein (SP+KL), laccase-TEMPO modified lignin-soy protein (SP+LL), and laccase-TEMPO modified lignin-soy protein from simplified process (SP+KL+Enz) adhesives. Means followed by different letters are significantly different at $p < 0.05$.

The SP and SP+KL+Enz were selected to continue on three-layer adhesion test. Wet adhesion strength significantly increased from 0.693 to 1.429 MPa (Table 5.3). No wood failure was observed on wet adhesion test of SP but partial wood failure was observed in SP+KL+Enz (Fig. 5.5a and b). The dry adhesion of the original SP was already good. An addition of lignin did not showed any negative impact on dry adhesion performance. Comparing to SP, the wet and dry adhesion strengths of SP+KL+Enz showed a better performance in the three-layer test indicating that the lignin-protein adhesive form the simplified process worked better in practical usage for plywood than in the laboratory scale test.

Table 5.3 Three layers adhesion of soy protein (SP), kraft lignin-soy protein (SP+KL), laccase-TEMPO modified lignin-soy protein (SP+LL), and laccase-TEMPO modified lignin-soy protein from simplified process (SP+KL+Enz) adhesives. Means followed by different letters are significantly different at $p < 0.05$.

Samples	Shear Strength (MPa)	
	Wet	Dry
SP	0.693 ± 0.182[a]	2.047 ± 0.197[a]
SP+KL+LL	1.429 ± 0.197[b]	1.906 ± 0.201[a]

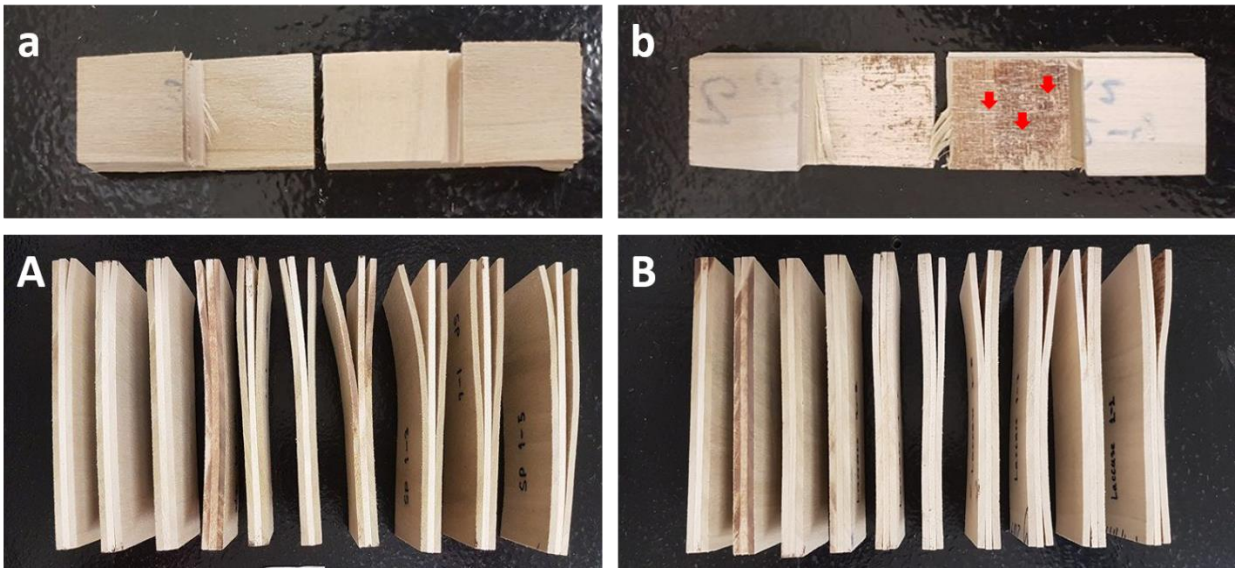

Figure 5.6 Wood specimens after wet adhesion test of soy protein (SP) (a), and laccase-TEMPO modified lignin-soy protein from simplified process (SP+KL+Enz) (b), and the delamination pattern of wood panels after the third cycle of soak strength test of SP (A) and SP+KL+Enz (B).

Three-cycle soaking test was performed on 10 replications for each sample. The delamination level was scored from 0 to 10. No visible delamination or completely intact plywood was scored 0. The score higher than 5 (major slippage 1-2 inch) is judged as failing to pass the three-cycle soak test. The evaluation was focused on the most delaminate part of the plywood. The data was recorded before and after drying of each cycle (Table 5.4). The wood extended under

water and shrunk during the drying process. The differences in each veneer and grain direction resulted in different shrinking rate, level, and direction. Therefore, the delamination before drying was equal or less than that after drying process. After drying of the first and second cycle, 100% of SP+KL+Enz plywood passed the standard, whereas 50% and 30% of SP passed the standard, respectively. Almost all (90%) of SP fail to pass the standard after soaking and drying of the third cycle. Fifty percent of plywood was scored 7 and 20% of them were almost split apart (Score 8 and 9) (Fig. 5.6A). The plywood was arranged from lowest to highest delamination levels. On the contrary, 100% of SP+KL+Enz still passed the standard after the third cycle soaking but 60% of them were scored 6 after drying of the last cycle. Forty percent of the plywood passed the standard. Ten percent of the sample was completely intact without any delamination and another 30% of the samples were scored from 2-4. The failed pieces were not as severe as observed in SP (Fig. 5.6A and B). Lignin-protein adhesive from the simplified process, SP+KL+Enz showed a great potential to be used as a wood adhesive in plywood industry and serves as a completely green resource in the biomaterial field.

Table 5.4 Three-cycle soak strength evaluation score of soy protein (SP), kraft lignin-soy protein (SP+KL), laccase-TEMPO modified lignin-soy protein (SP+LL), and laccase-TEMPO modified lignin-soy protein from simplified process (SP+KL+Enz) adhesives before and after drying process of each cycle.

Replication	1st cycle soaking				2nd cycle soaking				3rd cycle soaking			
	Before		After		Before		After		Before		After	
	SP	SP+KL+Enz	SP	SP+KL+Enz	SP	SP+KL+Enz	SP	SP+KL+Enz	SP	SP+KL+Enz	SP	SP+KL+Enz
1	6	0	7	4	7	4	7	8	5	8	8	6
2	0	4	4	5	4	5	5	7	5	5	7	6
3	5	4	5	5	6	5	5	4	5	6	6	6
4	6	0	8	4	8	5	5	9	5	9	9	6
5	5	3	5	5	6	5	5	7	5	5	7	6
6	7	0	7	0	7	0	0	7	0	5	7	0
7	5	0	6	4	6	4	5	7	5	5	7	6
8	5	0	6	0	6	0	2	7	2	5	7	2
9	0	0	0	0	5	3	3	6	3	6	6	4
10	0	0	0	0	2	0	3	2	3	3	3	3

Note: Higher score means larger delamination

5.5 Conclusion

Lignin increased water resistance and strengthened protein network by interacting with the $-COO^-$ and $-NH_2$ groups of protein. An increase thermal stability were observed with an addition of lignin. The most obvious changes were found in SP+KL+Enz obtained from the simplified process. The SP+KL+Enz showed a great improvement of 106% of wet shear strength, and partial wood failure was observed after wet adhesions strength. Since the simplified process is suitable for manufacturing practice and SP+KL+Enz contains only renewable materials; therefore, the SP+KL+Enz is a great candidate to fulfill the global demand for green products and technologies.

Chapter 6 - Conclusion and future work

6.1 Conclusion

Lignin showed a great potential to be utilized as water resistance enhancer for plant-protein adhesives. Lignin crosslinked with protein through hydroxyl, carboxylic, and amino groups and resulted in a strong lignin-protein network with high molecular weight. The crosslink interactions were supported mainly by H-bond and non-specific interactions. The lignin-protein interactions were observed through alkali (pH-8.5) and alkali-acid pH-shifting process (pH 12-4.5). The maximum increase (620%) in water resistance of SP adhesive was found at pH 12 with an addition of lignin. The formation of protein and lignin copolymer also improved flowability, thermal properties, and adhesion strength of soy protein (SP) adhesives.

Lignin particle size and the ratio of lignin to protein had a significant effect on spreadability and adhesion performance of the SP adhesives. The wet adhesion strength of SP adhesives increased as lignin particle size decreased. The optimum ratio of protein to lignin at 10:2 (w/w) with 12% total solid content provided the highest wet adhesion strength of 4.66 MPa, which was 53.3% higher than that of 10% pure SP adhesive.

Lignin depolymerization by laccase enzyme with the presence of mediator (TEMPO), provided reactive lignin intermediates and enhanced lignin-protein interactions. The laccase modified lignin-protein adhesive (SP+KL+Enz) had a high elastic modulus. A formation of strong lignin-protein network increased the wet adhesion strength of SP adhesive by 106% and the partial wood failure was observed when the three-layer plywood was tested. A better performance was also observed in the three-cycle soaking test.

Lignin-protein interaction can be enhanced by pH adjusting which can change protein folding behavior and lignin properties. Depolymerization of lignin and cleavage of β-O-4 bond

were found in alkali environment (pH 8.5 and 12). Protein aggregate, unfold and denature in acidic, basic and sever alkali environments, respectively. Therefore, pH had an effect on both properties and adhesion performance of lignin-protein adhesives and the effect extent varies depending on specific pH value. The better-wet adhesion performance was obtained at pH 4.5, 8.5-4.5 and 12 with rigid glue line.

Water resistance, glue line characteristics, lignin-protein interactions, and the balance of those factors contributed significantly to the adhesion performance. The protein-lignin adhesives using absolutely renewable materials have a great potential to replace the petroleum-based adhesives and fulfill the global demand for green products and technologies.

6.2 Future work

Utilization of lignin utilization for high value-added products still remained a challenge. Even many studies focus on lignin applications, the majority of lignin still be burned. In this research, lignin showed a great potential as a water resistance enhancer for protein adhesives. However, the knowledge and mechanism of lignin-protein interactions are still limited. The comprehensive studies are needed to understand the chemical pathways of lignin and protein polymer and the interactions between lignin subunits and amino acids at monomer, oligomer and polymer levels for development of affordable and durable biobased adhesives. More investigation is needed to study the effect of lignin on protein folding behavior and the formation of the lignin-protein network. So that the water resistance of plant-protein adhesives can be further improved.

The improvements in lignin modification and identification technologies are necessary to specify a suitable process and to develop derivatives for specific purpose and products. Further research is not only required for lignin modification research to develop a more reactive lignin

derivatives, but also needed for the conditions and parameters of lignin-protein interactions to enhance their interactions.

Scale-up and economical studies of the whole production process are the most for its commercialization and sustainability.

References

Adapa, P. K., Karunakaran, C., Tabil, L. G. and Schoenau, G. J. 2009. Potential applications of infrared and Raman spectromicroscopy for agricultural biomass. Agricultural Engineering International: CIGR Journal.

Aftabuddin, M. and Kundu, S. 2007. Hydrophobic, hydrophilic, and charged amino acid networks within protein. Biophysical journal 93:225-231.

Aracri, E., Blanco, C. D. and Tzanov, T. 2014. An enzymatic approach to develop a lignin-based adhesive for wool floor coverings. Green Chemistry 16:2597-2603.

ASTM, D. 2003. 1183-03. Standard practices for resistance of adhesives to cyclic laboratory aging conditions. USA.

Barreca, A. M., Fabbrini, M., Galli, C., Gentili, P. and Ljunggren, S. 2003. Laccase/mediated oxidation of a lignin model for improved delignification procedures. Journal of Molecular Catalysis B: Enzymatic 26:105-110.

Bertaud, F., Tapin-Lingua, S., Pizzi, A., Navarrete, P. and Petit-Conil, M. 2012. Development of green adhesives for fibreboard manufacturing, using tannins and lignin from pulp mill residues. Cellulose Chem. Technol 46:449-455.

Cao, J., Xiao, G., Xu, X., Shen, D. and Jin, B. 2013. Study on carbonization of lignin by TG-FTIR and high-temperature carbonization reactor. Fuel processing technology 106:41-47.

Cetin, N. S. and Özmen, N. 2002. Use of organosolv lignin in phenol-formaldehyde resins for particleboard production: II. Particleboard production and properties. International Journal of adhesion and adhesives 22:481-486.

Chen, H.-H., Xu, S.-Y. and Wang, Z. 2006a. Gelation properties of flaxseed gum. Journal of food engineering 77:295-303.

Chen, P., Zhang, L., Peng, S. and Liao, B. 2006b. Effects of nanoscale hydroxypropyl lignin on properties of soy protein plastics. Journal of applied polymer science 101:334-341.

Christopher, L. P., Yao, B. and Ji, Y. 2014. Lignin biodegradation with laccase-mediator systems. Frontiers in Energy Research 2:12.

Cong, F., Diehl, B. G., Hill, J. L., Brown, N. R. and Tien, M. 2013. Covalent bond formation between amino acids and lignin: cross-coupling between proteins and lignin. Phytochemistry 96:449-456.

Damodaran, S. 2008. Amino acids, peptides, and proteins. CRC Press: Boca Raton, FL.

de Meijer, M., Haemers, S., Cobben, W. and Militz, H. 2000. Surface energy determinations of wood: comparison of methods and wood species. Langmuir 16:9352-9359.

Dence, C. W. 1992. The determination of lignin. Pages 33-61 in: Methods in lignin chemistry. Springer.

Desai, S. and Nityanand, C. 2011. Microbial laccases and their applications: a review. Asian J Biotechnol 3:98-124.

Díaz-Rodríguez, A., Martínez-Montero, L., Lavandera, I., Gotor, V. and Gotor-Fernández, V. 2014. Laccase/2, 2, 6, 6-Tetramethylpiperidinoxyl Radical (TEMPO): An Efficient Catalytic System for Selective Oxidations of Primary Hydroxy and Amino Groups in Aqueous and Biphasic Media. Advanced Synthesis & Catalysis 356:2321-2329.

Diehl, B. G., Watts, H. D., Kubicki, J. D., Regner, M. R., Ralph, J. and Brown, N. R. 2014. Towards lignin-protein crosslinking: amino acid adducts of a lignin model quinone methide. Cellulose 21:1395-1407.

Doherty, W. O., Mousavioun, P. and Fellows, C. M. 2011. Value-adding to cellulosic ethanol: Lignin polymers. Industrial Crops and products 33:259-276.
Duval, A. and Lawoko, M. 2014. A review on lignin-based polymeric, micro-and nano-structured materials. Reactive and Functional Polymers 85:78-96.
Duval, A., Molina-Boisseau, S. and Chirat, C. 2013. Comparison of Kraft lignin and lignosulfonates addition to wheat gluten-based materials: Mechanical and thermal properties. Industrial crops and products 49:66-74.
El Mansouri, N.-E. and Salvadó, J. 2006. Structural characterization of technical lignins for the production of adhesives: Application to lignosulfonate, kraft, soda-anthraquinone, organosolv and ethanol process lignins. Industrial Crops and Products 24:8-16.
El Mansouri, N. E., Yuan, Q. and Huang, F. 2011. Characterization of alkaline lignins for use in phenol-formaldehyde and epoxy resins. BioResources 6:2647-2662.
EPA, E. P. A. 2013a. Formaldehyde Emissions Standards for Composite Wood Products: https://www.regulations.gov/document?D=EPA-HQ-OPPT-2012-0018-0001.
EPA, U. S. E. p. A. 2013b. Formaldehyde Emission Standards for Composite Wood Products: http://www.epa.gov/formaldehyde/formaldehyde-emission-standards-composite-wood-products#Formaldehyderegs.
Fabbrini, M., Galli, C. and Gentili, P. 2002. Comparing the catalytic efficiency of some mediators of laccase. Journal of Molecular Catalysis B: Enzymatic 16:231-240.
Fang, Z., Sato, T., Smith, R. L., Inomata, H., Arai, K. and Kozinski, J. A. 2008. Reaction chemistry and phase behavior of lignin in high-temperature and supercritical water. Bioresource Technology 99:3424-3430.
Fisher, A. B. and Fong, S. S. 2014. Lignin biodegradation and industrial implications. AIMS Bioengineering 1: 92-112
Fraenkel-Conrat, H. and Olcott, H. S. 1945. Esterification of proteins with alcohols of low molecular weight. Journal of Biological Chemistry 161:259-268.
Frigerio, P., Zoia, L., Orlandi, M., Hanel, T. and Castellani, L. 2014. Application of sulphur-free lignins as a filler for elastomers: effect of hexamethylenetetramine treatment. BioResources 9:1387-1400.
Frihart, C. R., Birkeland, M. J., Allen, A. J. and Wescott, J. M. 2010. Soy adhesives that can form durable bonds for plywood, laminated wood flooring, and particleboard. Proceedings of the International Convention of Society of Wood Science and Technology and United Nations Economic Commission for Europe – Timber Committee
Frihart, C. R., Hunt, C. G. and Birkeland, M. J. 2013. Recent Advances in Adhesion Science and Technology in Honor of Dr. Kash Mittal.
Geng, X. and Li, K. 2006. Investigation of wood adhesives from kraft lignin and polyethylenimine. Journal of adhesion science and technology 20:847-858.
Gennadios, A., BRANDENBURG, A., WELLER, C. and TESTIN, R. 1993. Effect of pH on properties of wheat gluten and soy protein isolate films. Journal of agricultural and food chemistry 41:1835-1839.
Gerrard, J., Meade, S., Miller, A., Brown, P., Yasir, S., Sutton, K. and Newberry, M. 2005. Protein Cross-Linking in Food. Annals of the New York Academy of Sciences 1043:97-103.
Gosselink, R., De Jong, E., Guran, B. and Abächerli, A. 2004. Co-ordination network for lignin—standardisation, production and applications adapted to market requirements (EUROLIGNIN). Industrial Crops and Products 20:121-129.

Grand View Research Inc. 2017a. Wood Adhesives Market Analysis By Product (Urea-Formaldehyde, Melamine Urea, Phenol-Formaldehyde, Isocyanate, Polyurethane, PVA, Soy-based), By Application (Flooring, Furniture, Doors & Windows), And Segment Forecasts, 2014 - 2025. Rep. Grand View REsearch Inc.

Grand View Research Inc. 2017b. Wood Adhesives Market Size Worth $6.18 Billion By 2025 | CAGR: 4.5%.

Hagerman, A. E. and Butler, L. G. 1981. The specificity of proanthocyanidin-protein interactions. Journal of Biological Chemistry 256:4494-4497.

Hagerman, A. E., Rice, M. E. and Ritchard, N. T. 1998. Mechanisms of protein precipitation for two tannins, pentagalloyl glucose and epicatechin16 (4→ 8) catechin (procyanidin). Journal of Agricultural and Food Chemistry 46:2590-2595.

Haslam, E. 1996. Natural polyphenols (vegetable tannins) as drugs: possible modes of action. Journal of natural products 59:205-215.

He, Z., Chapital, D. C., Cheng, H. N., Klasson, K. T., Olanya, O. M. and Uknalis, J. 2014. Application of tung oil to improve adhesion strength and water resistance of cottonseed meal and protein adhesives on maple veneer. Industrial Crops and Products 61:398-402.

Hejda, F., Solar, P. and Kousal, J. 2010. Surface free energy determination by contact angle measurements–A comparison of various approaches. WDS'10 Proceedings of Contributed Papers, Part III, 25–30, 2010.

Hemmilä, V., Trischler, J. and Sandberg, D. 2013. BIO-BASED ADHESIVES FOR THE WOOD INDUSTRY–AN OPPORTUNITY FOR THE FUTURE? Pages 118-125 in: Pro Ligno. Publishing House of Transilvania University of Brasov.

Hettiarachchy, N., Kalapathy, U. and Myers, D. 1995. Alkali-modified soy protein with improved adhesive and hydrophobic properties. Journal of the American Oil Chemists' Society 72:1461-1464.

Holladay, J. E., White, J. F., Bozell, J. J. and Johnson, D. 2007. Top Value Added Chemicals from Biomass-Volume II, Results of Screening for Potential Candidates from Biorefinery Lignin. Rep. Pacific Northwest National Lab.(PNNL), Richland, WA (United States); National Renewable Energy Laboratory (NREL), Golden, CO (United States).

HPVA. 2004. American National Standard for Hardwood and Decorative Plywood. H. P. V. Association, ed: Reston, VA.

Huang, J., Zhang, L. and Chen, F. 2003a. Effects of lignin as a filler on properties of soy protein plastics. I. Lignosulfonate. Journal of applied polymer science 88:3284-3290.

Huang, J., Zhang, L. and Chen, P. 2003b. Effects of lignin as a filler on properties of soy protein plastics. II. Alkaline lignin. Journal of applied polymer science 88:3291-3297.

Huang, W. and Sun, X. 2000a. Adhesive properties of soy proteins modified by sodium dodecyl sulfate and sodium dodecylbenzene sulfonate. Journal of the American Oil Chemists' Society 77:705-708.

Huang, W. and Sun, X. 2000b. Adhesive properties of soy proteins modified by urea and guanidine hydrochloride. Journal of the American Oil Chemists' Society 77:101-104.

Ibrahim, M. M., Nadiah, M. N. and Azian, H. 2006. Comparison studies between soda lignin and soda-anthraquinone lignin in terms of physic-chemical properties and structural features. Journal of Applied Sciences 6:292-296.

Ibrahim, M. N. M., Zakaria, N., Sipaut, C. S., Sulaiman, O. and Hashim, R. 2011. Chemical and thermal properties of lignins from oil palm biomass as a substitute for phenol in a phenol formaldehyde resin production. Carbohydrate polymers 86:112-119.

Ibrahim, V., Mamo, G., Gustafsson, P.-J. and Hatti-Kaul, R. 2013. Production and properties of adhesives formulated from laccase modified Kraft lignin. Industrial Crops and Products 45:343-348.

Ishino, K. and Okamoto, S. 1975. Molecular interaction in alkali denatured soybean proteins. Cereal chemistry.

Jiang, J., Chen, J. and Xiong, Y. L. 2009. Structural and emulsifying properties of soy protein isolate subjected to acid and alkaline pH-shifting processes. Journal of Agricultural and Food Chemistry 57:7576-7583.

Jiang, J., Xiong, Y. L. and Chen, J. 2010. pH shifting alters solubility characteristics and thermal stability of soy protein isolate and its globulin fractions in different pH, salt concentration, and temperature conditions. Journal of agricultural and food chemistry 58:8035-8042.

Khan, M. and Ashraf, S. 2005. Development and characterization of a lignin–phenol–formaldehyde wood adhesive using coffee bean shell. Journal of adhesion science and technology 19:493-509.

Khan, M. A., Ashraf, S. M. and Malhotra, V. P. 2004. Eucalyptus bark lignin substituted phenol formaldehyde adhesives: A study on optimization of reaction parameters and characterization. Journal of applied polymer science 92:3514-3523.

Kim, J.-Y., Oh, S., Hwang, H., Kim, U.-J. and Choi, J. W. 2013. Structural features and thermal degradation properties of various lignin macromolecules obtained from poplar wood (Populus albaglandulosa). Polymer degradation and stability 98:1671-1678.

Kim, M. J. and Sun, X. S. 2014. Adhesion properties of soy protein crosslinked with organic calcium silicate hydrate hybrids. Journal of Applied Polymer Science 131.

Kim, M. J. and Sun, X. S. 2015. Correlation between Physical Properties and Shear Adhesion Strength of Enzymatically Modified Soy Protein-Based Adhesives. Journal of the American Oil Chemists' Society 92:1689-1700.

Kunanopparat, T., Menut, P., Morel, M. H. and Guilbert, S. 2012. Improving wheat gluten materials properties by Kraft lignin addition. Journal of Applied Polymer Science 125:1391-1399.

Kuo, M. and Hse, C.-Y. 1991. Alkali treated kraft lignin as a component in flakeboard resins. Holzforschung-International Journal of the Biology, Chemistry, Physics and Technology of Wood 45:47-54.

Laurichesse, S. and Avérous, L. 2014. Chemical modification of lignins: Towards biobased polymers. Progress in Polymer Science 39:1266-1290.

Le Bourvellec, C. and Renard, C. 2012. Interactions between polyphenols and macromolecules: quantification methods and mechanisms. Critical reviews in food science and nutrition 52:213-248.

Lei, H., Du, G., Wu, Z., Xi, X. and Dong, Z. 2014. Cross-linked soy-based wood adhesives for plywood. International journal of adhesion and adhesives 50:199-203.

Leonowicz, A., Cho, N., Luterek, J., Wilkolazka, A., Wojtas-Wasilewska, M., Matuszewska, A., Hofrichter, M., Wesenberg, D. and Rogalski, J. 2001. Fungal laccase: properties and activity on lignin. Journal of Basic Microbiology 41:185-227.

Li, K., Peshkova, S. and Geng, X. 2004. Investigation of soy protein-Kymene® adhesive systems for wood composites. Journal of the American Oil Chemists' Society 81:487-491.

Li, N., Qi, G., Sun, X. S., Stamm, M. J. and Wang, D. 2012a. Physicochemical properties and adhesion performance of canola protein modified with sodium bisulfite. Journal of the American Oil Chemists' Society 89:897-908.

Li, N., Qi, G., Sun, X. S. and Wang, D. 2012b. Effects of sodium bisulfite on the physicochemical and adhesion properties of canola protein fractions. Journal of Polymers and the Environment 20:905-915.
Li, W., Van den Bulcke, J., Mannes, D., Lehmann, E., De Windt, I., Dierick, M. and Van Acker, J. 2014. Impact of internal structure on water-resistance of plywood studied using neutron radiography and X-ray tomography. Construction and Building Materials 73:171-179.
Lisperguer, J., Nunez, C. and Perez-Guerrero, P. 2013. Structure and thermal properties of maleated lignin-recycled polystyrene composites. Journal of the Chilean Chemical Society 58:1937-1940.
Liu, H.-M., Li, M.-F. and Sun, R.-C. 2013. Hydrothermal liquefaction of cornstalk: 7-lump distribution and characterization of products. Bioresource technology 128:58-64.
Liu, H. 2017. Wet adhesion properties of oilseed proteins stimulated by chemical and physical interactions and bonding. Kansas State University.
Liu, H., Li, C. and Sun, X. S. 2015. Improved water resistance in undecylenic acid (UA)-modified soy protein isolate (SPI)-based adhesives. Industrial Crops and Products 74:577-584.
Lora, J. H. and Glasser, W. G. 2002. Recent industrial applications of lignin: a sustainable alternative to nonrenewable materials. Journal of Polymers and the Environment 10:39-48.
Luo, J., Li, C., Li, X., Luo, J., Gao, Q. and Li, J. 2015a. A new soybean meal-based bioadhesive enhanced with 5, 5-dimethyl hydantoin polyepoxide for the improved water resistance of plywood. RSC Advances 5:62957-62965.
Luo, J., Li, X., Zhang, H., Gao, Q. and Li, J. 2016a. Properties of a soybean meal-based plywood adhesive modified by a commercial epoxy resin. International Journal of Adhesion and Adhesives 71:99-104.
Luo, J., Luo, J., Li, X., Gao, Q. and Li, J. 2016b. Effects of polyisocyanate on properties and pot life of epoxy resin cross-linked soybean meal-based bioadhesive. Journal of Applied Polymer Science 133.
Luo, J., Luo, J., Yuan, C., Zhang, W., Li, J., Gao, Q. and Chen, H. 2015b. An eco-friendly wood adhesive from soy protein and lignin: performance properties. RSC Advances 5:100849-100855.
Maestri, D. M., Labuckas, D. O., Meriles, J. M., Lamarque, A. L., Zygadlo, J. A. and Guzmán, C. A. 1998. Seed composition of soybean cultivars evaluated in different environmental regions. Journal of the Science of Food and Agriculture 77:494-498.
Mankar, S., Chaudhari, A. and Soni, I. 2012. Lignin in phenol-formaldehyde adhesives. International Journal of Knowledge Engineering, ISSN:0976-5816.
Migneault, I., Dartiguenave, C., Bertrand, M. J. and Waldron, K. C. 2004. Glutaraldehyde: behavior in aqueous solution, reaction with proteins, and application to enzyme crosslinking. Biotechniques 37:790-806.
Mo, X., Sun, X. and Wang, D. 2004. Thermal properties and adhesion strength of modified soybean storage proteins. Journal of the American Oil Chemists' Society 81:395-400.
Mo, X. and Sun, X. S. 2013. Soy proteins as plywood adhesives: formulation and characterization. Journal of Adhesion Science and Technology 27:2014-2026.
Morgan, K. T. 1997. A brief review of formaldehyde carcinogenesis in relation to rat nasal pathology and human health risk assessment. Toxicologic pathology 25:291-305.
Moubarik, A., Grimi, N., Boussetta, N. and Pizzi, A. 2013. Isolation and characterization of lignin from Moroccan sugar cane bagasse: Production of lignin–phenol-formaldehyde wood adhesive. Industrial Crops and Products 45:296-302.

Moxley, G., Gaspar, A. R., Higgins, D. and Xu, H. 2012. Structural changes of corn stover lignin during acid pretreatment. Journal of industrial microbiology & biotechnology 39:1289-1299.

Nasir, M., Gupta, A., Beg, M., Chua, G. and Kumar, A. 2014. PHYSICAL AND MECHANICAL PROPERTIES OF MEDIUM-DENSITY FIBREBOARDS USING SOY—LIGNIN ADHESIVES. Journal of tropical forest science:41-49.

Nordqvist, P., Nordgren, N., Khabbaz, F. and Malmström, E. 2013. Plant proteins as wood adhesives: Bonding performance at the macro-and nanoscale. Industrial Crops and Products 44:246-252.

Ozdal, T., Capanoglu, E. and Altay, F. 2013. A review on protein–phenolic interactions and associated changes. Food Research International 51:954-970.

Pandey, M. P. and Kim, C. S. 2011. Lignin depolymerization and conversion: a review of thermochemical methods. Chemical Engineering & Technology 34:29-41.

Park, S., Bae, D. and Rhee, K. 2000. Soy protein biopolymers cross-linked with glutaraldehyde. Journal of the American Oil Chemists' Society 77:879-884.

Pizzi, A. 2006. Recent developments in eco-efficient bio-based adhesives for wood bonding: opportunities and issues. Journal of adhesion science and technology 20:829-846.

Pizzi, A. and Salvadó, J. 2007. Lignin-based wood panel adhesives without formaldehyde. Holz als Roh-und Werkstoff 65:65.

Poletto, M. and Zattera, A. J. 2013. Materials produced from plant biomass: part III: degradation kinetics and hydrogen bonding in lignin. Materials Research 16:1065-1070.

Pouteau, C., Cathala, B., Dole, P., Kurek, B. and Monties, B. 2005. Structural modification of Kraft lignin after acid treatment: characterisation of the apolar extracts and influence on the antioxidant properties in polypropylene. Industrial Crops and Products 21:101-108.

Pradyawong, S., Qi, G., Li, N., Sun, X. S. and Wang, D. 2017. Adhesion properties of soy protein adhesives enhanced by biomass lignin. International Journal of Adhesion and Adhesives.

Prodpran, T., Benjakul, S. and Phatcharat, S. 2012. Effect of phenolic compounds on protein cross-linking and properties of film from fish myofibrillar protein. International journal of biological macromolecules 51:774-782.

Pu, Y., Chen, F., Ziebell, A., Davison, B. H. and Ragauskas, A. J. 2009. NMR characterization of C3H and HCT down-regulated alfalfa lignin. BioEnergy Research 2:198.

Pye, E. K. 2008. Industrial lignin production and applications. Biorefineries-industrial processes and products: status quo and future directions:165-200.

Qi, G., Li, N., Wang, D. and Sun, X. S. 2013a. Adhesion and physicochemical properties of soy protein modified by sodium bisulfite. Journal of the American Oil Chemists' Society 90:1917-1926.

Qi, G., Li, N., Wang, D. and Sun, X. S. 2013b. Physicochemical properties of soy protein adhesives modified by 2-octen-1-ylsuccinic anhydride. Industrial Crops and Products 46:165-172.

Qi, G., Li, N., Wang, D. and Sun, X. S. 2016. Development of High-Strength Soy Protein Adhesives Modified with Sodium Montmorillonite Clay. Journal of the American Oil Chemists' Society 93:1509-1517.

Qi, G. and Sun, X. S. 2011. Soy protein adhesive blends with synthetic latex on wood veneer. Journal of the American Oil Chemists' Society 88:271-281.

Qi, G., Venkateshan, K., Mo, X., Zhang, L. and Sun, X. S. 2011. Physicochemical properties of soy protein: effects of subunit composition. Journal of agricultural and food chemistry 59:9958-9964.

Ramalingam, B., Sana, B., Seayad, J., Ghadessy, F. and Sullivan, M. 2017. Towards understanding of laccase-catalysed oxidative oligomerisation of dimeric lignin model compounds. RSC Advances 7:11951-11958.
Rowell, R. M., Caldeira, F. and Rowell, J. K. 2010. Sustainable development in the forest products industry. Ed. Univ. Fernando Pessoa.
Salas, C., Ago, M., Lucia, L. A. and Rojas, O. J. 2014. Synthesis of soy protein–lignin nanofibers by solution electrospinning. Reactive and Functional Polymers 85:221-227.
Salas, C., Rojas, O. J., Lucia, L. A., Hubbe, M. A. and Genzer, J. 2012. On the surface interactions of proteins with lignin. ACS applied materials & interfaces 5:199-206.
Sánchez, O., Sierra, R. and Alméciga-Díaz, C. J. 2011. Delignification process of agro-industrial wastes an alternative to obtain fermentable carbohydrates for producing fuel in: Alternative fuel. InTech.
Santoni, I. and Pizzo, B. 2013. Evaluation of alternative vegetable proteins as wood adhesives. Industrial Crops and Products 45:148-154.
Schorr, D., Diouf, P. N. and Stevanovic, T. 2014. Evaluation of industrial lignins for biocomposites production. Industrial Crops and Products 52:65-73.
Shadid, K. A. 2016. Infrared Spectroscopy Theory and Interpretation of IR spectra. Dina Hopkins: http://slideplayer.com/slide/8335494.
Simon, C., Barathieu, K., Laguerre, M., Schmitter, J.-M., Fouquet, E., Pianet, I. and Dufourc, E. J. 2003. Three-dimensional structure and dynamics of wine tannin− saliva protein complexes. A multitechnique approach. Biochemistry 42:10385-10395.
Singh, S. K. and Ekhe, J. D. 2014. Towards effective lignin conversion: HZSM-5 catalyzed one-pot solvolytic depolymerization/hydrodeoxygenation of lignin into value added compounds. Rsc Advances 4:27971-27978.
Sofuoglu, S. C., Aslan, G., Inal, F. and Sofuoglu, A. 2011. An assessment of indoor air concentrations and health risks of volatile organic compounds in three primary schools. International journal of hygiene and environmental health 214:36-46.
Stewart, D. 2008. Lignin as a base material for materials applications: Chemistry, application and economics. Industrial crops and products 27:202-207.
Stuart, B. H. 2004. Infrared Spectroscopy : Fundamentals and Applications. John Wiley & Sons, Incorporated: Hoboken, UK.
Su, J.-F., Huang, Z., Yuan, X.-Y., Wang, X.-Y. and Li, M. 2010. Structure and properties of carboxymethyl cellulose/soy protein isolate blend edible films crosslinked by Maillard reactions. Carbohydrate Polymers 79:145-153.
Swain, S., Rao, K. and Nayak, P. 2004. Biodegradable polymers. III. Spectral, thermal, mechanical, and morphological properties of cross-linked furfural–soy protein concentrate. Journal of applied polymer science 93:2590-2596.
Tejado, A., Pena, C., Labidi, J., Echeverria, J. and Mondragon, I. 2007. Physico-chemical characterization of lignins from different sources for use in phenol–formaldehyde resin synthesis. Bioresource Technology 98:1655-1663.
Toledano, A., García, A., Mondragon, I. and Labidi, J. 2010. Lignin separation and fractionation by ultrafiltration. Separation and Purification Technology 71:38-43.
United Soybean Board. 2012. MARKET OPP0RTUNITY SUMMARY
Soy-Based Adhesives.
USDA. 2018. World Agricultural Supply and Demand Estimates. Page Agricultural Marketing Service. Farm Service Agency. The Department.

Wang, D., Sun, X., Yang, G. and Wang, Y. 2009a. Improved water resistance of soy protein adhesive at isoelectric point. Transactions of the ASABE 52:173-177.
Wang, S., Wang, K., Liu, Q., Gu, Y., Luo, Z., Cen, K. and Fransson, T. 2009b. Comparison of the pyrolysis behavior of lignins from different tree species. Biotechnology Advances 27:562-567.
Wang, Y., Mo, X., Sun, X. S. and Wang, D. 2007. Soy protein adhesion enhanced by glutaraldehyde crosslink. Journal of Applied Polymer Science 104:130-136.
Wang, Y., Wang, D. and Sun, X. 2005. Thermal properties and adhesiveness of soy protein modified with cationic detergent. Journal of the American Oil Chemists' Society 82:357-363.
Wei, M., Fan, L., Huang, J. and Chen, Y. 2006. Role of Star-Like Hydroxylpropyl Lignin in Soy-Protein Plastics. Macromolecular Materials and Engineering 291:524-530.
Wen, J.-L., Sun, S.-L., Xue, B.-L. and Sun, R.-C. 2013. Quantitative structures and thermal properties of birch lignins after ionic liquid pretreatment. Journal of agricultural and food chemistry 61:635-645.
Wescott, J., Frihart, C. and Traska, A. 2006. High-soy-containing water-durable adhesives. Journal of Adhesion Science and Technology 20:859-873.
Whitmore, F. 1978. Lignin-protein complex catalyzed by peroxidase. Plant Science Letters 13:241-245.
Whitmore, F. W. 1982. 6 Lignin-protein complex in cell walls of Pinus elliottii: Amino acid constituents. Phytochemistry 21:315-318.
Wool, R. and Sun, X. 2005. Bio-based polymers and composites.
Wool, R. and Sun, X. S. 2011. Bio-based polymers and composites. Academic Press.
Xiao, Z., Li, Y., Wu, X., Qi, G., Li, N., Zhang, K., Wang, D. and Sun, X. S. 2013. Utilization of sorghum lignin to improve adhesion strength of soy protein adhesives on wood veneer. Industrial Crops and Products 50:501-509.
Xin, J., Zhang, P., Wolcott, M. P., Zhang, X. and Zhang, J. 2014. Partial depolymerization of enzymolysis lignin via mild hydrogenolysis over Raney Nickel. Bioresource technology 155:422-426.
Yang, S., Wen, J.-L., Yuan, T.-Q. and Sun, R.-C. 2014. Characterization and phenolation of biorefinery technical lignins for lignin–phenol–formaldehyde resin adhesive synthesis. RSC Advances 4:57996-58004.
Yang, S., Yuan, T. Q., Li, M. F. and Sun, R. C. 2015. Hydrothermal degradation of lignin: products analysis for phenol formaldehyde adhesive synthesis. Int J Biol Macromol 72:54-62.
Yuan, T.-Q., Sun, S.-N., Xu, F. and Sun, R.-C. 2011. Characterization of lignin structures and lignin–carbohydrate complex (LCC) linkages by quantitative 13C and 2D HSQC NMR spectroscopy. Journal of agricultural and food chemistry 59:10604-10614.
Zhang, J., Chen, Y., Sewell, P. and Brook, M. A. 2015. Utilization of softwood lignin as both crosslinker and reinforcing agent in silicone elastomers. Green Chemistry 17:1811-1819.
Zhang, W., Ma, Y., Xu, Y., Wang, C. and Chu, F. 2013. Lignocellulosic ethanol residue-based lignin–phenol–formaldehyde resin adhesive. International Journal of Adhesion and Adhesives 40:11-18.
Zhang, Y.-J., Tanaka, T., Betsumiya, Y., Kusano, R., Matsuo, A., Ueda, T. and Kouno, I. 2002. Association of tannins and related polyphenols with the cyclic peptide gramicidin S. Chemical and pharmaceutical bulletin 50:258-262.

Zhang, Y., Zhu, W., Lu, Y., Gao, Z. and Gu, J. 2014. Nano-scale blocking mechanism of MMT and its effects on the properties of polyisocyanate-modified soybean protein adhesive. Industrial Crops and Products 57:35-42.

Zhong, Z. and Sun, X. S. 2007. Plywood adhesives by blending soy protein polymer with phenol-formaldehyde resin. Journal of Biobased Materials and Bioenergy 1:380-387.

Zhu, W. 2015. Precipitation of Kraft Lignin: Yield and Equilibrium. Chalmers University of Technology.

Zhu, X., Wang, D., Li, N. and Sun, X. S. 2017. Bio-Based Wood Adhesive from Camelina Protein (a Biodiesel Residue) and Depolymerized Lignin with Improved Water Resistance. ACS Omega 2:7996-8004.